Aero

(3) GALCIT REPORT NO. 321

(2) GUGGENHEIM AERONAUTICS LABORATORY

(1) CALIFORNIA INSTITUTE OF TECHNOLOGY

REPORT ON

WIND TUNNEL TESTS ON A 1/4TH SCALE MODEL OF

THE CURTISS-WRIGHT XP[illegible]

REPORT 321

NOTE

Because of the Emergency National Defense Program the GALCIT wind tunnel operations have been considerably intensified, and the supervisory staff has been reduced through calls on some of its members for government service. In view of the pressure for rapid presentation of wind tunnel results to government contractors and the shortage of wind tunnel staff personnel it has been found necessary to modify the usual GALCIT Report procedure for the duration of the emergency. During this period experimental data will be analysed as carefully as possible and the Reports will remain self-contained and complete, but the detailed discussion of results, which has been a feature of GALCIT reports, will be greatly shortened or omitted. The following Report has been prepared in accordance with this procedure.

Clark B. Millikan

Clark B. Millikan

January 16, 1941

GUGGENHEIM AERONAUTICS LABORATORY

CALIFORNIA INSTITUTE OF TECHNOLOGY

PASADENA

REPORT ON

WIND TUNNEL TESTS ON A 1/4TH SCALE MODEL OF THE CURTISS-WRIGHT XP-55 AIRPLANE

PREPARED BY

Clark B. Millikan

No. of pages 91
No. of figures 61
No. of photos 26

Date July 21, 1941

Wind Tunnel Section

TABLE OF CONTENTS

INDEX OF RUNS

Run	Configuration	Test	q gm/cm^2	Settings (degrees)	Fig. No. Ref.
1	$W_N A^*$	MDP	25	$a_r = a_\ell = 0$	7,8,10,11
2	" + wing tufts	P+tuft pict.	"	"	8,9,23
3	$W_N A^* V_I$ + " "	"	"	$a_r = a_\ell = r = 0$	8,9,22,24
4	$W_N A V_I$ + " "	"	"	"	8,21,22,25
5	$W_N A V_I f_1$ + " "	"	"	"	21,22,26
6	$W_N A V_I f_2$ + " "	"	"	"	21,22,27
7	$W_N A V_I f_3$ + " "	"	"	"	21,22,28
8	$W_N A V_I f_4$ + " "	"	"	"	21,22,29, 30,31
9	$W_N A^* V_I f_4$ + " "	"	"	"	30,31,32
10	$W_N A^* V_I f_5$ + " "	"	"	"	30,31,34
11	$W_N A^* V_I f_5$ + " "	"	"	"	30,31,33
12	$W_N A^* V_I B_N P^{30}_{FIN} P^{30}_{RIW}$	MDP	"	" , $i = 2.25$	10,11
13	$W_N A^* V_I B_N D$	"	"	" , "	9,10,11
14	" + wing tufts	P+tuft pict.	"	" , "	9,11,35,36
15	$W_N A^* V_I X_N B_N D$ + " "	"	"	" , "	9,10,11,35, 37
16	$W_N A^* V_I X_N B_N D f_4$ + " "	"	"	" , "	9,35,38
17	$W_N A V_I X_N B_N D f_4$ + " "	"	"	" , "	9,35,39,40, 41
17A	" + " "	"	"	" , "	
18	$W_N A V_I X_N B_N D f_4 S_i$ + " "	"	"	" , "	40,41,42
19	$W_N A V_I X_N B_N D f_4 S_m$ + " "	"	"	" , "	40,41,43
20	$W_N A V_I X_N B_N D f_4 S^6_i$ + " "	"	"	" , "	40,41,44
21	$W_N A^* V_I f_4 B_N D X_N$	MDP	"	" , "	10,11

INDEX OF RUNS (Cont'd)

Run	Configuration	Test	$\frac{q}{gm/cm^2}$	Settings (degrees)	Fig. No. Ref.
22	$W_{NA}{}^{*}V_{I}f_{4}B_{N}{}^{X}{}_{N}{}^{P}{}_{RRW}^{30}$	P	25	$a_r=a_l=r=0, i=2.25$	10,11,12, 13,15,17, 19,20
23	$W_{NA}{}^{*}V_{I}f_{4}B_{N}{}^{X}{}_{N}{}^{P}{}_{RRW}^{30}F^{45}$	"	"	" , "	12
24	$W_{NA}V_{I}f_{4}B_{N}{}^{X}{}_{N}{}^{P}{}_{RRW}^{30}F^{45}$	"	"	" , "	12
25	"	"	"	$a_r=a_l=-10, r=0, i=2.25$	12,51
25A	" +wing tufts	P+tuft pict.	"	$a_r=a_l=-10, r=0, i=2.25$	54
26	$W_{NA}{}^{*}V_{I}f_{4}B_{N}{}^{X}{}_{N}{}^{P}{}_{RRW}^{30}F^{45}$ + " "	"	"	" , " , "	12,55,51
27	$W_{NA}{}^{*}V_{I}B_{N}{}^{X}{}_{N}LL_{N}{}^{P}{}_{RRW}^{30}F^{45}f_{4}$ +wing tufts	P	"	" , " , "	12,50,51
28	" $+S_{\Delta}+$ " "	P+tuft pict.	"	" , " , "	50,51,56
29	$W_{NA}{}^{*}V_{I}B_{N}{}^{X}{}_{N}LL_{N}{}^{P}{}_{RRW}^{30}f_{4}F^{45}$ +wing tufts	"	"	$a_r=a_l=0$, $r=0$, "	12,53,51
30	$W_{NA}{}^{*}V_{I}B_{N}{}^{X}{}_{N}LL_{N}{}^{P}{}_{RRW}^{30}F^{45}$ +wing tufts	"	"	" , " , "	12,52,51
31	$W_{NA}{}^{*}V_{I}B_{N}{}^{X}{}_{N}{}^{P}{}_{RRW}^{30}f_{4}$ + " "	P	"	" , " , " (3650 rpm)	10,11,12, 45,46
32	$W_{NA}{}^{*}V_{I}B_{N}{}^{X}{}_{N}f_{4}H_{1}P_{RRW}^{30}$	HMMDP	"	" , " , " $e=e_t=0$	13,14,15, 16,17,18, 19,20
33	"	HMP	"	" , " , $i=2.25$ $e=+5$, $e_t=0$	13,14
34	"	"	"	" , " , $i=2.25$ $e=+10$, $e_t=0$	13,14
35	"	"	"	" , " , $i=2.25$ $e=-5$, $e_t=0$	13,14
36	"	"	"	" , " , $i=2.25$ $e=-10$, $e_t=0$	13,14
37	"	"	"	" , " , $i=2.25$ $e=0$, $e_t=-10$	15,16

INDEX OF RUNS (Cont'd)

Run	Configuration	Test	q gm/cm^2	Settings (degrees)	Fig. No. Ref.
38	$W_N A^* V_I B_N X_N f_4 H_1 P^{30}_{RRW}$	HMP	25	$a_r=a_\ell=0$, r=0 , i=2.25 e=+5 , e_t=-10	15,16
39	"	"	"	" , " , i=2.25 e=+10 , e_t=-10	15,16
40	"	"	"	" , " , i=2.25 e=+10 , e_t=-15	17,18
41	$W_N V_I A^* f_4 H_1 B_N X_N P^{30}_{RRW}$	"	"	" , " , i=2.25 e=+5 , e_t=-15	17,18
42	"	"	"	" , " , i=2.25 e=0 , e_t=-15	17,18
43	"	P	"	" , " , i=2.25 e=free, e_t=0	19,20
44	$W_N V_I A^* B_N X_N f_4 P^{30}_{RRW} + S^2_\Delta$ +wing tuft	P+tuft pict.	"	" , " , i=2.25	45,46,47
45	" $+ S^3_\Delta$ +wing tuft	"	"	" , " , i=2.25	45,46,48
46	" $+ S'_\Delta$	"	"	" , " , "	45,46,49

Definition of Tests

P = Complete polar

MDP = Minimum drag + complete polar

Tuft pict. = Photographs of stall patterns using tufts

HM = Elevator hinge moments

HMP = Elevator hinge moments + P

HMMDP = Elevator hinge moments + MDP

INDEX OF FIGURES

General

Wing Alone Characteristics

Effects of Model Build-up and Miscellaneous Modifications

Horizontal Tail Effects

INDEX OF FIGURES (Cont'd)

Investigation of Flow Conditions and Pitching Moments Especially Near the Stall

INDEX OF FIGURES (Cont'd)

INDEX OF PHOTOS

1. $W_N A V_I f_1$, lower side view showing f_1
2. $W_N A V_I f_2$, side view showing f_2
3. $W_N A V_I f_3$, " " " f_3
4. $W_N A V_I f_4$, " " " f_4
5. $W_N A^* V_I f_5$, " " " f_5
6. $W_N A^* V_I B_N D$, 3/4 front view
7. " + Wing Tufts, 3/4 rear view
8. " , side view
9. $W_N A^* V_I B_N X_N D$ + Wing Tufts, side view showing fillet X_N
10. " + " " , front " " " " "
11. " + " " , rear " " " " "
12. " + " " , 3/4 rear view showing fillet X_N
13. $W_N A V_I X_N B_N D f_4 S_i$ + Wing Tufts, upper front view showing spoiler S_i
14. $W_N A V_I X_N B_N D f_4 S_m$ + " " , " " " " " " S_m
15. $W_N A V_I X_N B_N D f_4 S_i^6$ + " " , " " " " " " S_i^6
16. $W_N A^* V_I X_N B_N f_4 P_{FLW}^{30} P_{RRW}^{30}$, rear view
17. " , side view
18. $W_N A^* V_I f_4 B_N X_N P_{RRW}^{30}$, rear view
19. " , side view
20. $W_N A^* V_I f_4 B_N X_N P_{RRW}^{30} F^{45}$, rear view showing flaps F^{45}
21. " , 3/4 side view " " "
22. $W_N A^* V_I f_4 B_N X_N LL_N P_{RRW}^{30} F^{45} S_\Delta$ + Wing Tufts, front view showing landing gear LL_N and spoiler S_Δ
23. $W_N A^* V_I f_4 B_N X_N LL_N P_{RRW}^{30} F^{45} S_\Delta$ + Wing Tufts, side view showing landing gear LL_N and spoiler S_Δ
24. $W_N A^* V_I f_4 B_N X_N LL_N P_{RRW}^{30} F^{45} S_\Delta$ + Wing Tufts, front view of right wing showing landing gear LL_N and spoiler S_Δ
25. $W_N A^* V_I f_4 B_N X_N H_1 P_{RRW}^{30}$, front view showing tail H_1
26. " , side view showing tail H_1

TABLE 1

Notation Used to Describe Configurations Tested

		Curtiss-Wright Drawing No.	Photo No.	Fig. No.
W_N	= Wing with symmetrical section (modified NA - 75 section)	24-279		1,2a,2b
B_N	= Fuselage (new to tests of the XP-55)	2 4-281,4,5	6,7,8	1
X_N	= Large wing-fuselage fillet	24-317	9,10,11, 12	2b
D	= Dummy conical tail cone used on tests without propellers	24-281	7,8	
A	= Ailerons	24-279		2a,2b, 2c
A*	= A, with gaps sealed with tape			
F^{45}	= Split flaps, down 45°	24-313	20,21	
S_i	= Inboard spoiler on each wing of 1/16" welding rod 1-1/2" long, placed 1/4" above wing leading edge, centered 2" from wing-fuselage fillet (model scale)		13	2e
S_i^6	= 6" spoiler of 1/16" welding rod, placed 1/4" above wing leading edge, (model scale) with inboard end at same position as inboard end of S_i		15	2e
S_m	= Same as S_i, but centered midway between fillet and vertical surface		14	2e
S_Δ	= 2" spoiler with equilateral triangle cross-section 1/8" per side, placed 1/8" above wing leading edge, centered midway between side of fuselage and vertical surface. (model scale)		22,23,24	2e
S'_Δ	= Spoiler similar to S_Δ, but 1/4" per side (model scale) in same position as S_i			2e
S^2_Δ	= S'_Δ in same position as S_Δ			2e
S^3_Δ	= Spoiler similar to S'_Δ, but 4" long (model scale), in same position as S_Δ			2e
L	= Main landing gear wheels	24-288	22,23,24	
L_N	= Nose wheel	24-291	22,23,24	

TABLE 1 (Cont'd)

		Curtiss-Wright Drawing No.	Photo No.	Fig. No.
H_1	= Nose elevator	24-312	25,26	2f
V_I	= Vertical surfaces without fin extension (99.69" outboard, full scale)	24-293		2d
f_1	= Very small wood fin extension fairing on V_I		1	2d
f_2	= Larger " " " " " "		2	2d
f_3	= Next larger " " " " " "		3	2d
f_4	= Largest " " " " " ", extending ahead of leading edge of wing		4	2d
f_5	= f_4 with metal extension		5	2d
P^{30}_{FLW}	= Front propeller at $\beta = 30^\circ$, left-hand rotation, windmilling		16,17	
P^{30}_{RRW}	= Rear propeller at $\beta = 30^\circ$, right-hand rotation, windmilling.		16,17,18, 19	
	[Propellers have high-speed airfoil section blades]			
α_u	= Angle of attack relative to fuselage reference line (relative to root chord for wing alone), uncorrected for wind tunnel wall interference			
α	= Angle of attack relative to fuselage reference line (relative to root chord for wing alone), corrected for wind tunnel wall interference			
i	= Angle of incidence of root chord relative to fuselage reference line			
a_r	= Right aileron angle , relative to wing chord plane			
a_ℓ	= Left aileron angle , relative to wing chord plane			
e	= Nose elevator angle relative to fuselage reference line			
e_t	= Elevator tab angle, relative to elevator chord			
r	= Rudder angle relative to plane of symmetry			
β	= Propeller blade angle measured at 0.75R			
q	= Dynamic pressure ($\rho/2\ V^2$, gm/cm^2)			

TABLE 2

Full Scale Dimensions Model Scale = 1/4

Wing: W_M

Root section

Profile = Modified NA-73 symmetrical section, maximum thickness 15 % at 40 % chord

Chord = 92 in.

Tip section

Profile = Modified NA-73 symmetrical section, maximum thickness 15% at 40 % chord

Chord = 29.40 in.

Taper ratio = 3.13:1

Sweepback of 25 % chord line = 28.5° in chord plane

Dihedral = 4.5° measured to trailing edge

Geometric twist

0°, root chord to 99.69" outboard of fuselage center line

-1.5° (washout), 99.69" outboard of fuselage center line to tip, twisted about trailing edge

Mean aerodynamic chord (MAC) = 66.52 in.

Location: 89.45" outboard fuselage center line, 7.06" above root chord, leading edge 55.92" aft of leading edge of root chord at fuselage center line

Incidence = 0° relative to root chord

	Wing	Vertical Surfaces	Flaps	
			Inboard	Outboard
Area, $ft.^2$	183.5	25.2 **	9.00*	11.22*
Span, ft.	36.58	4.58	6.67*	10.00*
Aspect ratio, AR	7.3	1.67**	--	--

* Includes both surfaces

** Without fairing

Vertical surfaces located 99.75" outboard fuselage center line

TABLE 2 (Cont'd)

	Nose elevator	Rudders	Ailerons
Area, ft.^{2}	10.31*	11.44**	13.06**
Span, ft.	8.16	4.58	14.70(tot.)
Area aft of hinge line, ft.^{2}	8.76*	11.44	13.06
Percent balance	15 %	0	0
Area affected by movable surfaces, ft.^{2}	10.3	25.2	--
Mean chord aft of hinge line, ft.	1.48	1.25	0.85
Total Tab area, ft.^{2}	3.16	0	0

* Movable surface
** Both surfaces

Distance from trunnion axis to nose elevator hinge line = 186.12"

Longitudinal distance from trunnion axis to rudder hinge line = 62.48"

Proper area of fuselage = 13.54 ft.^{2}

Propellers, P:

Curtiss-Wright 101330 Design (NACA 16 Sections), full-scale and model

Diameter = 9 ft. (27" model scale); three blades; $\beta = 30^\circ$ at 0.75R; right- and left-hand rotation

REPORT ON WIND TUNNEL TESTS ON A 1/4TH SCALE MODEL OF THE CURTISS-WRIGHT XP-55 AIRPLANE

I. Introduction, General Description of Model and Tests

This Report describes the results of wind tunnel tests on a 1/4th scale model of the Curtiss-Wright XP-55 Airplane. The experiments were made in the closed working section of the 10-foot wind tunnel of the GALCIT (Guggenheim Aeronautics Laboratory at the California Institute of Technology).* The tests were made at a wind speed of approximately 150 m.p.h. (dynamic pressure 25 gm/cm^2), corresponding to Reynolds Number based on mean wing chord of about 1,670,000. The critical Reynolds Number at which a 15 cm. sphere has a drag coefficient of 0.3 is about 525,000, indicating a wind stream with rather low turbulence. The model was lacquered and rubbed down to a fairly high polish.

During the course of the investigation, many modifications were made. Table 1 (page 10) gives the notation employed throughout the Report in designating the various elements and configurations.

A three-view of the model with full-scale dimensions is given in Fig. 1. Diagrams of various model components appear in Figs. 2a - 2f. On Fig. 3 are indicated the trunnion location which represented the axis relative to which moments were determined, and the root and mean chord locations and dimensions. The full-scale data which were furnished by the Curtiss-Wright Corporation and used throughout the Report are given in Table 2 (page 12). For other details of the model and its parts, reference must be made to the original drawings.

---

*cf. Clark B. Millikan and A. L. Klein: "Description and Calibration of 10-foot Wind Tunnel at California Institute of Technology", presented at the Berkeley meeting, Aeronautics Section of the A.S.M.E., June 1932.

The tests were divided into the following broad groups:

1) Wing alone characteristics

2) Effects of model build-up and miscellaneous modifications

3) Horizontal tail effects

4) Investigation of flow conditions and pitching moments, especially near the stall

The figures are collected in terms of the above grouping at the end of the Report.

II. Method of Making Tests and Calculations, and of Presenting Results; Notation

The normal experimental setup is indicated schematically in Figs. 4 and 5, and is illustrated by the Photos at the end of the Report. The tare drag and moment of the supporting system were estimated from the experimental results of previous GALCIT investigations. The tare drag at cruising attitudes was approximately 60% of the minimum net parasite drag.

The model was equipped with counter-rotating propellers which were mounted and allowed to windmill freely in certain tests. Because of trouble with the propeller shaft bearings it was necessary, for most of the tests with rotating propellers, to remove one propeller and use only a single propeller.

Elevator hinge moments were measured by an electrical strain gage developed by Curtiss-Wright and mounted on the elevator control arms. This system operated very well and gave very satisfactory hinge moment results.

All drags and angles of attack were corrected by the Millikan theory of tunnel wall interference* to give free-air conditions. No correction was made for the influence of wind tunnel wall interference on the tail pitching moment.

All observations were reduced to the standard American system of absolute units.

$$C_L = \frac{\text{Lift}}{qS} \qquad C_D = \frac{\text{Drag}}{qS} \qquad C_M = \frac{\text{Stalling Moment}}{qSt} \qquad C_H = \frac{\text{Hinge Moment}}{q\, S_{aft} t_{aft}}$$

where

q = dynamic pressure, $\rho/2\, V^2$, in grams per cm^2.

ρ = mass density of air (note: a correction was applied to the experimental observations so that in this formula ρ is to be taken as the free air density uncorrected for compressibility effects, at least up to 200 m.p.h.

V = Velocity

S = main wing area (see Table 2)

t = mean chord (see Table 2)

b = span (see Table 2)

S_{aft} = Area of movable control surface aft of hinge line (see Table 2)

t_{aft} = Mean chord of movable control surface aft of hinge line (see Table 2)

The conventions and signs are the same as those used by the N.A.C.A. and are as follows: C_M is positive when it tends to raise the nose; control surface and tab angles are positive when they tend to increase the lift on

---

*Millikan, C. B.: "On the Lift Distribution for a Wing of Arbitrary Plan Form in a Circular Wind Tunnel"; Trans. A.S.M.E., App. Mech., Sept. 1932.

the surface; hinge moments are positive when they tend to increase the angle of the movable surface in question.

In certain cases the parasite drag coefficient, C_{D_p}, was determined. For the wing alone the profile drag coefficient, C_{D_o}, and the effective angle of attack were also obtained. The formulae employed in obtaining these quantities were:

$$C_{D_p} \text{ (or } C_{D_o}) = C_D - \frac{C_L^2}{\pi AR}$$

$$\alpha_o = \alpha - \frac{C_L}{\pi AR}$$

where AR = aspect ratio = $\frac{(\text{span})^2}{\text{area}}$. It will be noticed that the lift distribution was assumed to be elliptical.

Pitching moments are referred to an axis through the trunnion position, cf. Fig. 3, except for the wing-alone, infinite aspect ratio results which are referred to a point on the M.A.C. 30% of its length aft of its leading edge. The angle of attack is referred to the thrust line of Fig. 3, except for the wing-alone, infinite aspect ratio data which are referred to the root chord line. Elevator hinge moments refer to the hinge axis (Fig. 2f)

For the investigation of flow characteristics silk tufts were attached to the wing with cellophane tape. The tufts were observed visually and photographically. The "stall pattern" figures given in the report were prepared as a result of studies of the photographs as well as of the sketches made during the visual observations.

It should be mentioned that the plotted experimental points represent direct observations with no fairing, except that the tare drag results were faired before being subtracted from the observed total drags to give the final values. All numerical results are presented in the form of experimental points and faired curves. Tabular data are available in the GALCIT files.

III. Experimental Results and Discussion

1) Wing Alone Characteristics (Fig. 7)

The most important infinite aspect ratio characteristics of the wing alone, determined from Fig. 7, are collected in Table 3.

TABLE 3

Infinite Aspect Ratio Characteristics Of The Wing Alone
($R \doteq 1.67 \times 10^6$)

α_o ($C_L=0$) = Angle of attack of root chord for zero lift	0.4°
$\eta = \frac{dC_L/d\alpha_e \text{ (radians)}}{2\pi}$ = airfoil efficiency factor	0.82
$C_{D_{o_{min}}}$ = Minimum profile drag coefficient (Fig. 11)	0.0073
$C_{L_{opt}}$ = Lift coefficient at $C_{D_{o_{min}}}$	0.1
e = Airplane efficiency factor for wing alone	0.70
$C_{L_{max}}$ = Maximum lift coefficient	1.12
C_{M_o} = Moment coefficient at zero lift	0.017
$\frac{C_{L_{max}}}{C_{D_{o_{min}}}}$ =	154

In view of the considerable sweepback of the wing the reduction of the data to infinite aspect ratio conditions is of doubtful significance. Certain of the results are, however, of considerable interest. The value of $C_{D_{o_{min}}}$ is quite low for wings tested in the GALCIT tunnel at Reynolds Numbers of the order of 1.5×10^6. This indicates that, in spite of the turbulence level of this tunnel, the advantages of the "laminar flow" airfoil section begin to be apparent. The rapid increase in stalling moment near and above the stall suggests the premature tip stall whose investigation is the subject of Section III, 4 below.

2) Effects of Model Build-Up and Miscellaneous Modifications (Figs. 8 - 12)

A complete model build-up was not one of the primary purposes of the present investigation, and as a result the results of this section are neither complete nor systematic. The most important items, together with certain values obtained from other sections of the report, are collected in tabular form in Table 4. The proper drag coefficients, shown in the table are defined by:

$$C_{D_\pi} = \Delta C_{D_p} \times \frac{S}{S_\pi}$$

where S_π is the "proper" area of the element in question, defined as the projected frontal area for the fuselage, and the normal projected area for horizontal and vertical surfaces (cf. Table 2).

TABLE 4

Summary of Lift and Drag Values

A. Parasite Drag of Various Configurations

Configuration		$C_{D_{p_{min}}}$ at $C_L = 0.15$	Run
$W_N A^*$		0.0074	1
$W_N A^*$ + Wing Tufts	≐	0.0090	2
$W_N A^* V_I$ + Wing Tufts	≐	0.0111	3
$W_N A V_I$ + Wing Tufts	≐	0.0119	4
$W_N A^* V_I$	≐	0.0095	--
$W_N A V_I$	≐	0.0103	--
$W_N A^* V_I B_N D$		0.0156	13
$W_N A^* V_I X_N B_N D$	≐	0.0159	--
$W_N A^* V_I X_N B_N D f_4$		0.0163	21
$W_N A^* V_I X_N B_N f_4 H_1 D$	≐	0.0172	--
$W_N A^* V_I X_N B_N f_4 P^{30}_{RRW}$		0.0210	22
$W_N A^* V_I X_N B_N f_4 H_1 P^{30}_{RRW}$		0.0219	32

TABLE 4 (Cont'd)

B. Parasite and Proper Drag Increments of Various Components

Element		$\Delta C_{D_{P_{min}}}$	C_{D_π}	Runs
A-A*		0.0008		4-3
V_I	≐	0.0021	0.0153	3-2
$B_N D$	≐	0.0061	0.084	--
$V_I B_N D$		0.0082		13-1
X_N	≐	0.0003		--
f_4	≐	0.0004		--
$X_N f_4$		0.0007		21-13
P^{30}_{RRW}		0.0047		22-21
H_1		0.0009	0.0160	32-22
$W_N A^*$		0.0074		
$V_I H_1$		0.0030	0.0155	
Wing Tufts	≐	0.0016		2-1

C. Maximum Lift Value or Increment

Element or Configuration		$\Delta C_{L_{max}}$ or $C_{L_{max}}$	Runs
$W_N A^* V_I f_4 B_N D X_N$		1.09	21
$W_N A^* V_I X_N B_N f_4 L L_N F^{45} P^{30}_{RRW}$ + Wing Tufts		1.465	29
$W_N A^* V_I X_N B_N f_4 L L_N H_1 F^{45} P^{30}_{RRW}$	≐	1.50	29 + 32 - 22
H_1	≐	.03	32 - 22
Wing Tufts		0	26 - 23

NOTE: The symbol ≐ means "estimated from tuft runs or from normal polars"

The proper drags of both horizontal and vertical surfaces are rather high as would be expected while that of the fuselage is low as is natural in view of its good shape and fineness ratio.

One noteworthy characteristic which does not appear in Table 4 is the fact that the windmilling propellers have a stabilizing effect equivalent to a forward c.g shift of about 3% M.A.C.

The effect of flap and symmetrical aileron deflection on trim (Fig. 12) is discussed in the next section in connection with horizontal tail effects.

3) Horizontal Tail Effects (Figs. 13 - 20)

Certain of the results of this section (and Fig. 12) are so striking as to warrant special mention:

a) The horizontal surface at a fixed incidence has a powerful destabilizing effect reducing the stability until it is roughly neutral.

b) The horizontal surface floating freely has an appreciable stabilizing effect.

c) With fixed controls an elevator deflection of $+10^{\circ}$ to $+15^{\circ}$ should permit trim at the stall with flaps up.

d) A tab deflection of -15° does not make it possible for the elevator to quite reach $+10^{\circ}$ near the stall with zero hinge moment (free control)

e) Elevator deflection giving trim at the stall does not appreciably affect $C_{L_{max}}$.

f) Flap deflection does not appreciably alter the trim

g) With deflected flaps a symmetrical aileron deflection of -10° produces a stalling moment roughly equivalent to a $+10^{\circ}$ elevator deflection.

In general the longitudinal trim and stability characteristics would appear to be satisfactory below the stall with elevator free with the single possible difficulty of obtaining trim at the stall. This point should be further investigated with elevator free, flaps up and down, and ailerons neutral and deflected symmetrically up.

4) Investigation of Flow Conditions and Pitching Moments, Especially Near the Stall (Figs. 21 - 56)

This section contains the results of the portion of the investigation which was considered of primary importance: namely the improvement of longitudinal stability conditions at and above the stall. Previous studies had shown that, because of the taper and sweepback, severe tip stall leading to static longitudinal instability occurred near the stall. The inboard location of the vertical surfaces V_I had been found to improve the situation somewhat, and it was hoped that forward extension of V_I might give still more improvement. Figs. 21 and 22 show that the so-called "dorsal" fin extensions did not have much effect until f_4 was reached, when the fin extended around the wing leading edge, and the instability above the stall at once disappeared. The stall patterns of Figs. 23 - 29 are very instructive although an exact correlation with the pitching moments of Fig. 22 is somewhat difficult. In general it appears that often portions of the wing which appear to be stalled in the stall diagrams must actually continue to contribute materially to the lift and hence to the pitching moments.

Figs. 30 - 34 show that a further extension of the fins forward (f_5) has a deleterious effect and that opening the aileron slot, although it changes the apparent separation picture below the stall, has little effect on the longitudinal stability in the stall region.

The above results were obtained without any fuselage. Figs. 35 - 39 again show the favorable effect of the fin extension f_4, although with the complete model a slight instability above the stall remains even with f_4 in place.

In an attempt to improve this situation small spoilers with circular cross-section (S_i and S_m) were tried (Figs. 2e and 40 - 44). These gave a small improvement if they were not located too close to the fuselage. Larger

triangular section spoilers (Figs. 2e and 45 - 49) placed well out from the fuselage gave a still greater improvement, and the longest ones, S_{Δ}^{3} led to a moment curve having a very satisfactory slope to the largest angle of attack investigated. However this spoiler appreciably increased drag and decreased maximum lift.

Figs. 50 - 56 indicate that with flaps deflected the stability conditions above the stall are more favorable. Although f_4 is still necessary to avoid instability, the spoiler S_{Δ} is not required and seriously decreases $C_{L_{max}}$.

The general conclusion to be drawn from these results is that the fin extensions f_4 are themselves nearly sufficient to ensure static longitudinal stability for several degrees above the stall. Spoilers may prove advantageous in order to further increase the stability but their effects are so slight that a definite conclusion can probably only be reached by flight tests. It may also reasonably be inferred that satisfactory longitudinal stability in this case also indicates the absence of lateral instability associated with tip stall.

Conclusion

The investigation described above was carried out from June 29 to July 5, 1941 under the direction of Dr. Clark B. Millikan who was largely assisted by Mr. J. E. Smith, Dr. H. J. Stewart, Mr. W. H. Bowen and other members of the GALCIT wind tunnel staff. Mr. L. B. Rumph, Jr. acted as the Curtiss-Wright representative during the investigation.

Guggenheim Aeronautics Laboratory
California Institute of Technology
July 21, 1941

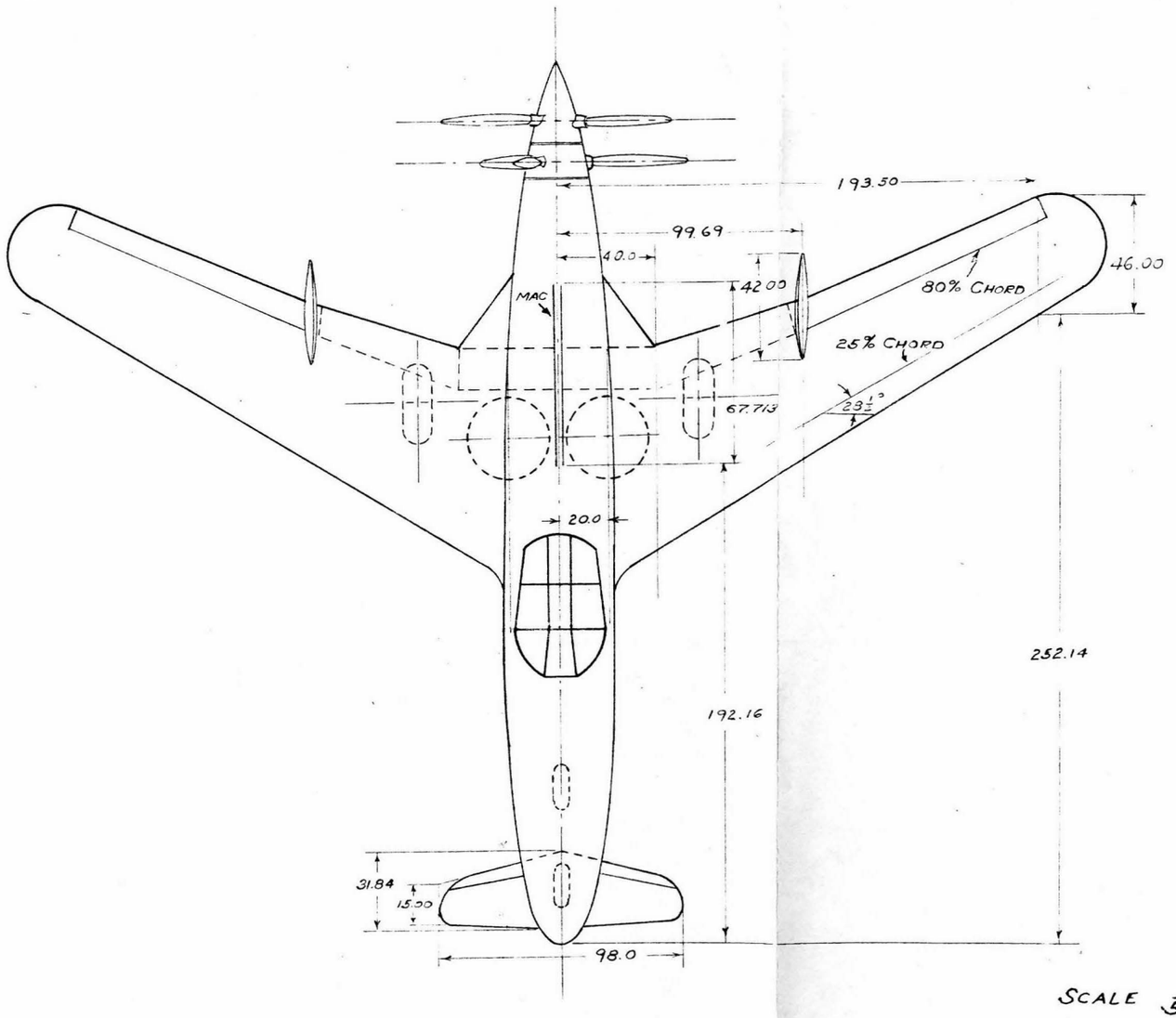

THREE VIEW SKETCH OF CURTISS-WRIGHT MODEL CW-24 (XP-55)

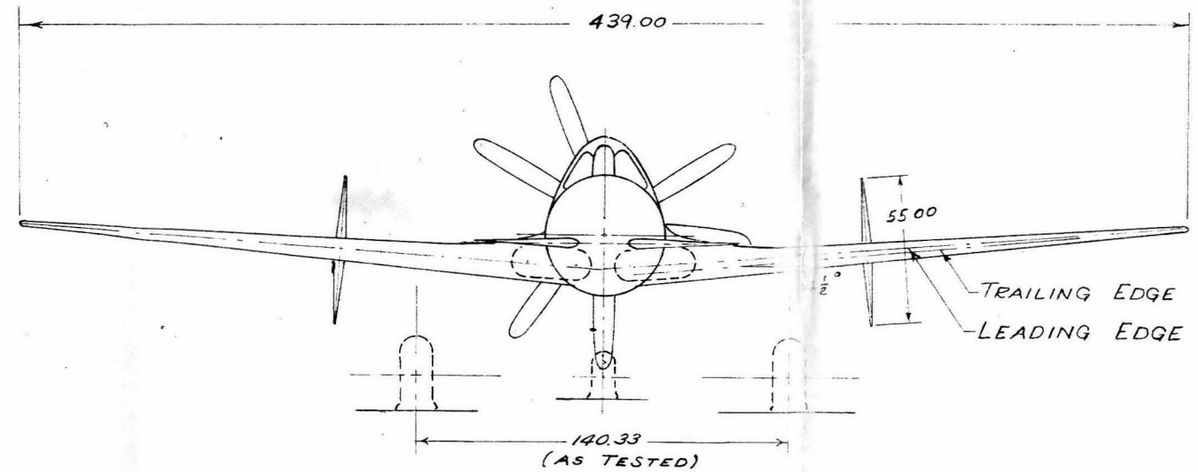

ACTUAL TREAD 124.33

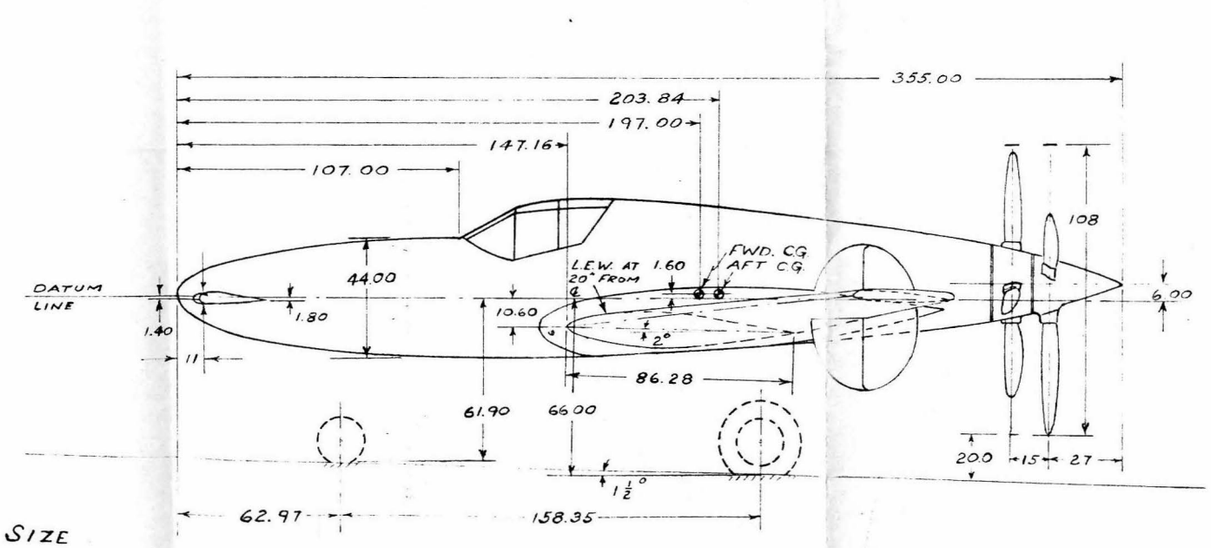

SCALE $\frac{1}{50}$ SIZE

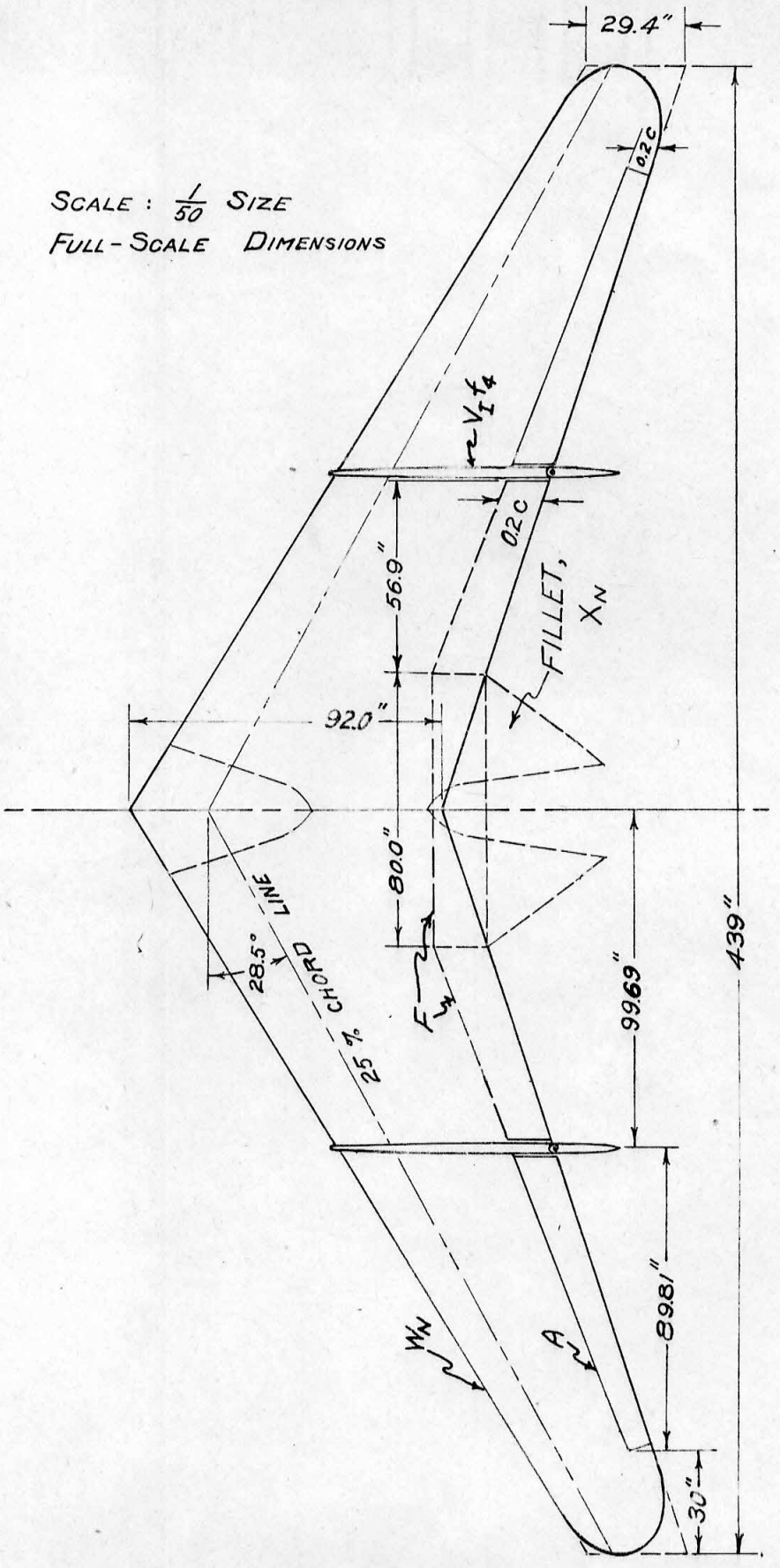

SKETCH SHOWING WING AND COMPONENTS

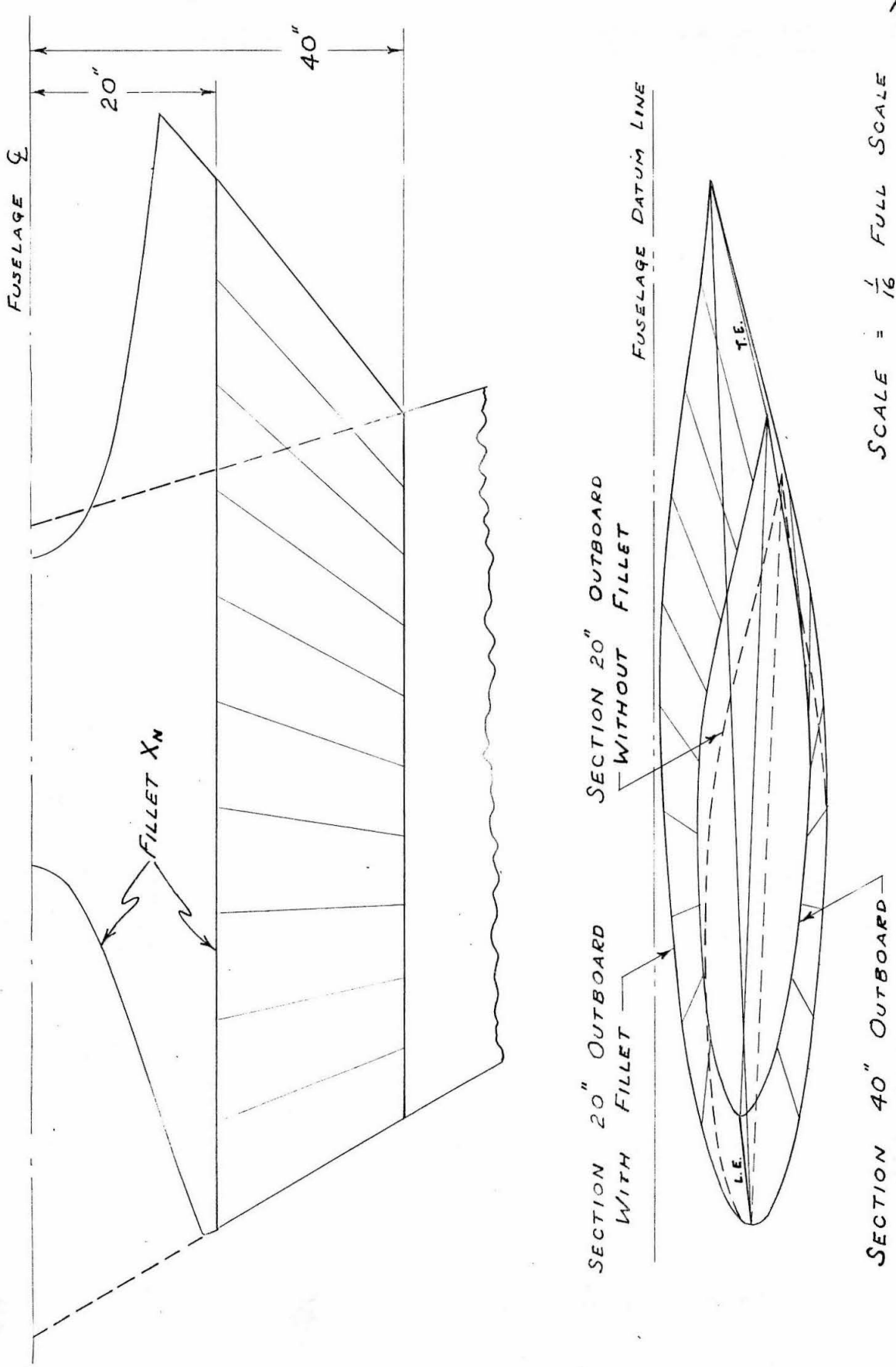

SKETCH SHOWING WING PROFILES AND FILLET X_N

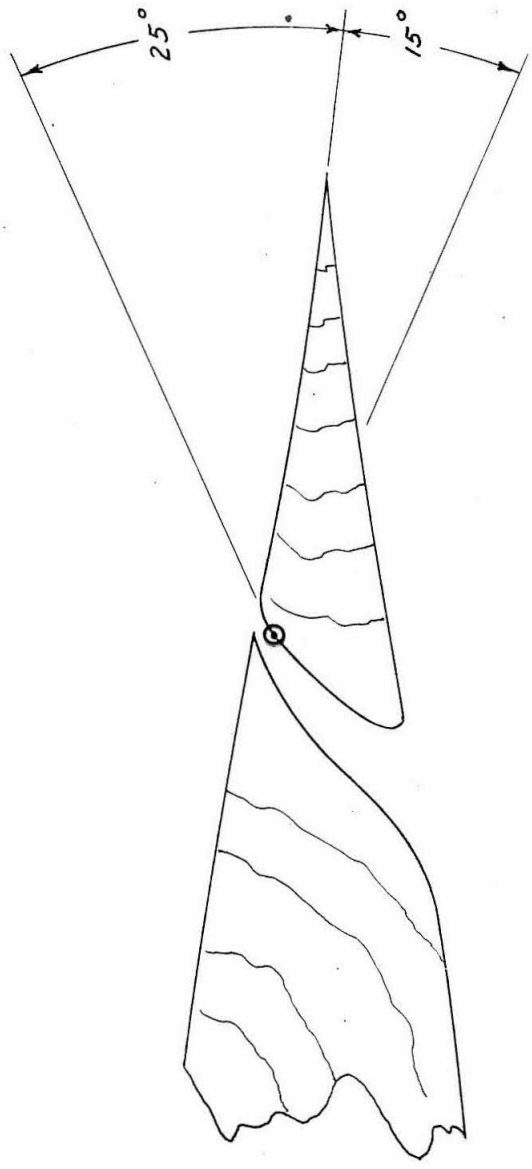

MEAN CHORD AFT OF HINGE LINE = 0.83 FT.

SKETCH OF AILERON CROSS-SECTION

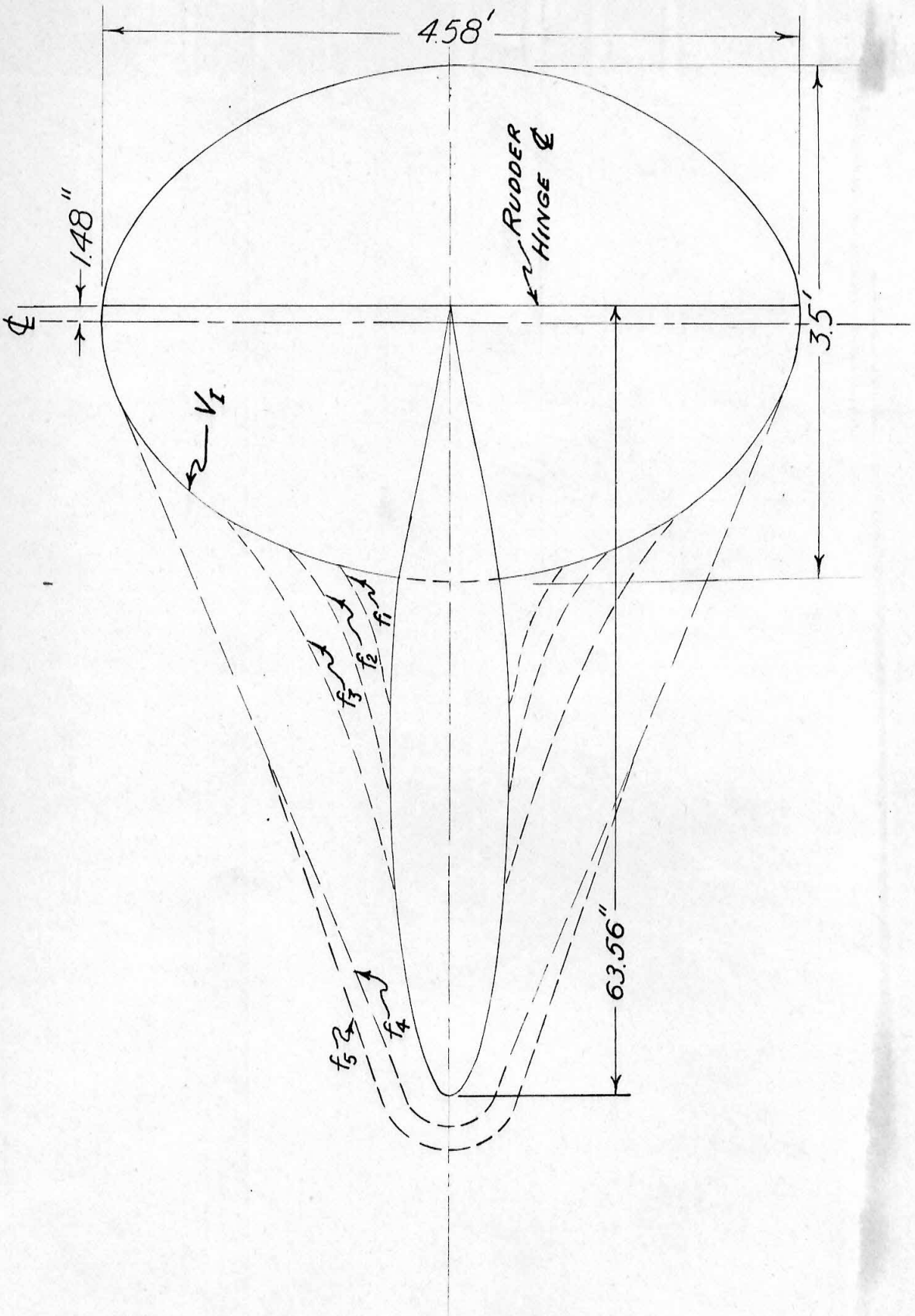

SKETCH OF VERTICAL SURFACES AND VARIOUS FAIRINGS

SKETCH SHOWING VARIOUS SPOILERS

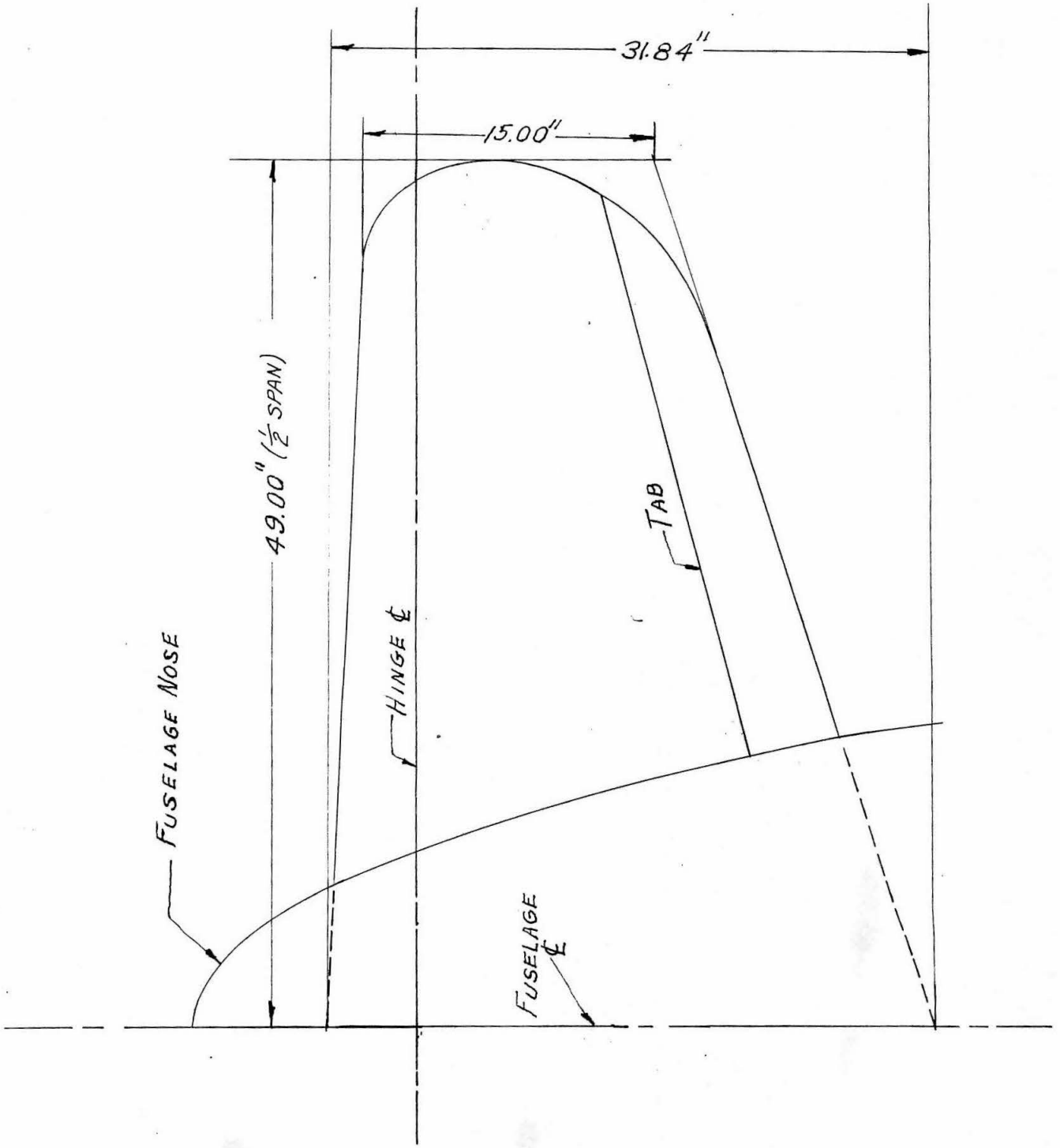

SKETCH SHOWING HORIZONTAL SURFACE H,

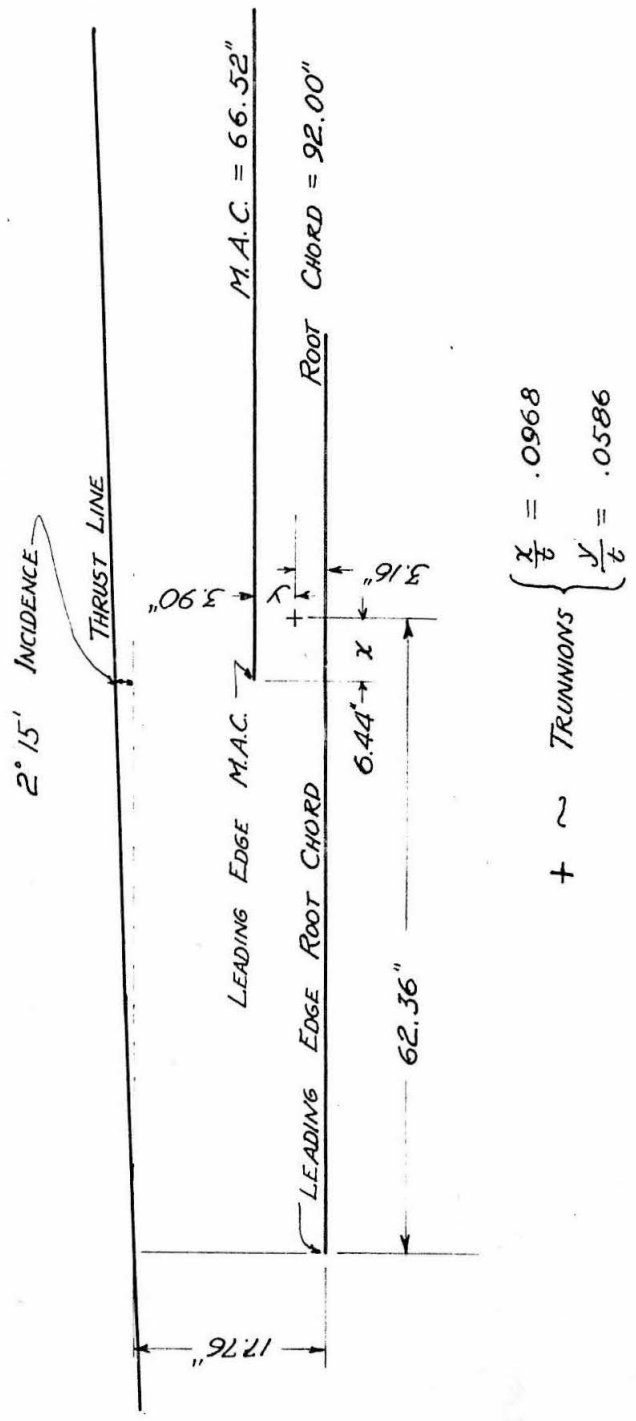

MOMENT AXIS DIAGRAM

VERTICAL SECTION THROUGH 10 FT. WIND TUNNEL

GUGGENHEIM AERONAUTICS LABORATORY
CALIFORNIA INSTITUTE OF TECHNOLOGY, PASADENA

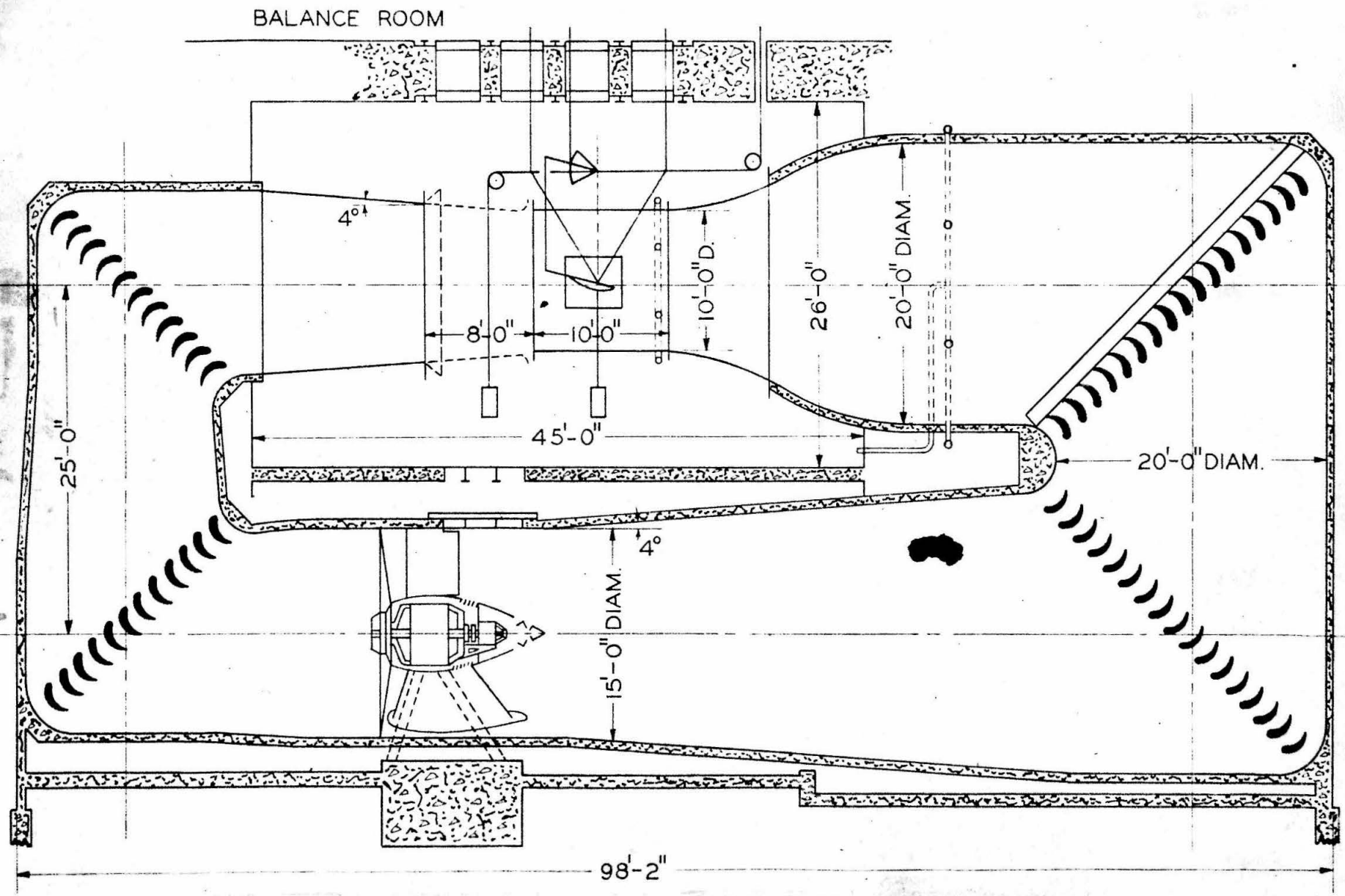

FIG 5

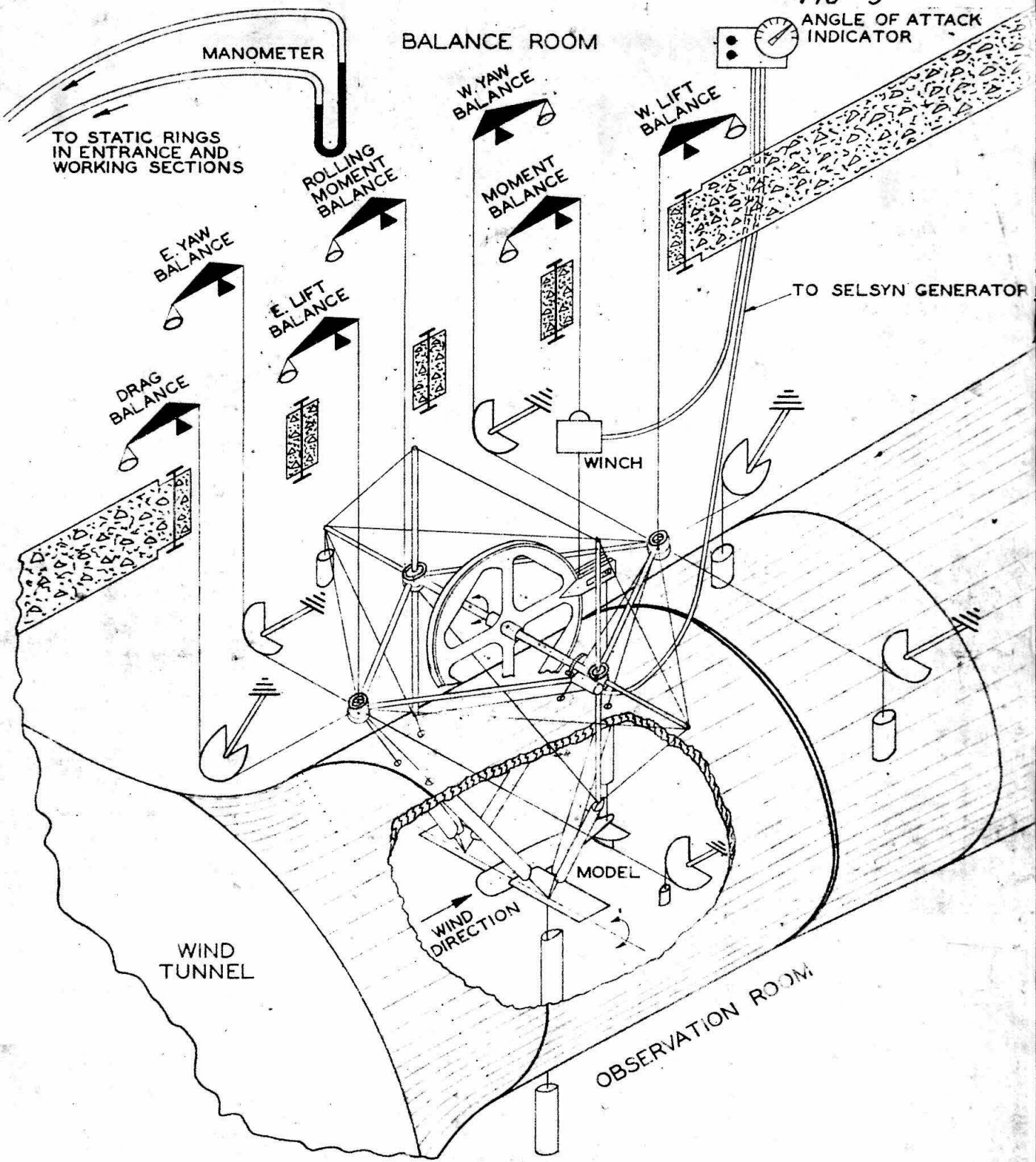

SIX COMPONENT SETUP FOR TEN FOOT WIND TUNNEL TESTS
AT GUGGENHEIM AERONAUTICS LABORATORY
CALIFORNIA INSTITUTE OF TECHNOLOGY

FIG.

DWG. WT 26

CURTISS WRIGHT 101330 DESIGN (NACA 16 SECTIONS)

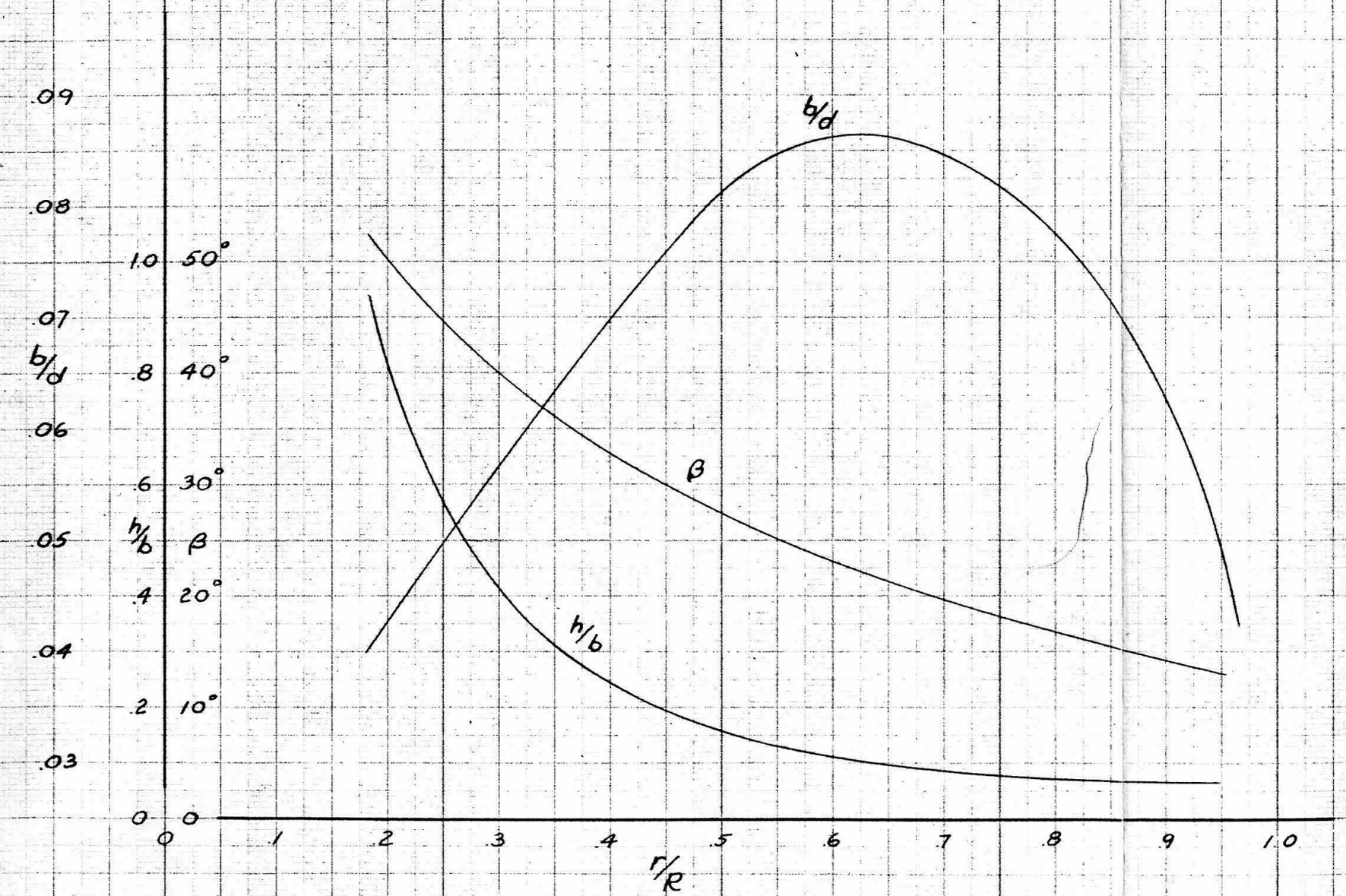

PROPELLER BLADE FORM CHARACTERISTICS

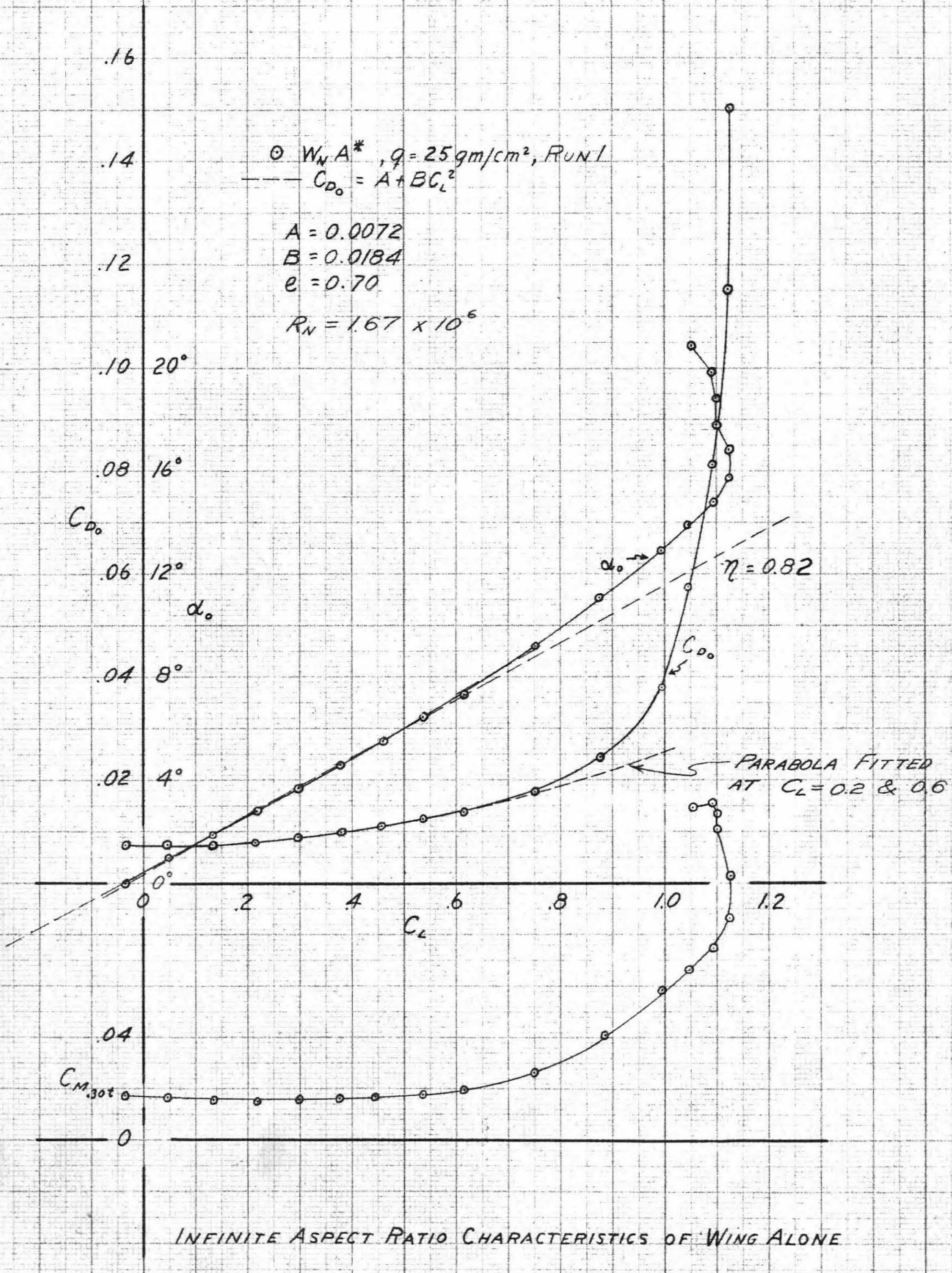

INFINITE ASPECT RATIO CHARACTERISTICS OF WING ALONE

$q = 25\ gm/cm^2$, $\alpha_T = \alpha_E = 0°$

○ $W_N A^*$, RUN 1
△ $W_N A^*$ + WING TUFTS , " 2 (SEE FIG. 23)
□ $W_N A^* V_t$ + WING TUFTS, $r = 0°$, " 3 (" " 24)
⊽ $W_N A V_t$ + " " , " , " 4 (" " 25)

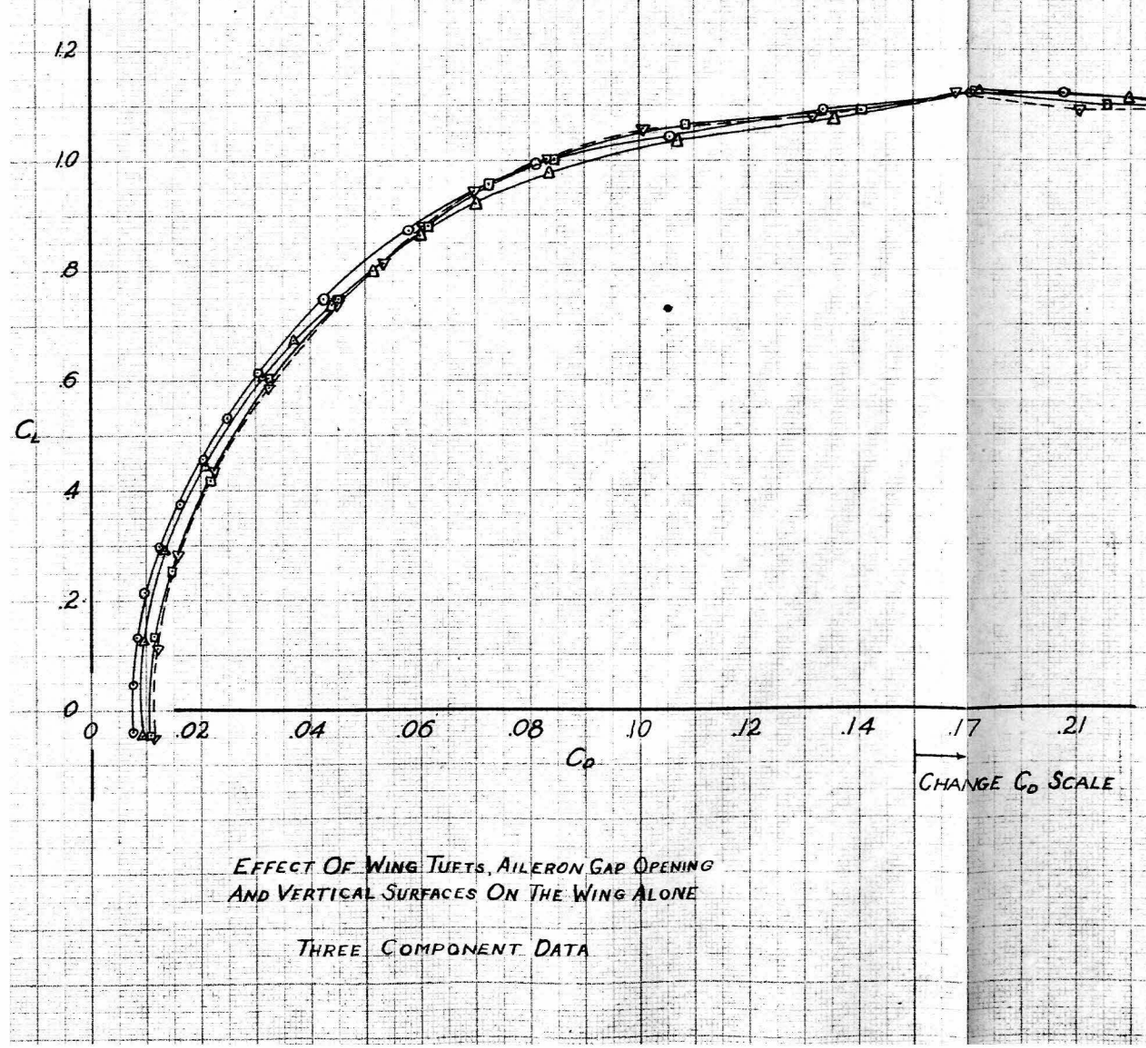

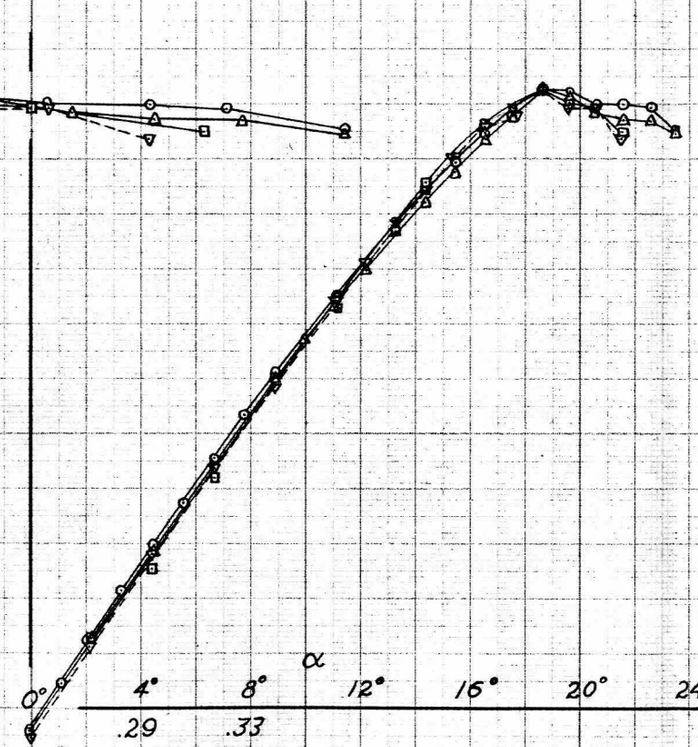

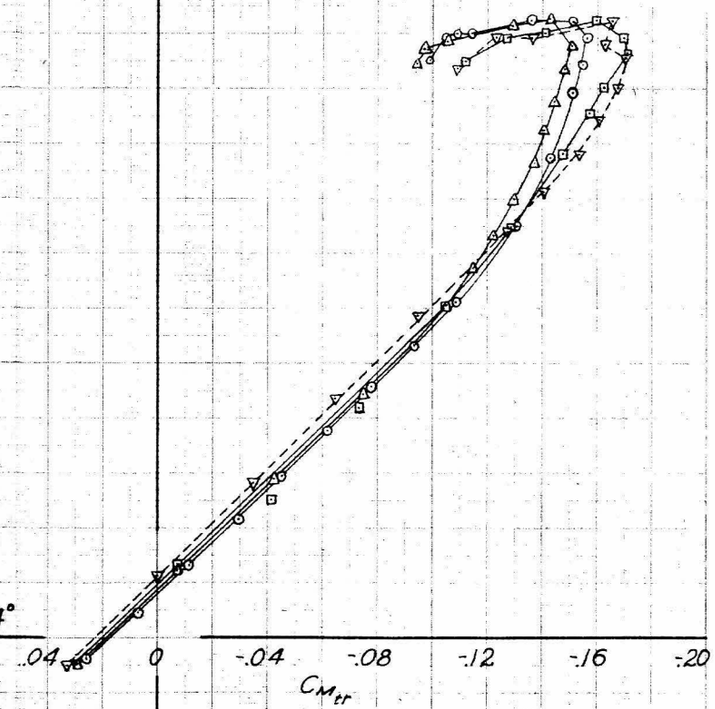

EFFECT OF WING TUFTS, AILERON GAP OPENING AND VERTICAL SURFACES ON THE WING ALONE

THREE COMPONENT DATA

$q = 25\ gm/cm^2$
$a_f = a_e = 0°$

○	$W_N A^*$ + WING TUFTS,	RUN 2 (SEE FIG. 23)
△	$W_N A^* V_1$ + " " , $r = 0°$,	" 3 (" " 24)
□	$W_N A^* V_1 B_N D$, " , $i = 2.25°$,	" 13
▽	" + WING TUFTS, " , " ,	" 14 (SEE FIG. 36)
◇	$W_N A^* V_1 X_N B_N D$ + " " , " , " ,	" 15 (" " 37)
×	$W_N A^* V_1 X_N B_N D f_4$ + " " , " , " ,	" 16 (" " 38)
+	$W_N A V_1 X_N B_N D f_4$ + " " , " , " ,	" 17 (" " 39)

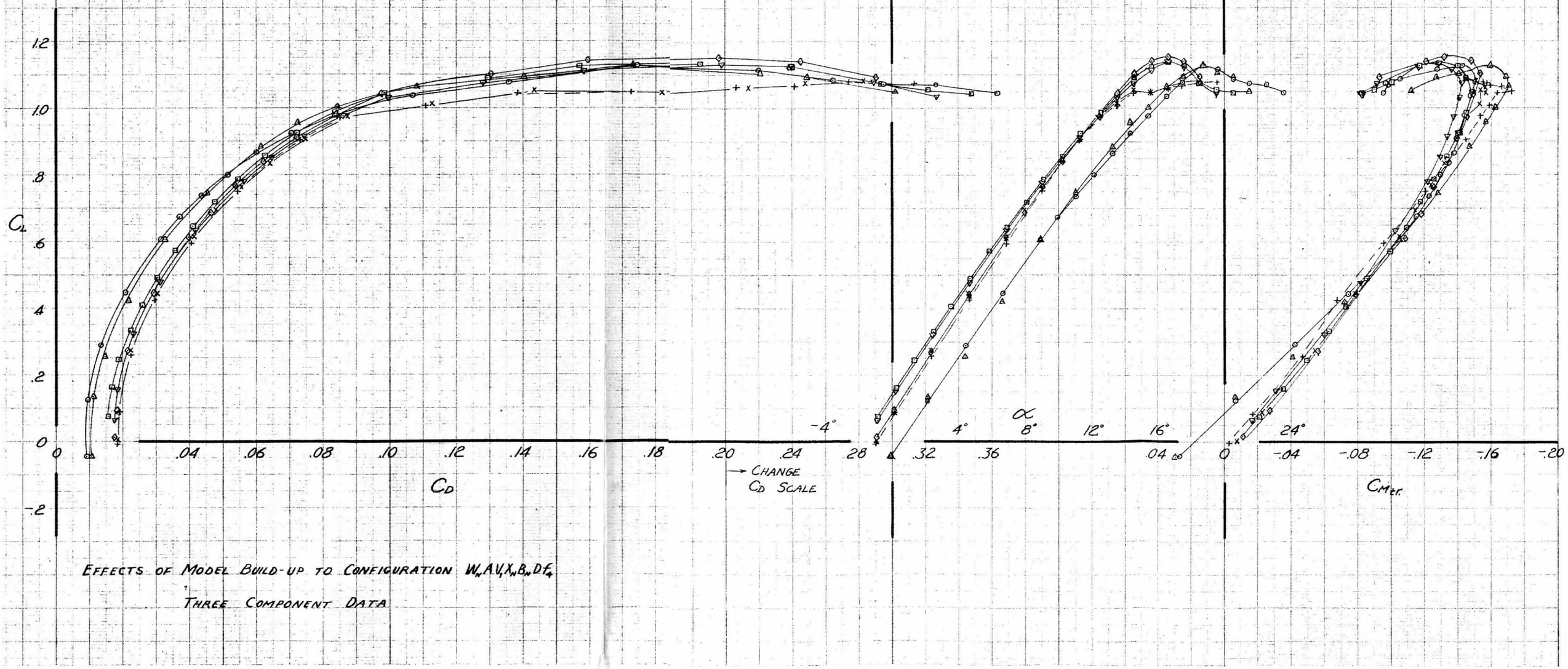

EFFECTS OF MODEL BUILD-UP TO CONFIGURATION $W_N A V_1 X_N B_N D f_4$

THREE COMPONENT DATA

$q = 25\ gm/cm^2$, $a_r = a_l = 0°$

○	$W_N A^*$		RUN 1
X	" $+ V_I B_N D$	$i = 2.25°$, $r = 0°$,	" 13
△	" $+ V_I B_N P^{30}_{FLW} P^{30}_{RRW}$	" " "	" 12
□	" $+ V_I f_w B_N D X_N$	" " "	" 21
▽	" $+ V_I f_w B_N X_N P^{30}_{RRW}$	" " "	" 22
◇	" $+ V_I X_N B_N D$ + WING TUFTS	" " "	" 15 (SEE FIG. 37)
▽	" $+ V_I B_N X_N P^{30}_{RRW} f_4$ + WING TUFTS	" " "	" 31 (" " 46)

FOR P^{30}_{FLW} P^{30}_{RRW} AND P^{30}_{RRW}, $J = 1.59$

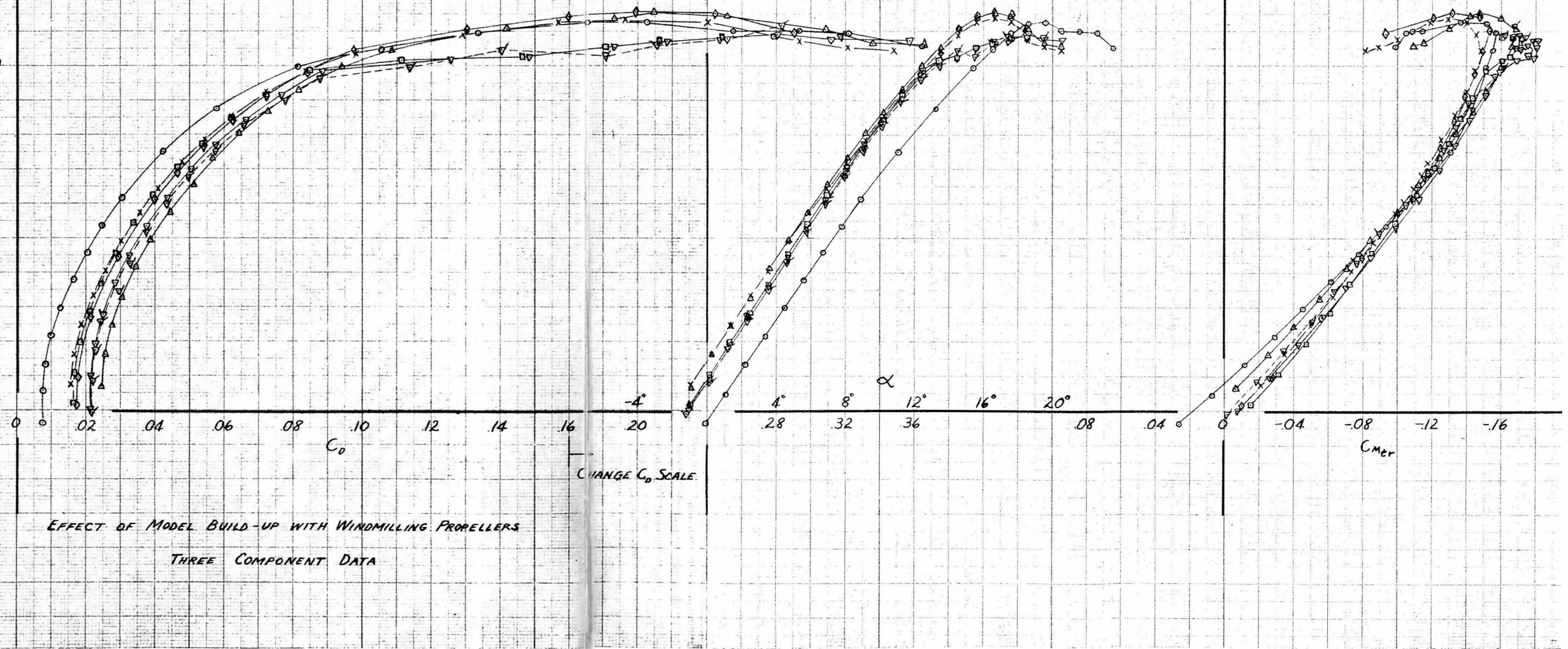

EFFECT OF MODEL BUILD-UP WITH WINDMILLING PROPELLERS

THREE COMPONENT DATA

FIG. 11

$q = 25 gm./cm^2$, $a_r = a_l = 0°$

○	$W_N A^*$	RUN 1
×	" $+V_I B_N D$	$i = 2.25°, r = 0°$, " 13
△	" $+V_I B_N P_{FLW}^{30} P_{RRW}^{30}$	" " " " 12
□	" $+V_I f_4 B_N D X_N$	" " " " 21
▽	" $+V_I f_4 B_N X_N P_{RRW}^{30}$	" " " " 22
◇	" $+V_I X_N B_N D$ + WING TUFTS	" " " " 15
▽	" $+V_I B_N X_N P_{RRW}^{30} f_4$ + WING TUFTS	" " " " 31
•	" $+V_I B_N D$ + " "	" " " " 14
+	" $+V_I B_N X_N f_4 H_1 P_{RRW}^{30}, e = e_t = 0°$	" " " " 32

SEE FIG 13

FOR P_{RRW}^{30} AND $P_{FLW}^{30} P_{RRW}^{30}$, $J = 1.59$

C_{D_P}

.030
.025
.020
.015
.010

-1 0 .1 .2 .3 .4 .5 .6 .7 .8

C_L

EFFECT OF MODEL BUILD-UP WITH WINDMILLING PROPELLERS
PARASITE DRAG

$q = 25$ gm/cm.^{2}, $i = 2.25°$, $r = 0°$

- ○ $W_N A^* V_L f_4 B_N X_N P^{30}_{RRW}$, $a_r = a_l = 0°$, RUN 22
- △ $W_N A^* V_L f_4 B_N X_N P^{30}_{RRW} F^{45}$, " " " 23
- □ $W_N A V_L f_4 B_N X_N P^{30}_{RRW} F^{45}$, " " " 24
- ▽ $W_N A^* V_L f_4 B_N X_N P^{30}_{RRW} F^{45}$ + WING TUFTS, $a_r = a_l = -10°$, " 26 (SEE FIG. 55)
- ◇ $W_N A V_L f_4 B_N X_N P^{30}_{RRW} F^{45}$, " " " 25
- × $W_N A^* V_L B_N X_N L L_N P^{30}_{RRW} F^{45}_{f_4}$ + " " " " " 27
- ⊘ $W_N A^* V_L B_N X_N P^{30}_{RRW} f_4$ + WING TUFTS, $a_r = a_l = 0°$, " 31
- • $W_N A^* V_L B_N X_N L L_N P^{30}_{RRW} f_4 F^{45}$ + " " " " " 29 (SEE FIG. 53)
- + $W_N A^* V_L B_N X_N L L_N P^{30}_{RRW} F^{45}$ + " " " " " 30 (" " 52)

FOR P^{30}_{RRW}, $J = 1.59$

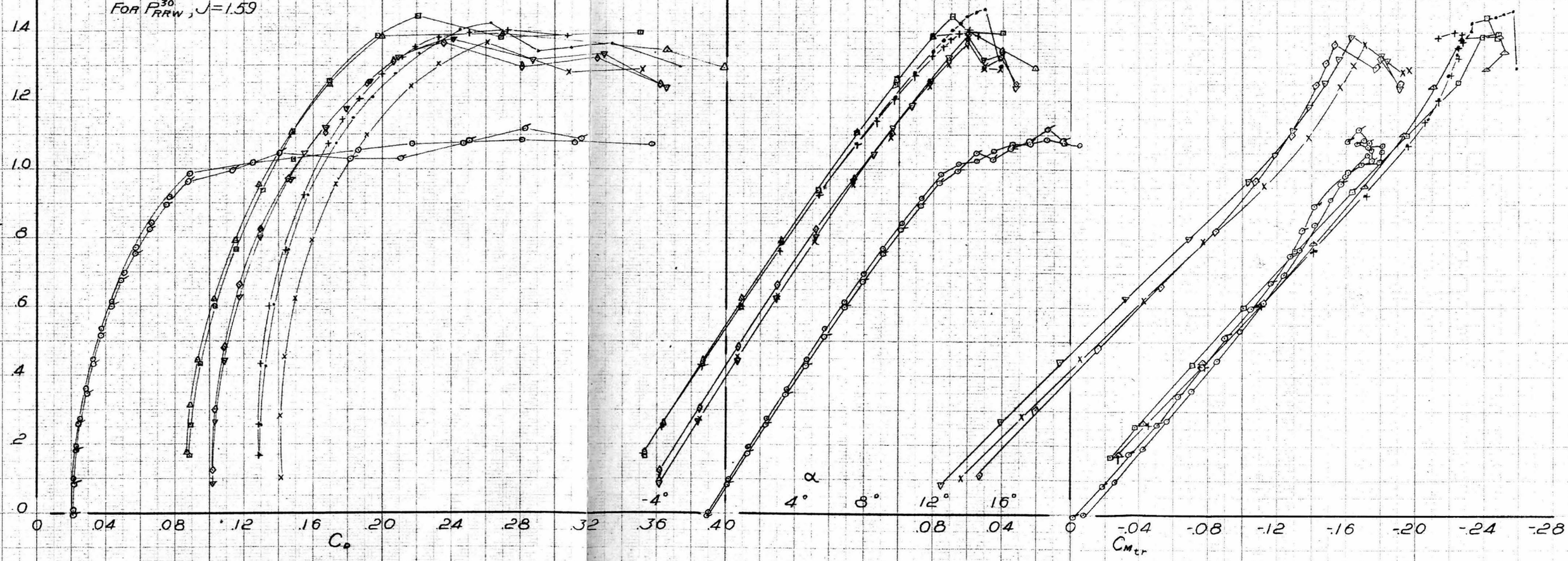

EFFECTS OF SPLIT FLAPS DOWN 45°, LANDING GEAR DOWN, AILERON SLOT OPENING, AND f_4 ON CONFIGURATION $W_N A^* V_L B_N X_N P^{30}_{RRW}$ WITH AND WITHOUT UP AILERONS

THREE COMPONENT DATA

$q = 25 gm/cm^2$, $a_r = a_l = r = 0°$, $i = 2.25°$

×	$W_N A^* V_1 \xi_4 B_N X_N P^{30}_{RRW}$	RUN 22
○	$W_N A^* V_1 \xi_4 B_N X_N H_1 P^{30}_{RRW}$, $e_t = 0°$, $e = -10°$,	" 36
△	" , " , $e = -5°$,	" 35
□	" , " , $e = 0°$,	" 32
▽	" , " , $e = +5°$,	" 33
◇	" , " , $e = +10°$,	" 34

FOR P^{30}_{RRW}, $J = 1.59$

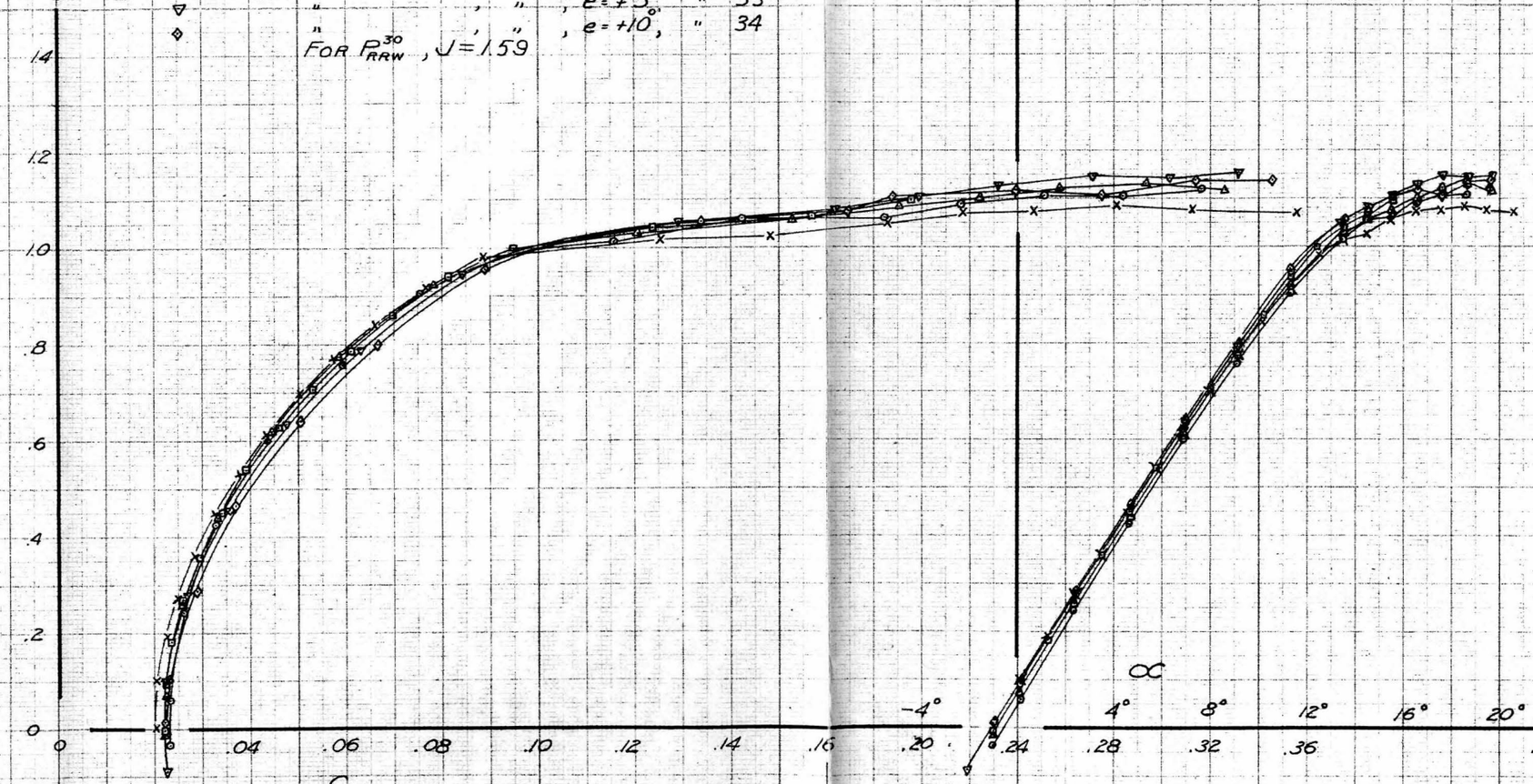

→ CHANGE C_D SCALE

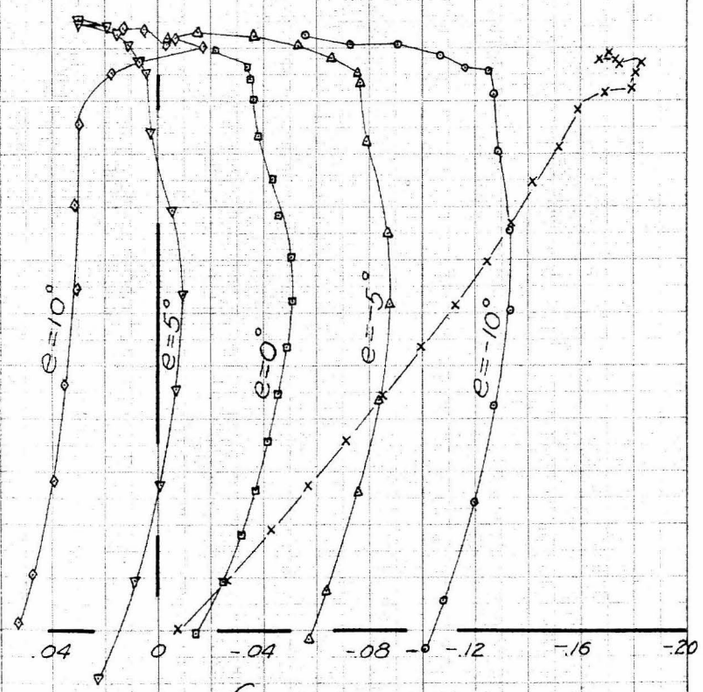

ELEVATOR EFFECTIVENESS WITH COMPLETE MODEL AND WINDMILLING PROPELLER, $e_t = 0°$

THREE COMPONENT DATA

$q = 25 gm/cm^2$; $a_r = a_l = r = e_t = 0°$, $J = 1.59$, $i = 2.25°$

⊙	$W_N A^* V_I B_N X_N f_4 H_1 P_{RRW}^{30}$	$e = -10°$,	RUN 36
△	"	$e = -5°$,	" 35
⊡	"	$e = 0°$,	" 32
▽	"	$e = 5°$,	" 33
◇	"	$e = 10°$,	" 34

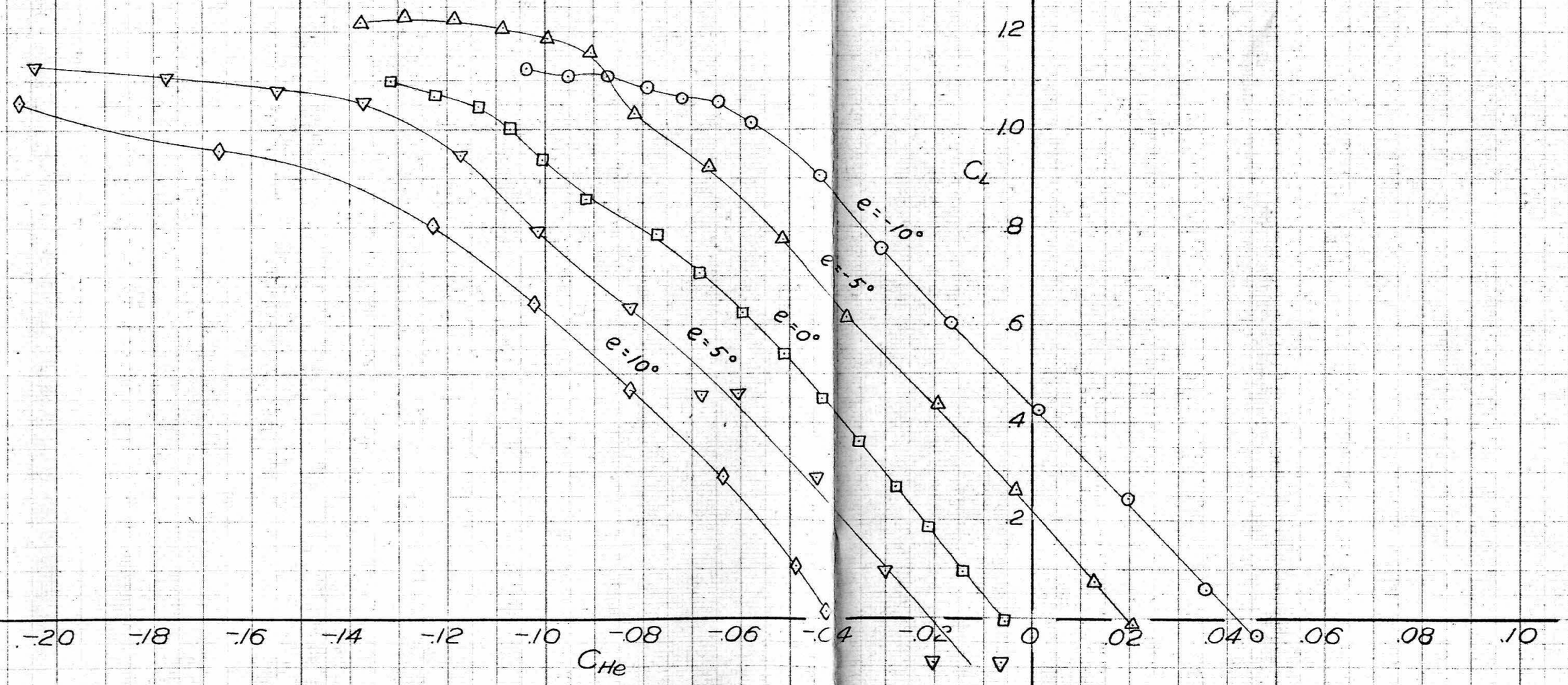

ELEVATOR EFFECTIVENESS WITH COMPLETE MODEL AND WINDMILLING PROPELLER, $e_t = 0°$

ELEVATOR HINGE MOMENTS

$q = 25 gm/cm^2$, $i = 2.25°$, $a_r = a_t = r = 0°$, $J = 1.59$

×	$W_H A^* V_t f_4 B_H X_H P^{30}_{RRW}$,				Run 22
□	"	$+H_1$,	$e = 0°$,	$e_t = -10°$,	" 37
▽	"	+ " ,	$e = 5°$,	$e_t =$ " ,	" 38
◇	"	+ " ,	$e = 10°$,	$e_t =$ " ,	" 39
⊙	"	+ " ,	$e = 0°$,	$e_t = 0°$,	" 32

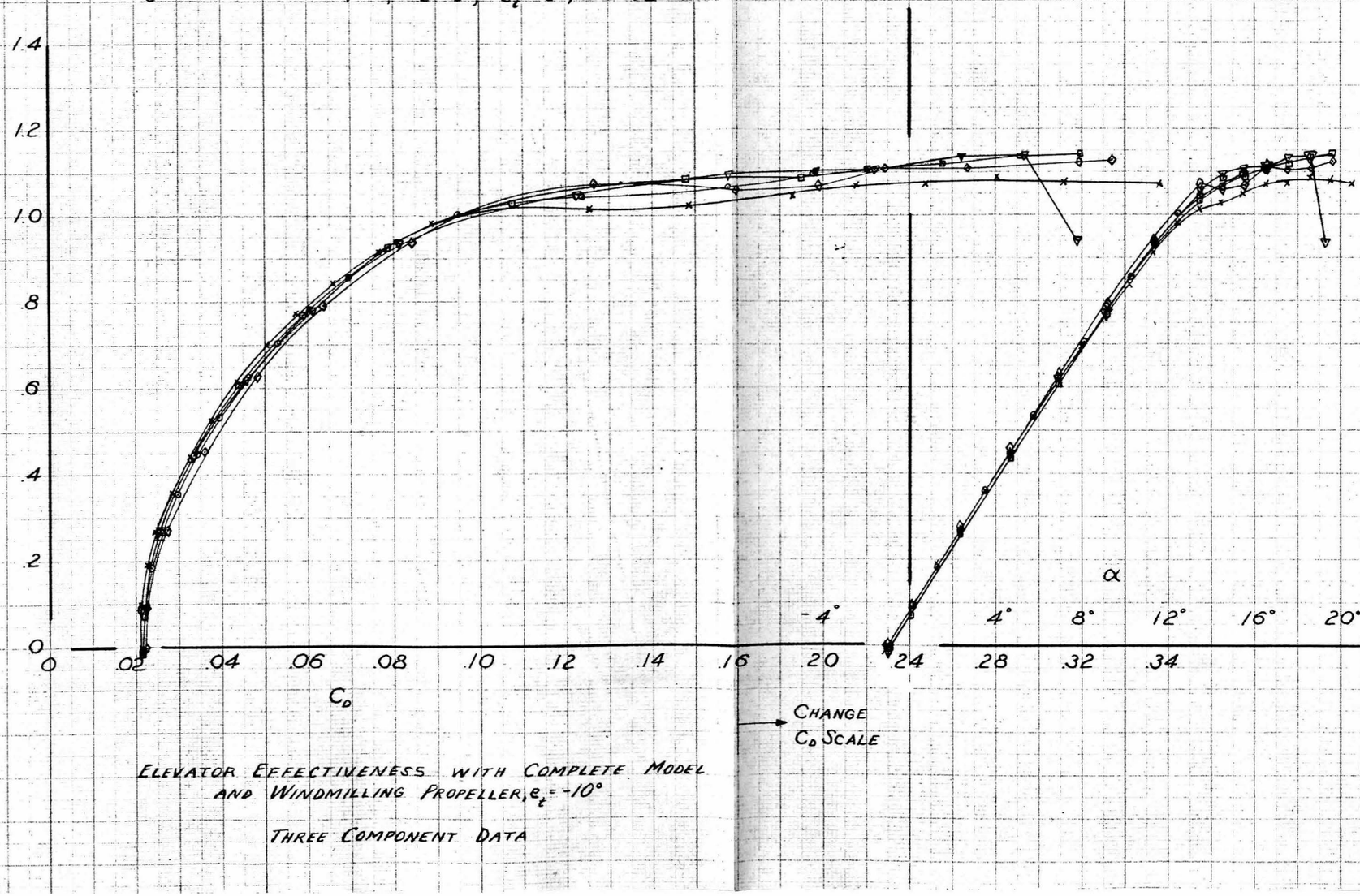

CHANGE C_D SCALE

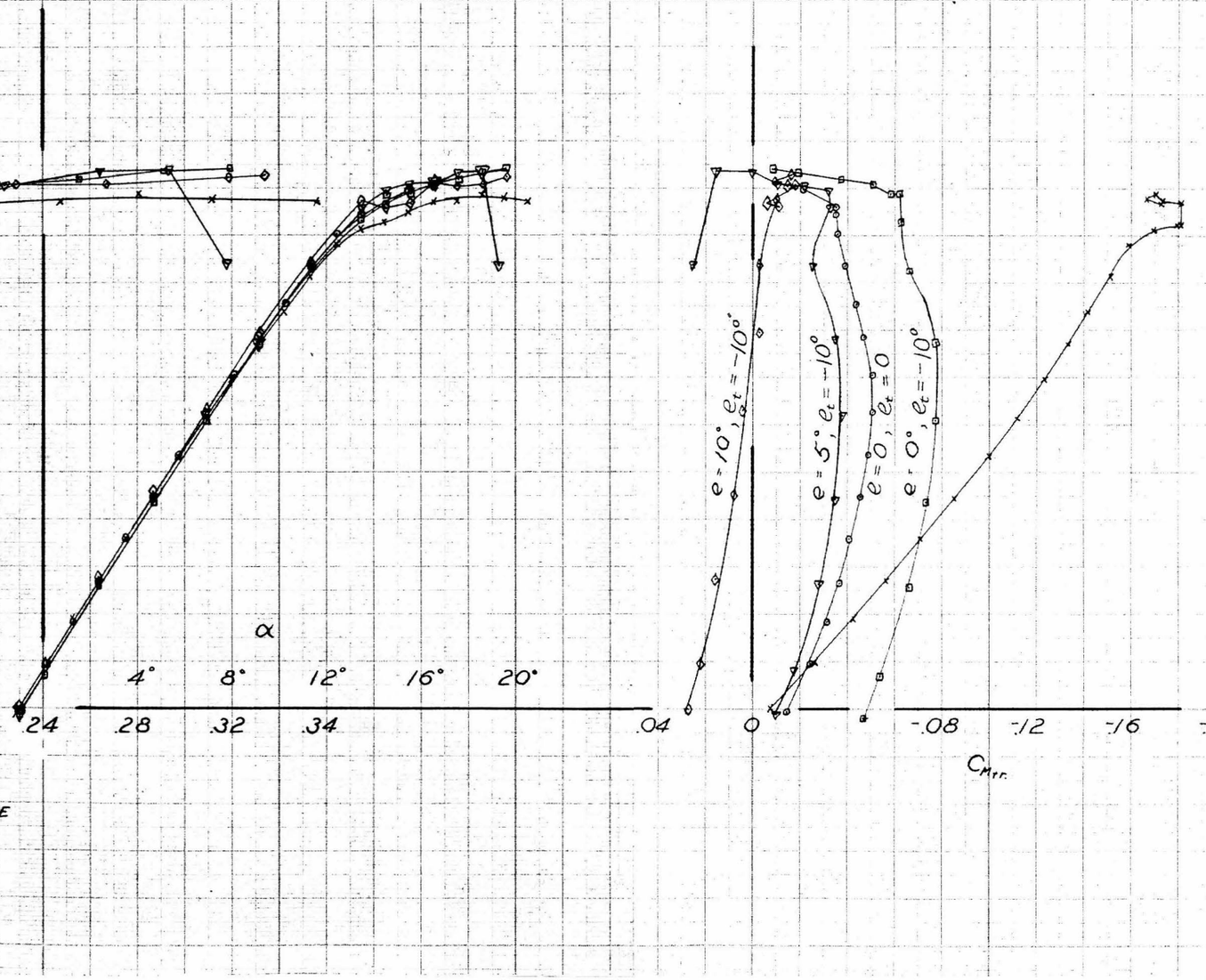

ELEVATOR EFFECTIVENESS WITH COMPLETE MODEL AND WINDMILLING PROPELLER, $e_t = -10°$

THREE COMPONENT DATA

$q = 25\ gm/cm^2$; $a_p = a_t = i_t = 0°$; $J = 1.59$; $\epsilon = 2.25°$

- ○ $W_N A^* V_I B_N X_N f_4 H, P^{30}_{RRW}$, $e = 0°$; $e_t = 0°$; RUN 32
- ⊡ " , " , $e_t = -10°$; " 37
- ▽ " , $e = 5°$, " , " 38
- ◇ " , $e = 10°$, " , " 39

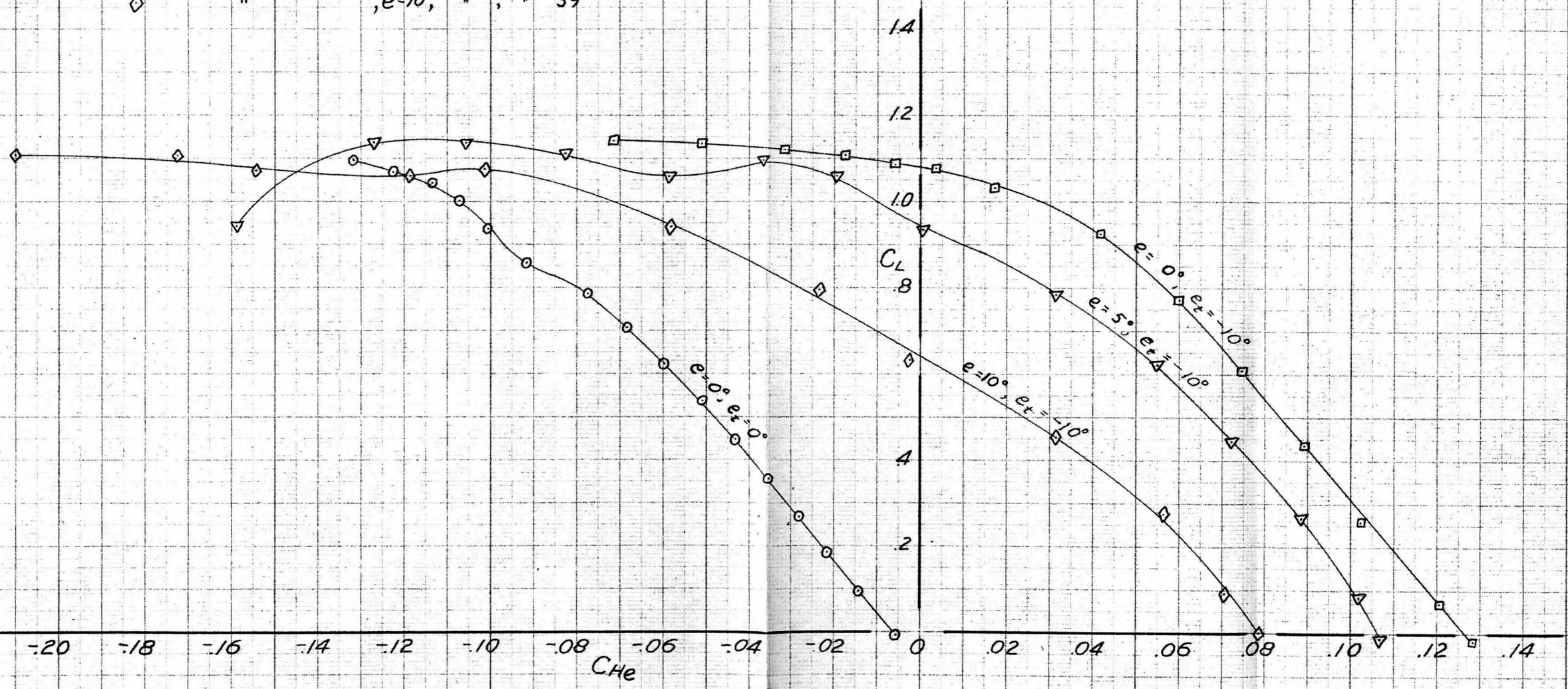

ELEVATOR EFFECTIVENESS WITH COMPLETE MODEL AND WINDMILLING PROPELLER. $e_t = -10°$

ELEVATOR HINGE MOMENTS

$q = 25\ gm/cm^2$, $i = 2.25°$, $\alpha_r = \alpha_l = r = 0°$

×	$W_N A^* V_t f_4 B_N X_N P^{30}_{RRW}$	,	RUN 22
⊡	"	$+H_t$, $e=0°$, $e_t=-15°$,	" 42
▽	"	$+H_t$, $e=5°$, $e_t=-15°$,	" 41
◇	"	$+H_t$, $e=10°$, $e_t=-15°$,	" 40
⊙	"	$+H_t$, $e=0°$, $e_t=0°$,	" 32

FOR P^{30}_{RRW}, $J=1.59$

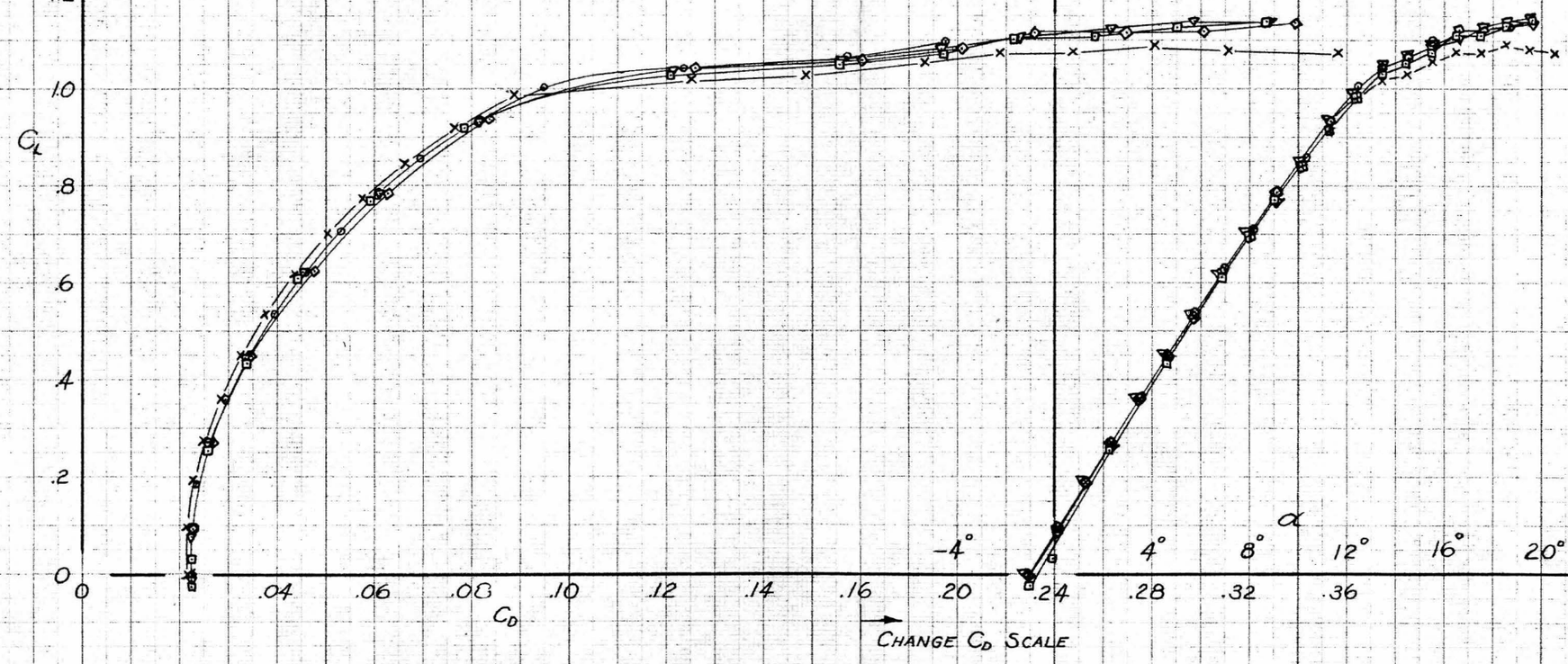

ELEVATOR EFFECTIVENESS WITH COMPLETE MODEL AND WINDMILLING PROPELLER, $e_t = -15°$

THREE COMPONENT DATA

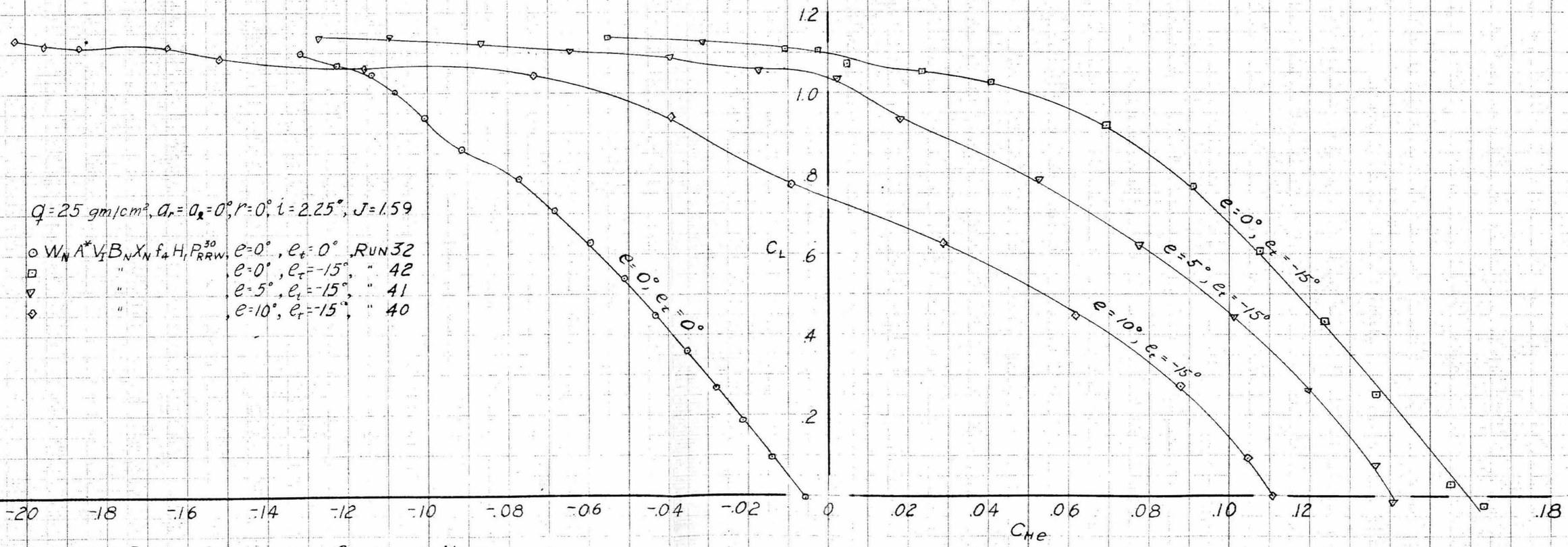

ELEVATOR EFFECTIVENESS WITH COMPLETE MODEL AND WINDMILLING PROPELLER, $e_t = -15°$

ELEVATOR HINGE MOMENTS

$q = 25$ gm/cm², $i = 2.25°$, $\alpha_t = \alpha_0 = r = 0°$

× $W_N A^* V_1 f_4 B_N X_N P^{30}_{RRW}$, Run 22

□ " + H_1, $e = 0°$, $e_t = 0°$, 32

◇ " + ", e = FREE, $e_t = 0°$, 43

FOR P^{30}_{RRW}, $J = 1.59$

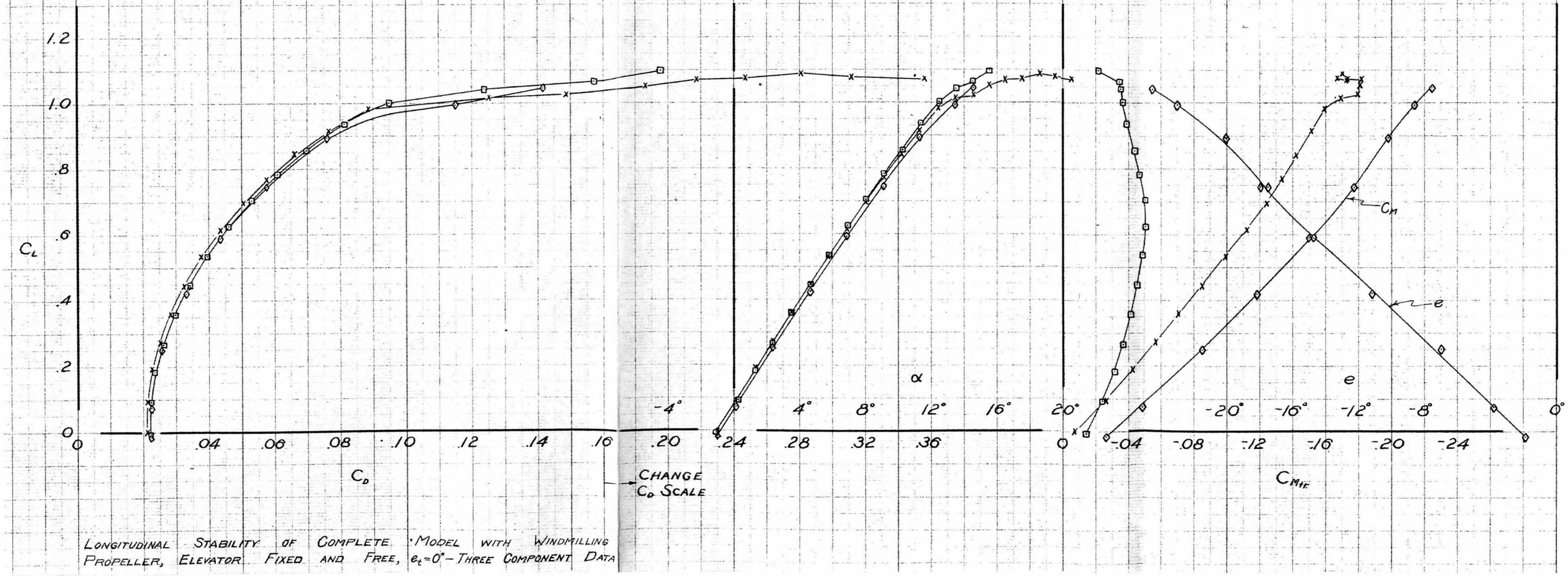

LONGITUDINAL STABILITY OF COMPLETE MODEL WITH WINDMILLING PROPELLER, ELEVATOR FIXED AND FREE, $e_t = 0°$ – THREE COMPONENT DATA

BASIC CONFIGURATION: $W_N A^* V_I f_4 B_N X_N P_{RRW}^{30}$
$q = 25$ gm./cm.^{2}; $i = 2.25°$; $a_r = a_e = r = 0°$

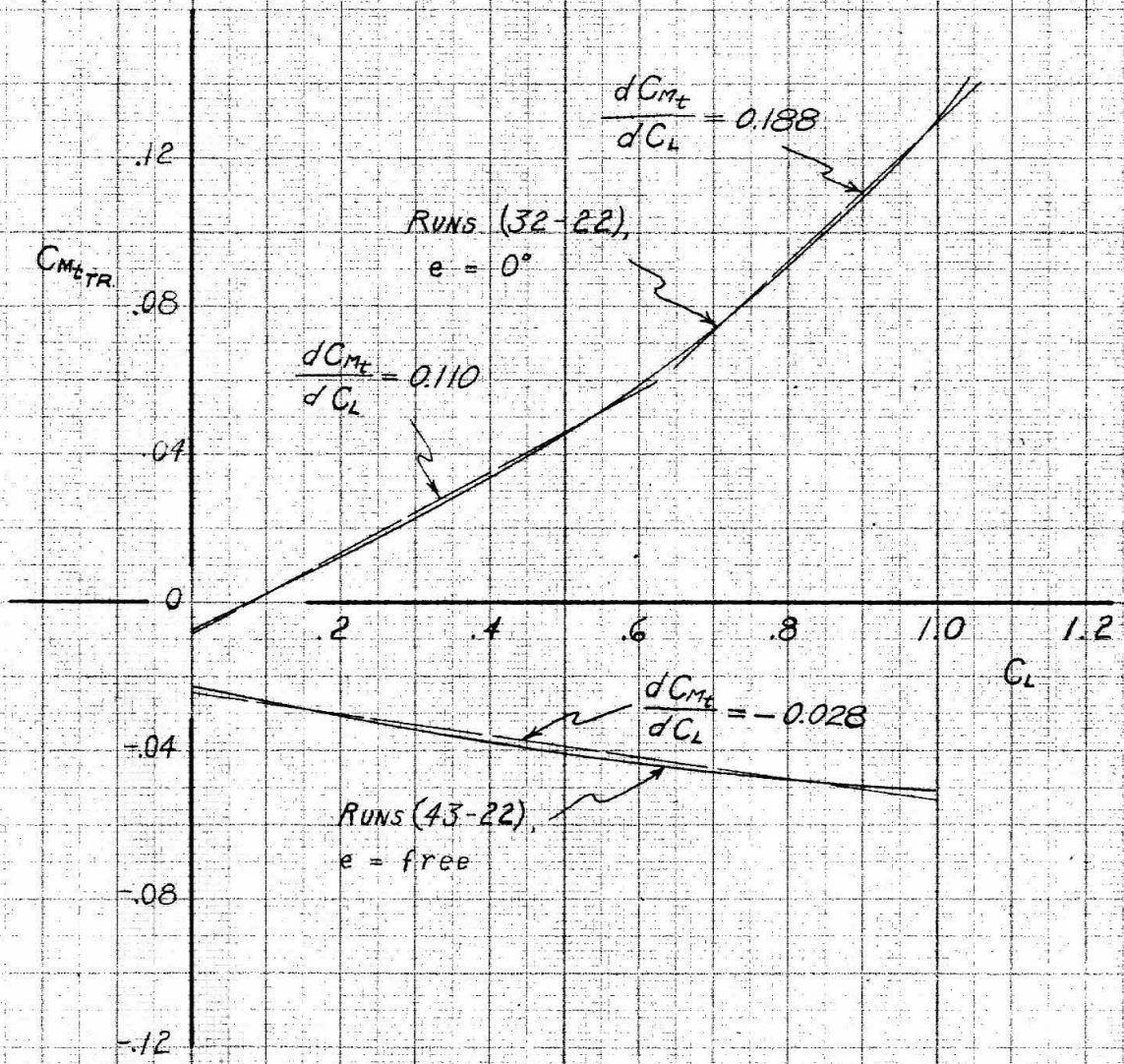

PITCHING MOMENTS DUE TO HORIZONTAL TAIL H_1

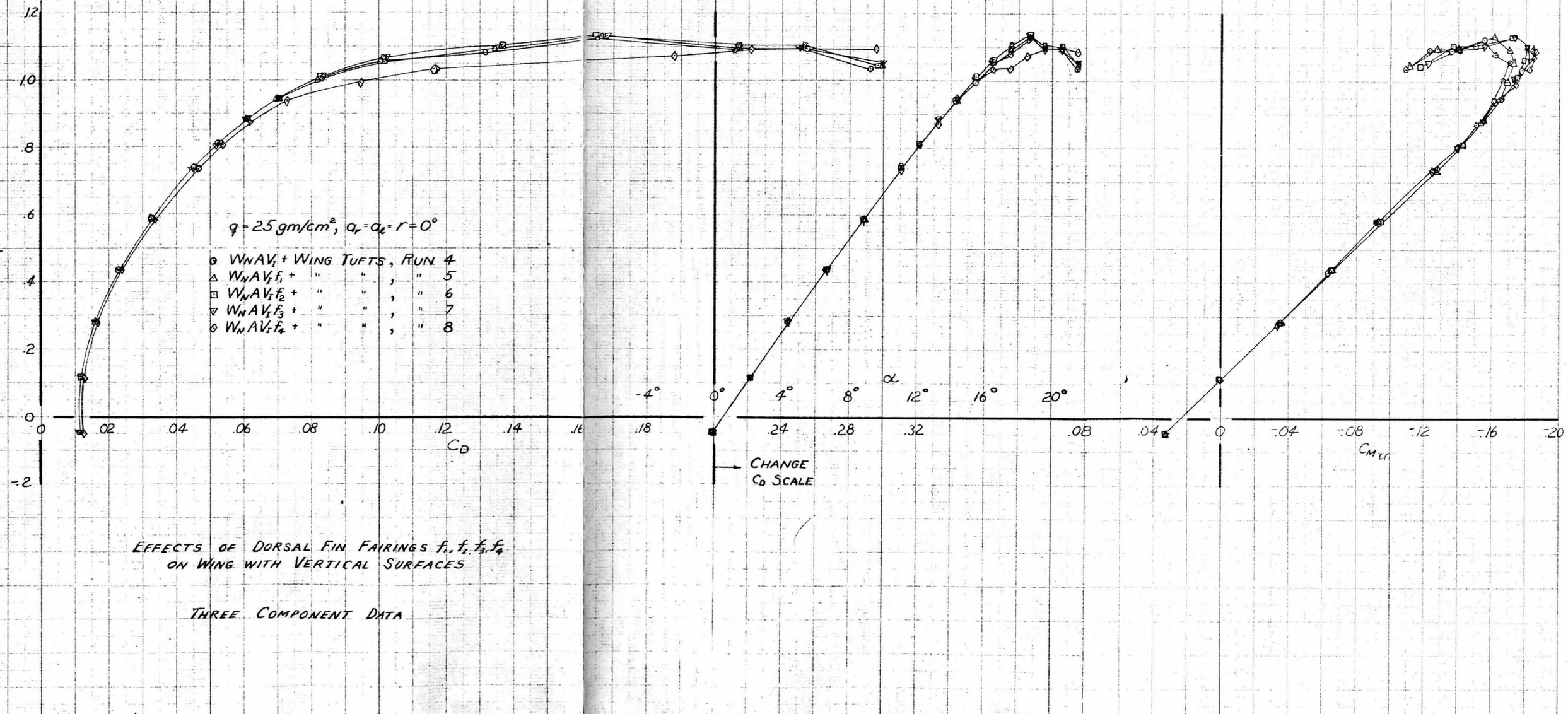

EFFECTS OF DORSAL FIN FAIRINGS f_1, f_2, f_3, f_4
ON WING WITH VERTICAL SURFACES

THREE COMPONENT DATA

FIG 22

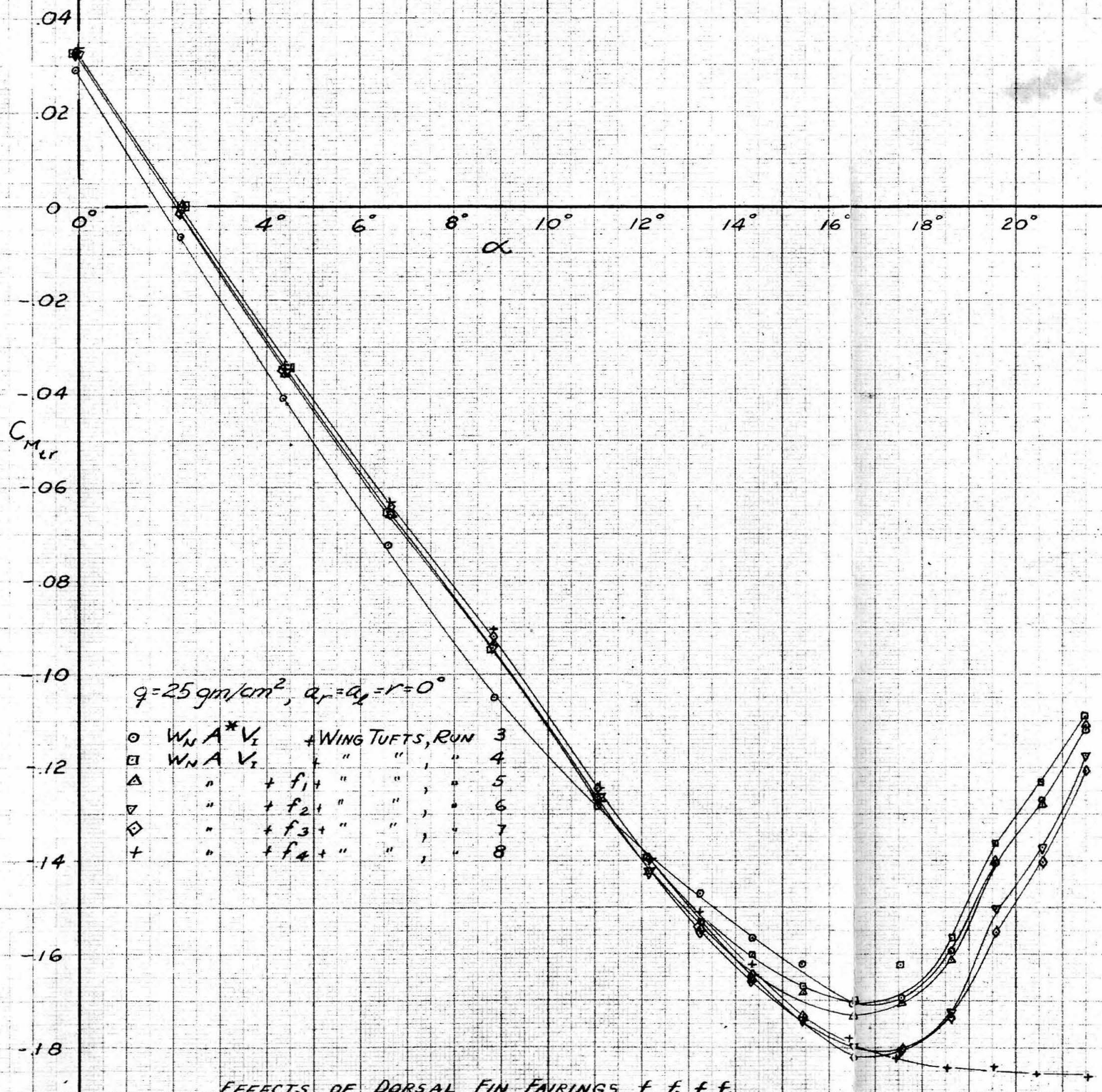

EFFECTS OF DORSAL FIN FAIRINGS f_1, f_2, f_3, f_4 ON WING WITH VERTICAL SURFACES

PITCHING MOMENT VS α

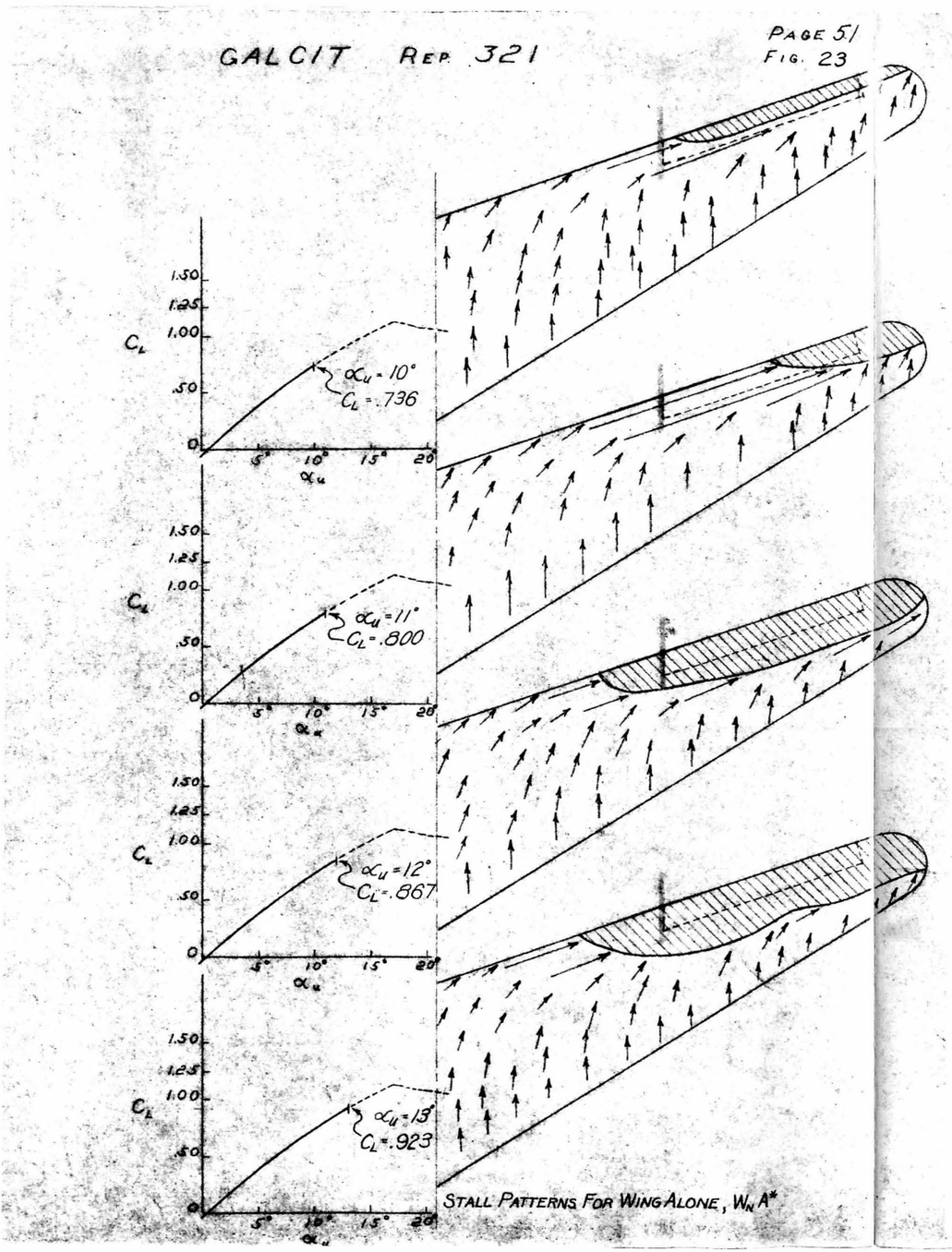

STALL PATTERNS FOR WING ALONE, $W_N A^*$

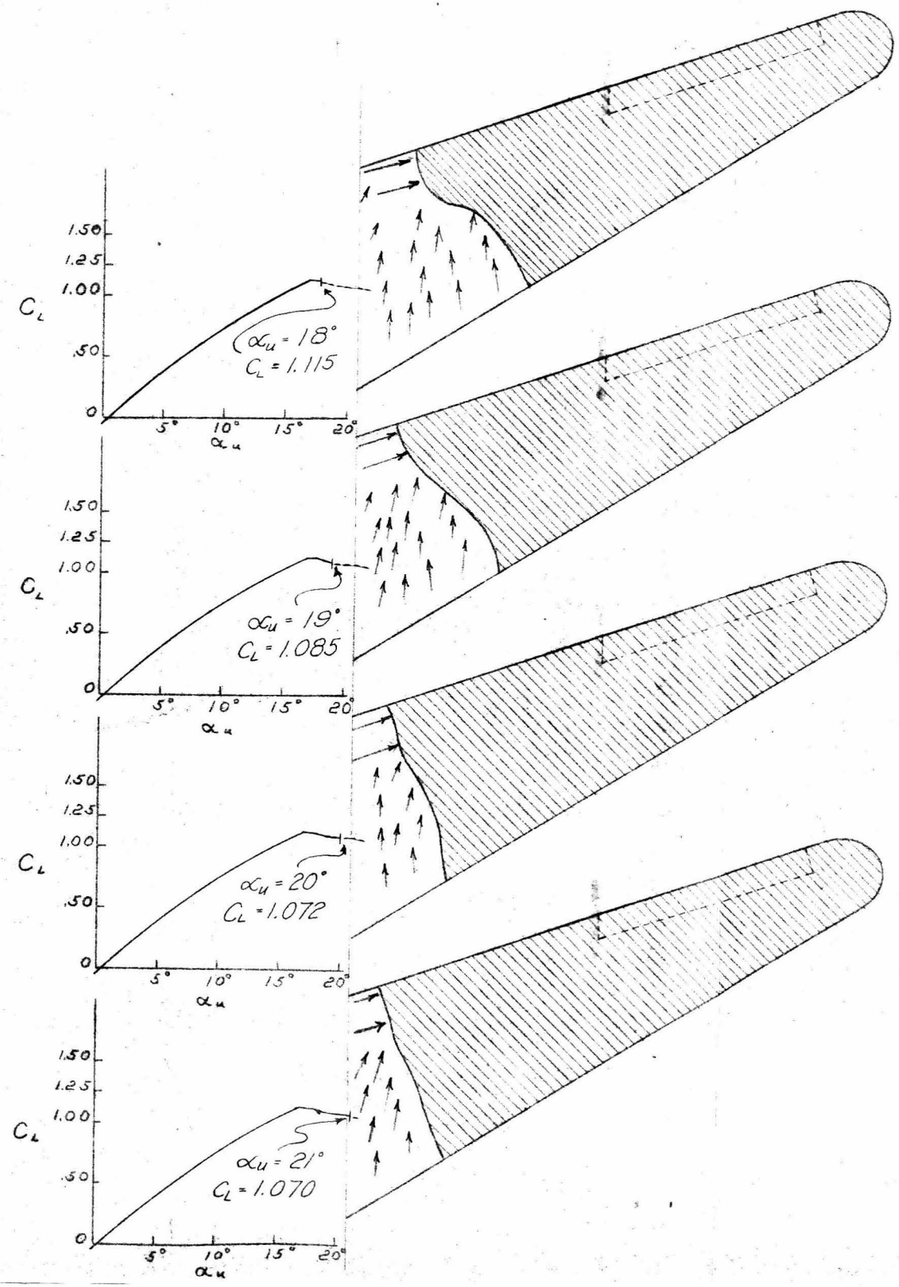

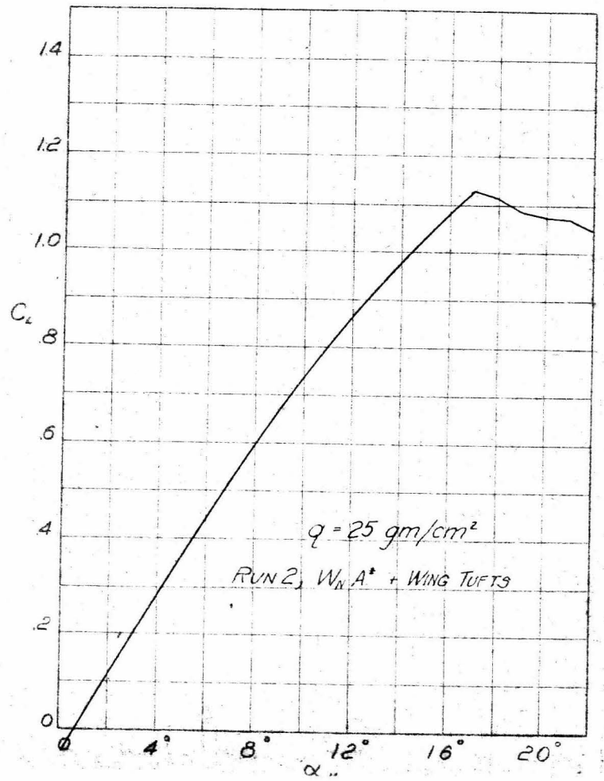

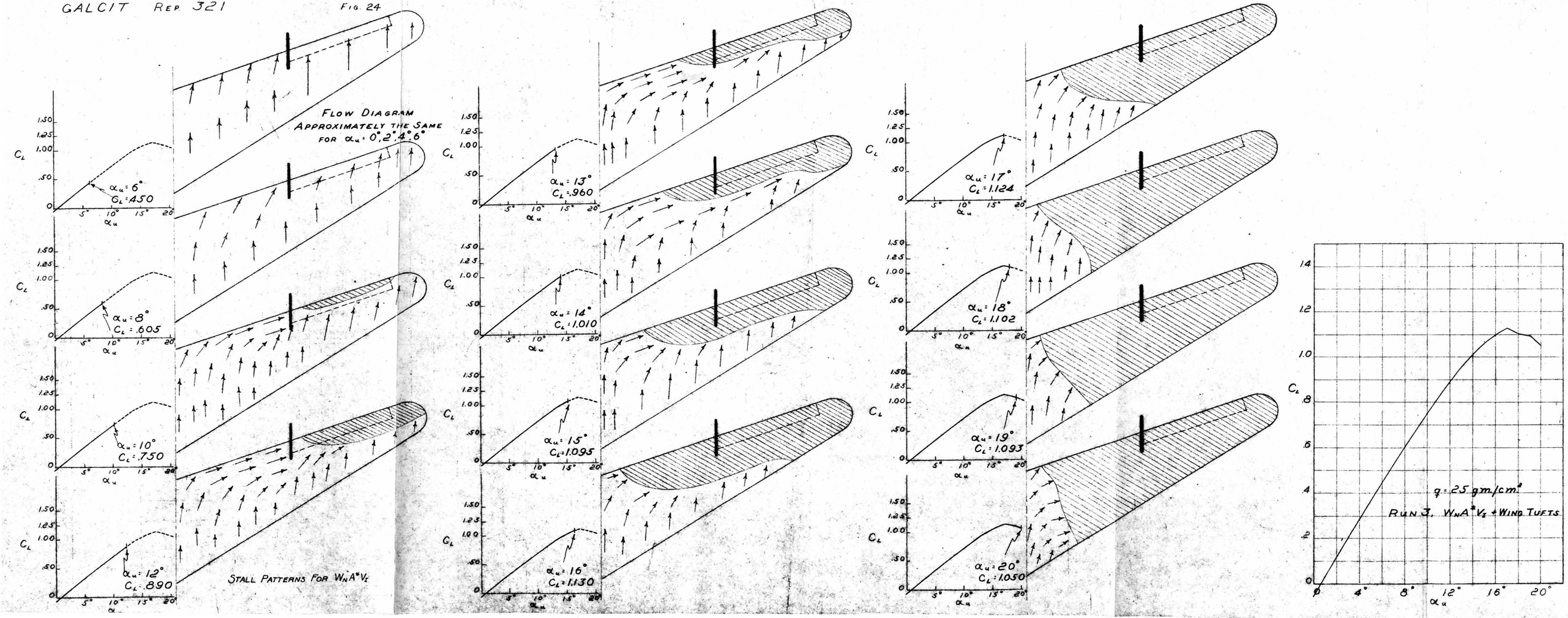
FLOW DIAGRAM
APPROXIMATELY THE SAME
FOR $\alpha_u = 0°, 2°, 4°, 6°$
$\alpha_u = 6°$
$C_L = .450$
$\alpha_u = 8°$
$C_L = .605$
$\alpha_u = 10°$
$C_L = .750$
$\alpha_u = 12°$
$C_L = .890$
$\alpha_u = 13°$
$C_L = .960$
$\alpha_u = 14°$
$C_L = 1.010$
$\alpha_u = 15°$
$C_L = 1.095$
$\alpha_u = 16°$
$C_L = 1.130$
$\alpha_u = 17°$
$C_L = 1.124$
$\alpha_u = 18°$
$C_L = 1.102$
$\alpha_u = 19°$
$C_L = 1.093$
$\alpha_u = 20°$
$C_L = 1.050$
C_L
α_u
STALL PATTERNS FOR $W_N A^* V_f$

C_L
α_u
$q = 25$ gm./cm²
RUN 3. $W_N A^* V_f$ + WIND TUFTS

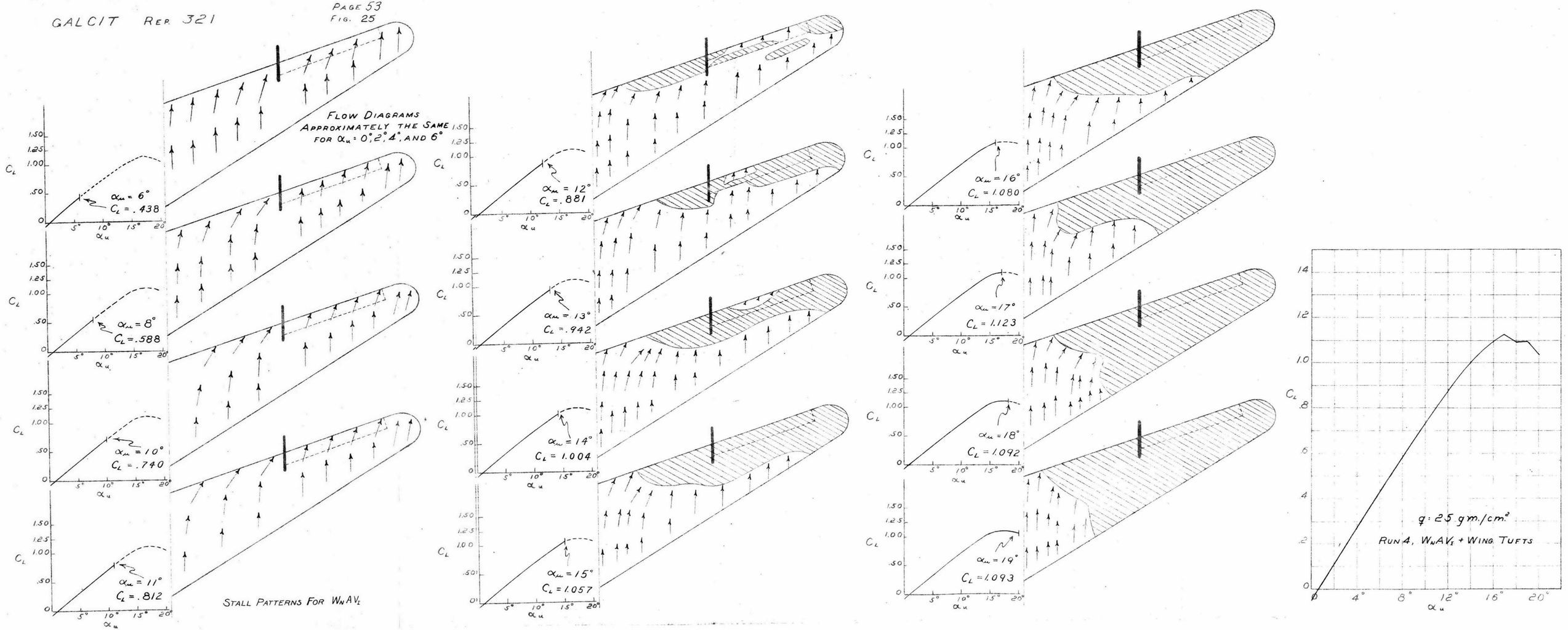
FLOW DIAGRAMS
APPROXIMATELY THE SAME
FOR $\alpha_u = 0°, 2°, 4°$, AND 6°
$\alpha_u = 6°$
$C_L = .438$
$\alpha_u = 8°$
$C_L = .588$
$\alpha_u = 10°$
$C_L = .740$
$\alpha_u = 11°$
$C_L = .812$
$\alpha_u = 12°$
$C_L = .881$
$\alpha_u = 13°$
$C_L = .942$
$\alpha_u = 14°$
$C_L = 1.004$
$\alpha_u = 15°$
$C_L = 1.057$
$\alpha_u = 16°$
$C_L = 1.080$
$\alpha_u = 17°$
$C_L = 1.123$
$\alpha_u = 18°$
$C_L = 1.092$
$\alpha_u = 19°$
$C_L = 1.093$
C_L
α_u
STALL PATTERNS FOR $W_N A V_L$

C_L
α_u
$q = 25$ gm./cm.²
RUN 4, $W_N A V_L$ + WING TUFTS

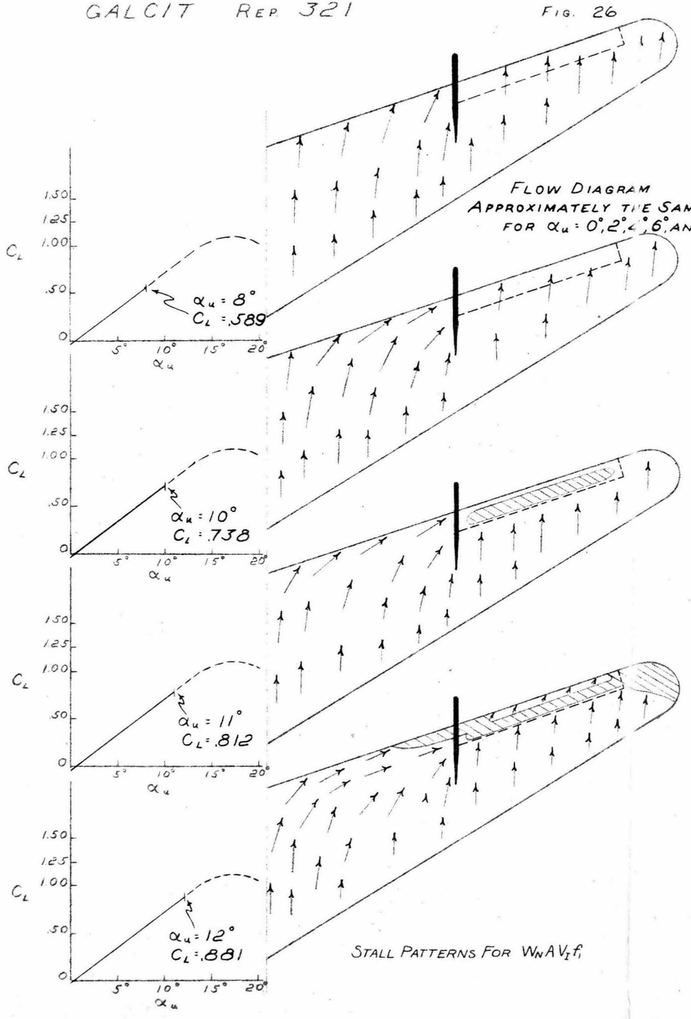
FLOW DIAGRAM
APPROXIMATELY THE SAME
FOR α_u = 0°, 2°, 6°, AND 8°
α_u = 8°
C_L = .589
α_u = 10°
C_L = .738
α_u = 11°
C_L = .812
α_u = 12°
C_L = .881
STALL PATTERNS FOR $W_N A V_1 f_1$

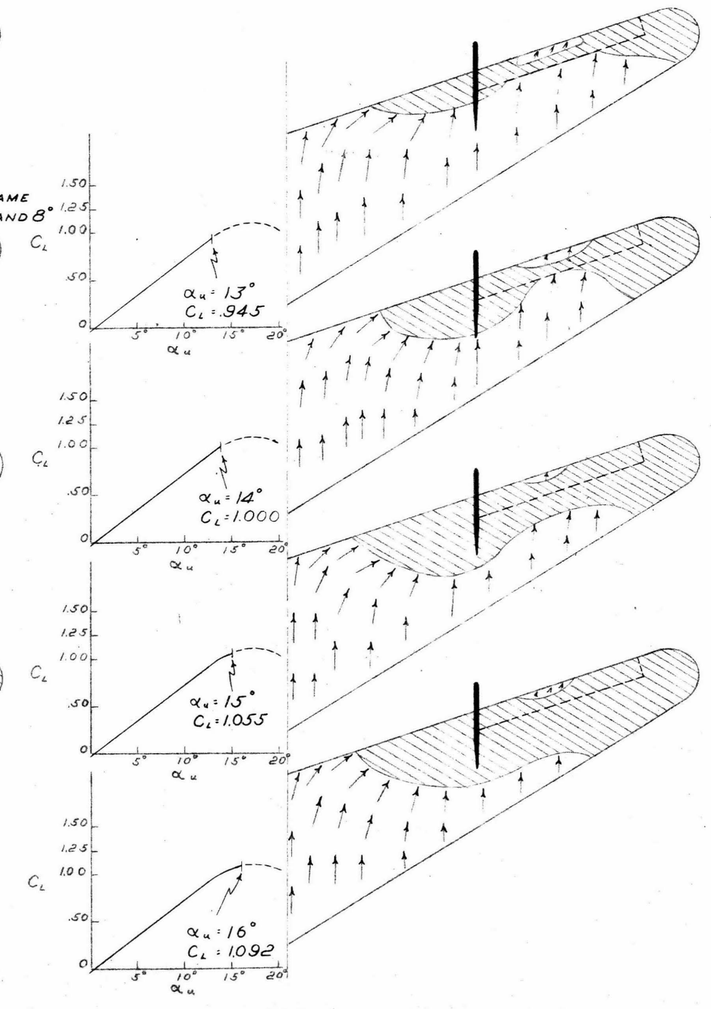
α_u = 13°
C_L = .945
α_u = 14°
C_L = 1.000
α_u = 15°
C_L = 1.055
α_u = 16°
C_L = 1.092

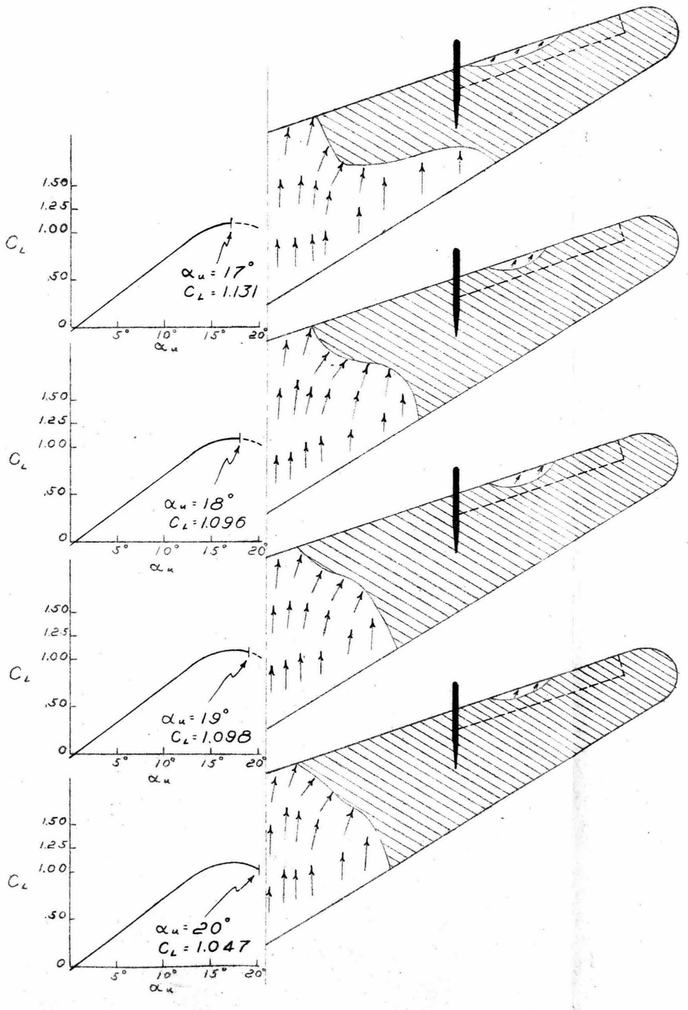
α_u = 17°
C_L = 1.131
α_u = 18°
C_L = 1.096
α_u = 19°
C_L = 1.098
α_u = 20°
C_L = 1.047

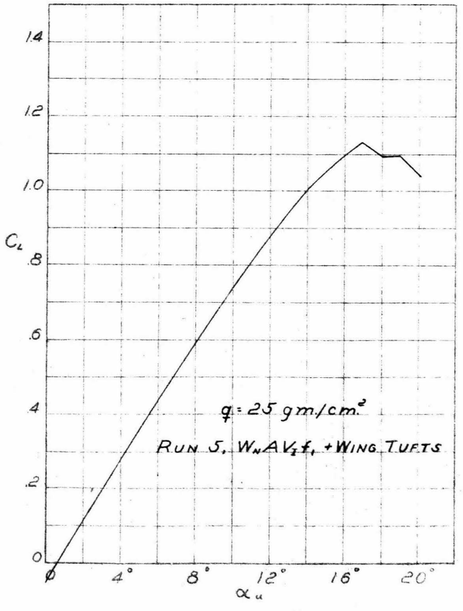
q = 25 gm./cm.²
RUN 5. $W_N A V_2 f_1$ + WING TUFTS

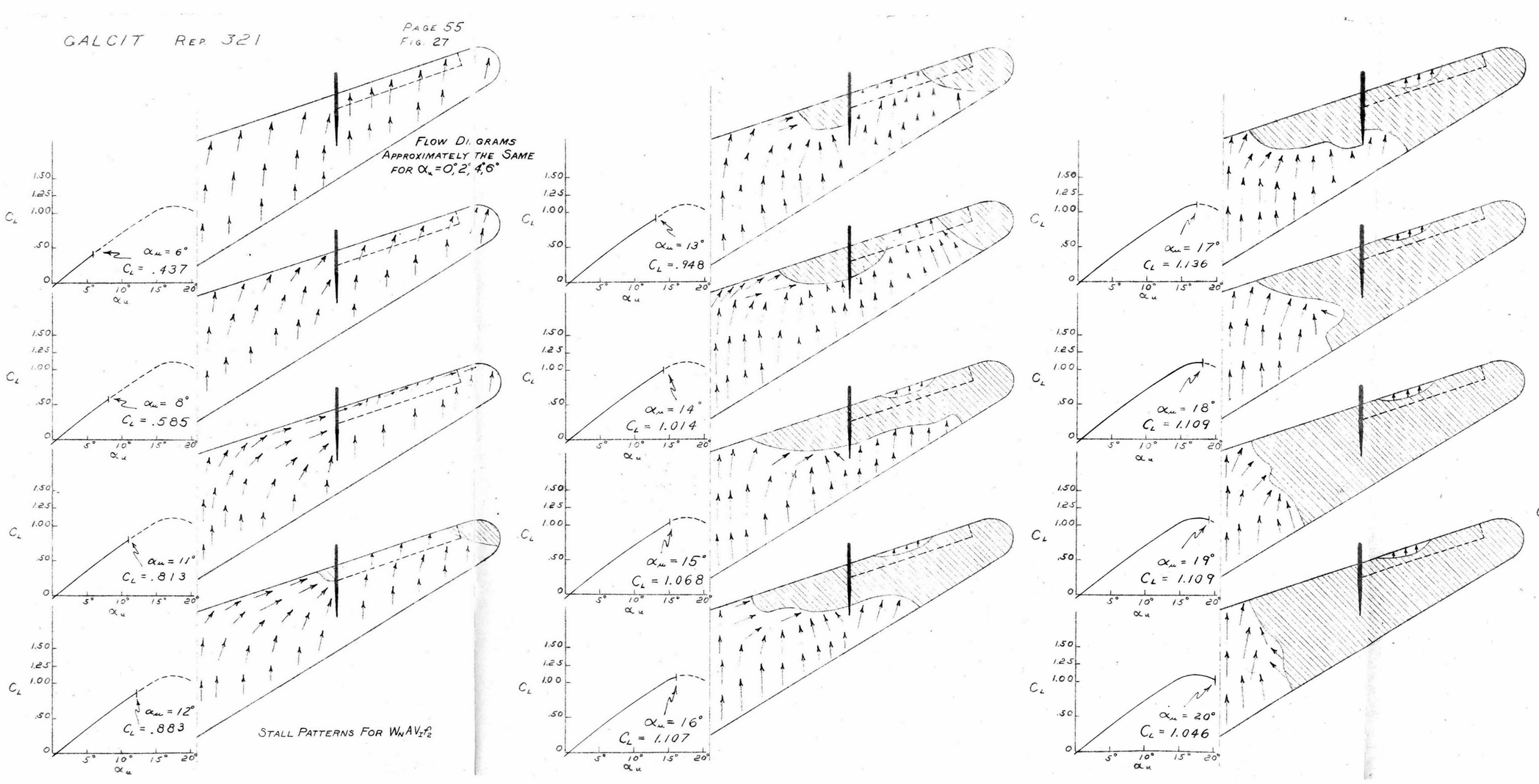
FLOW DIAGRAMS
APPROXIMATELY THE SAME
FOR α_u = 0°, 2°, 4°, 6°
α_u = 6°
C_L = .437
α_u = 8°
C_L = .585
α_u = 11°
C_L = .813
α_u = 12°
C_L = .883
α_u = 13°
C_L = .948
α_u = 14°
C_L = 1.014
α_u = 15°
C_L = 1.068
α_u = 16°
C_L = 1.107
α_u = 17°
C_L = 1.136
α_u = 18°
C_L = 1.109
α_u = 19°
C_L = 1.109
α_u = 20°
C_L = 1.046
C_L
α_u
STALL PATTERNS FOR $W_N A V_1 f_2$

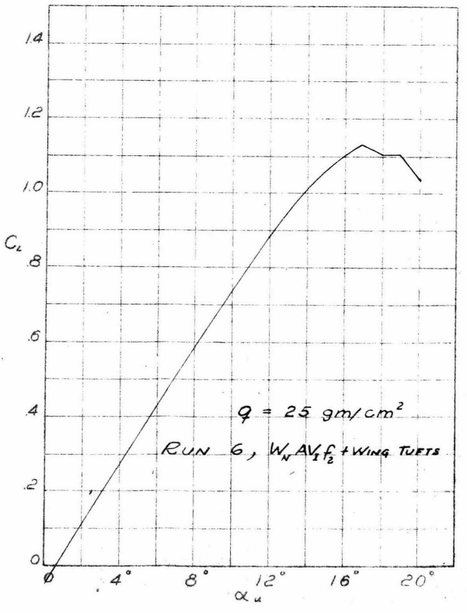
C_L
α_u
q = 25 gm/cm²
RUN 6, $W_N A V_1 f_2$ + WING TUFTS

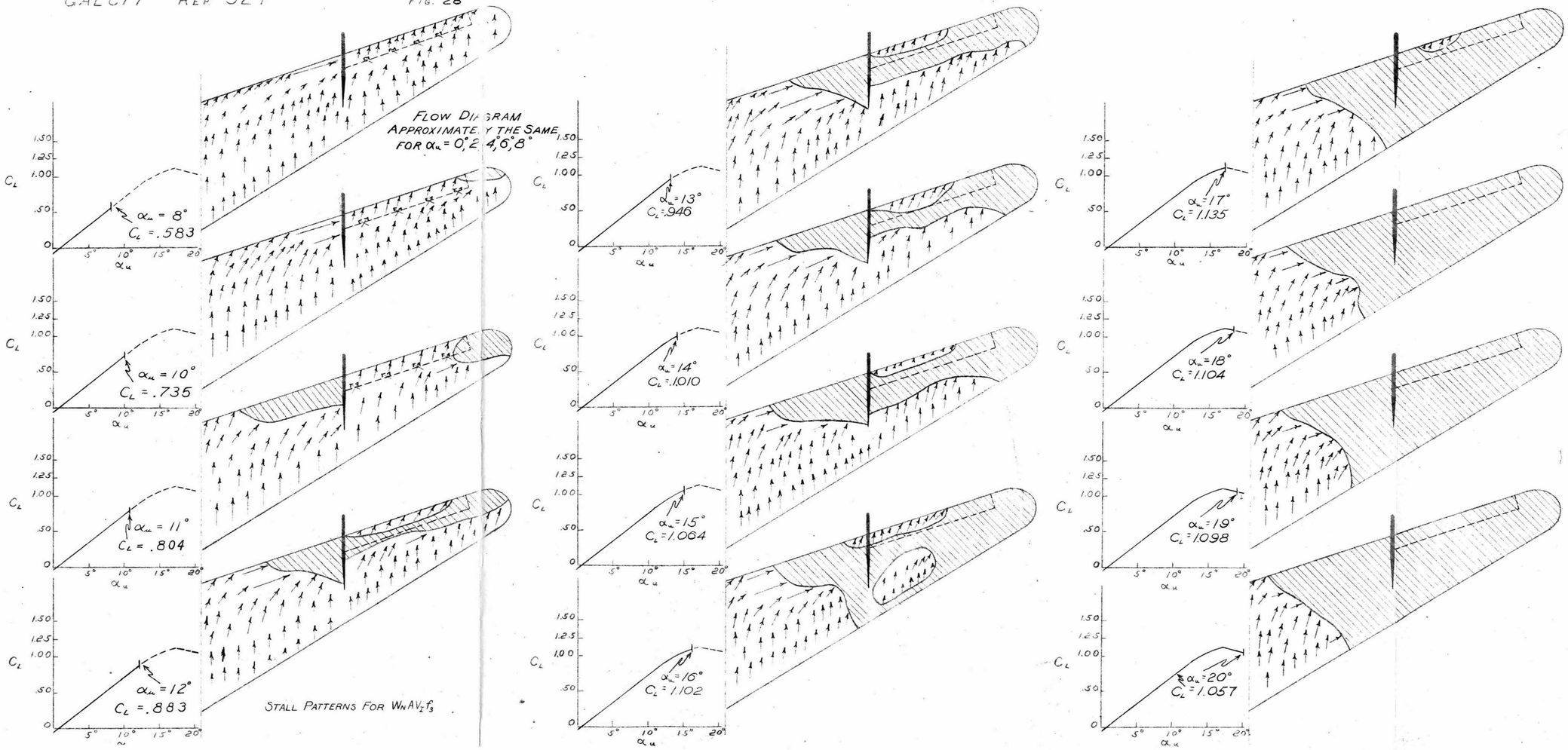

STALL PATTERNS FOR $W_N A V_I f_3$

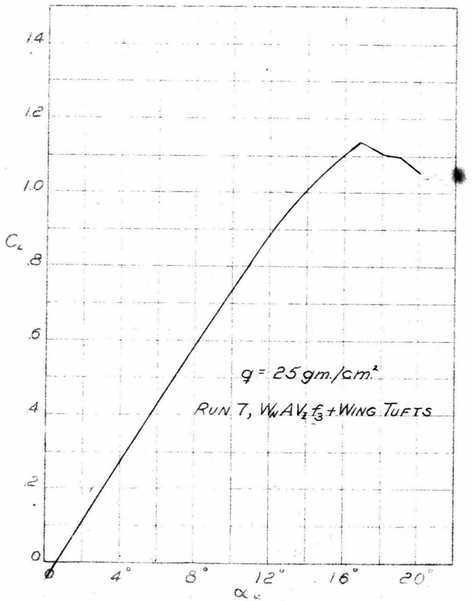

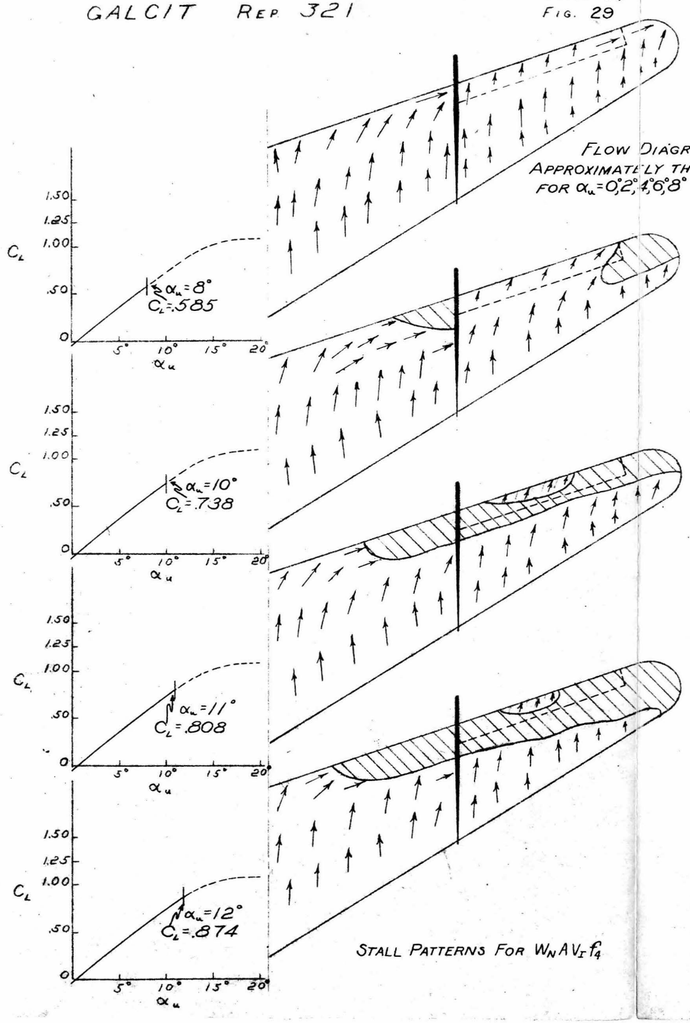

FLOW DIAGRAMS APPROXIMATELY THE SAME FOR α_u=0°,2°,4°,6°,8°

STALL PATTERNS FOR $W_N A V_I f_4$

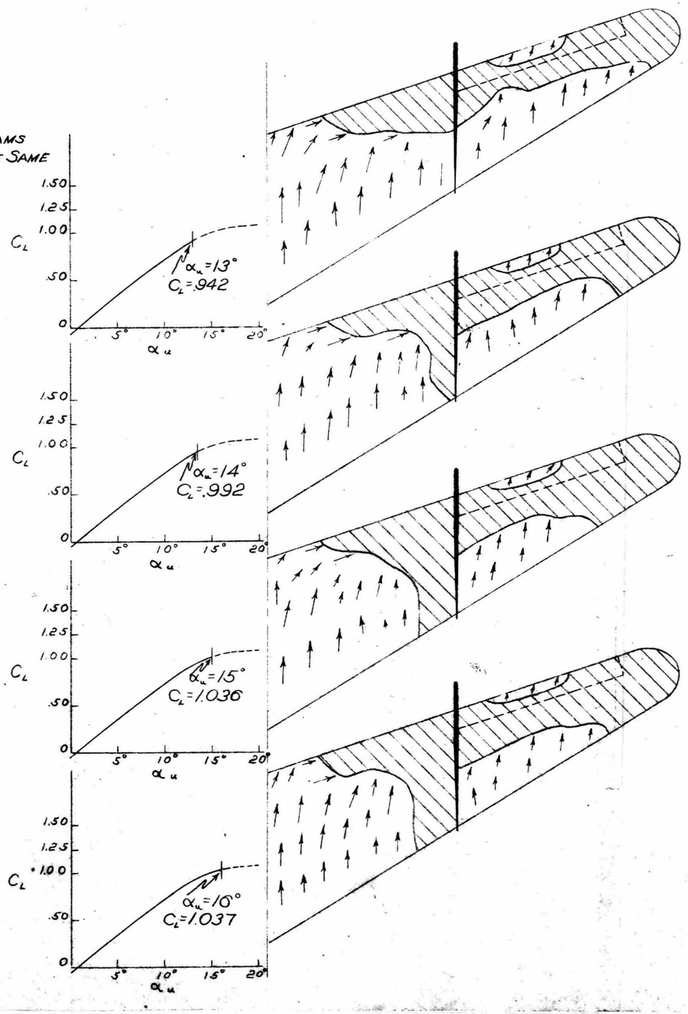

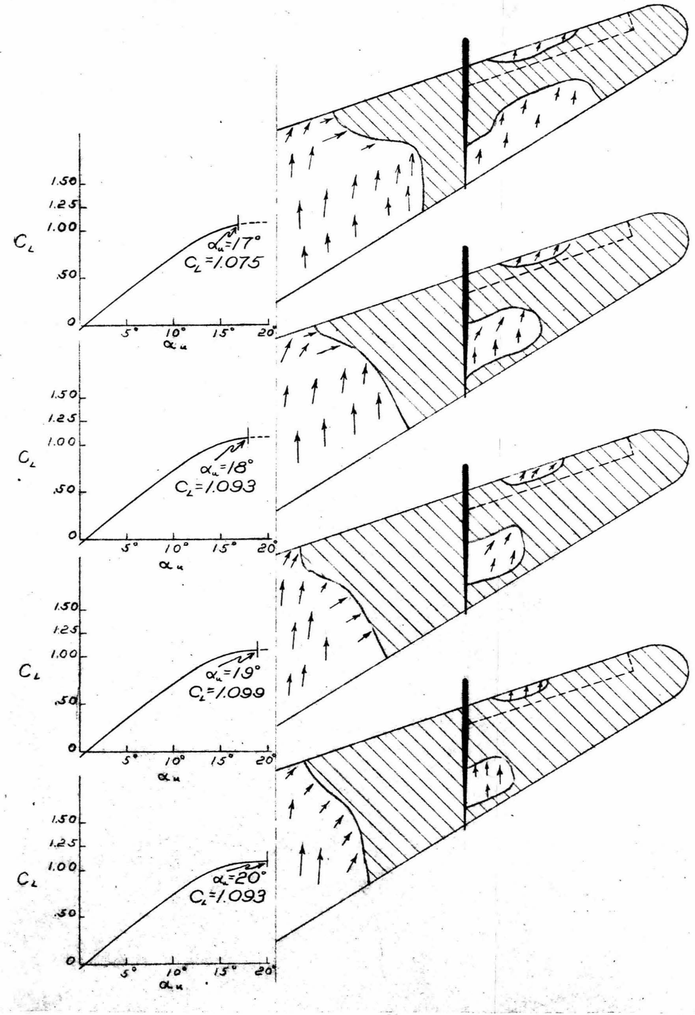

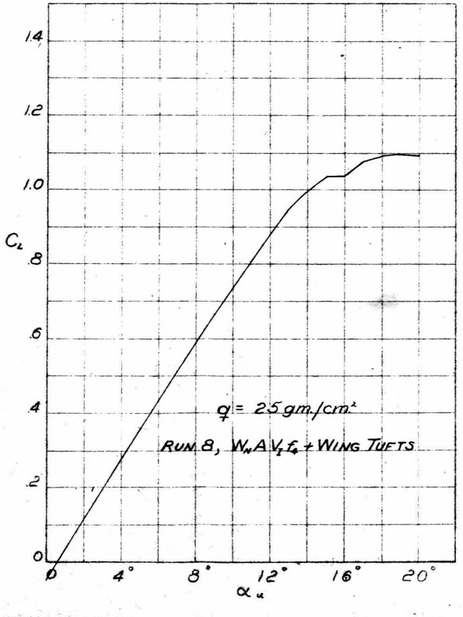

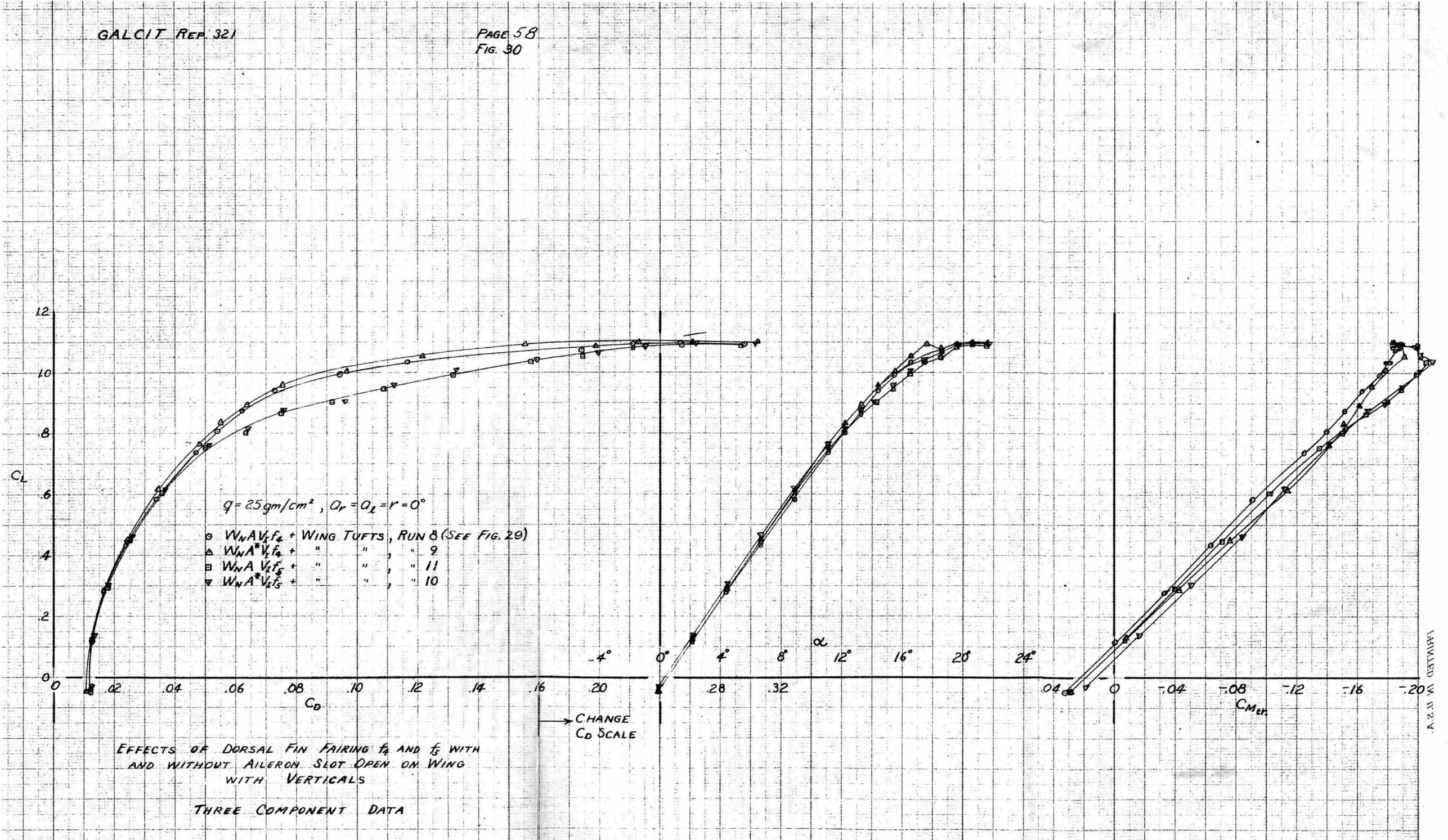

Effects of Dorsal Fin Fairing f_4 and f_5 with and without Aileron Slot Open on Wing with Verticals

Three Component Data

FIG. 31

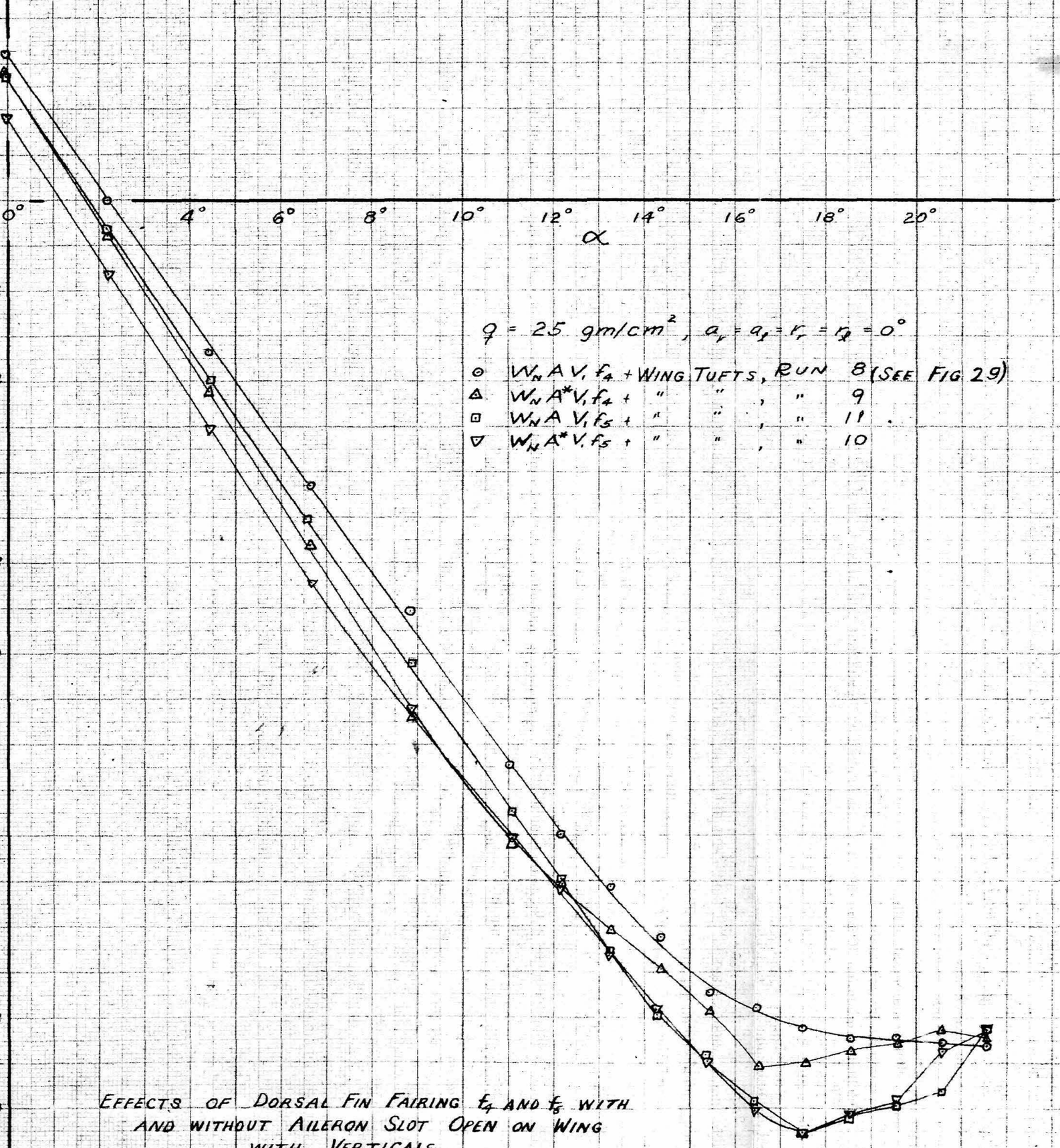

EFFECTS OF DORSAL FIN FAIRING f_4 AND f_5 WITH AND WITHOUT AILERON SLOT OPEN ON WING WITH VERTICALS
PITCHING MOMENT VS α

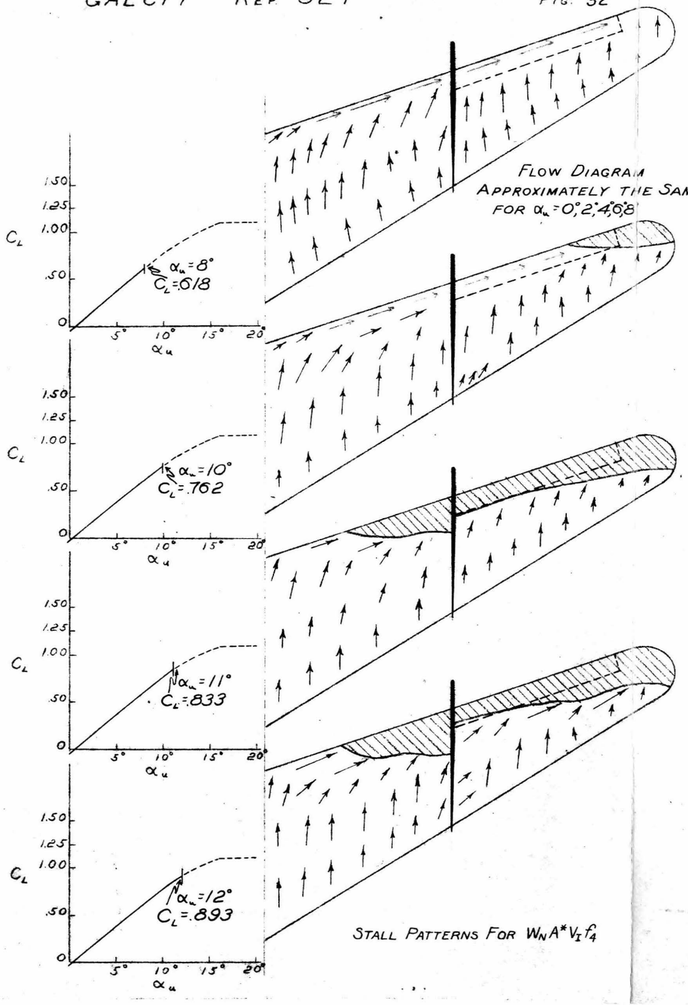
FLOW DIAGRAM
APPROXIMATELY THE SAME
FOR α_w = 0°, 2°, 4°, 6°, 8°
α_w = 8°
C_L = .618
α_w = 10°
C_L = .762
α_w = 11°
C_L = .833
α_w = 12°
C_L = .893
C_L
α_u
STALL PATTERNS FOR $W_N A^* V_I f_4$

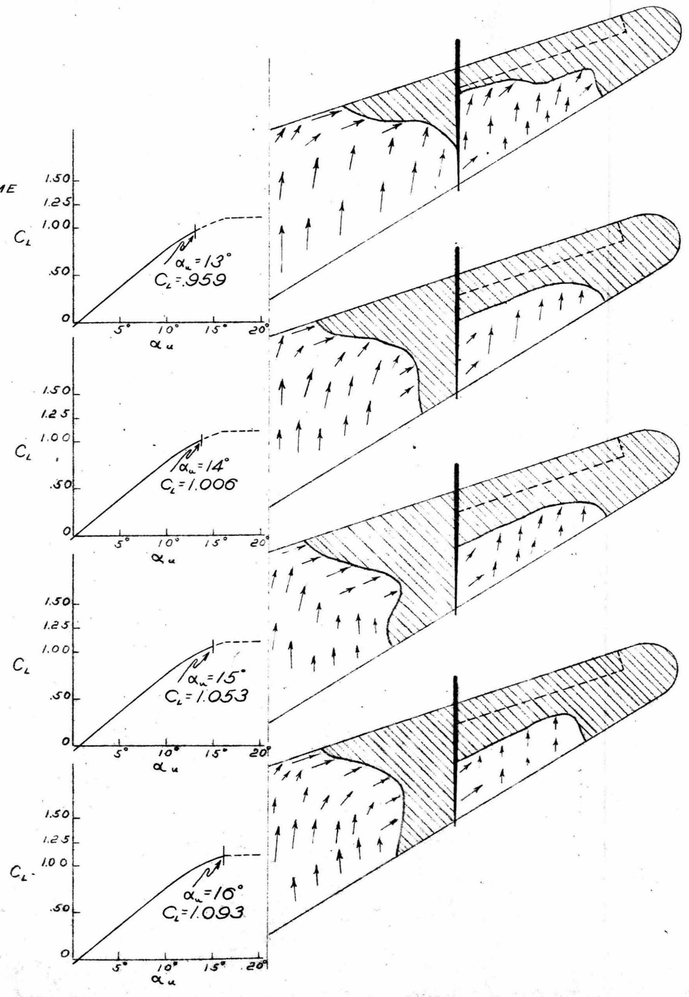
α_w = 13°
C_L = .959
α_w = 14°
C_L = 1.006
α_w = 15°
C_L = 1.053
α_w = 16°
C_L = 1.093
C_L
α_u

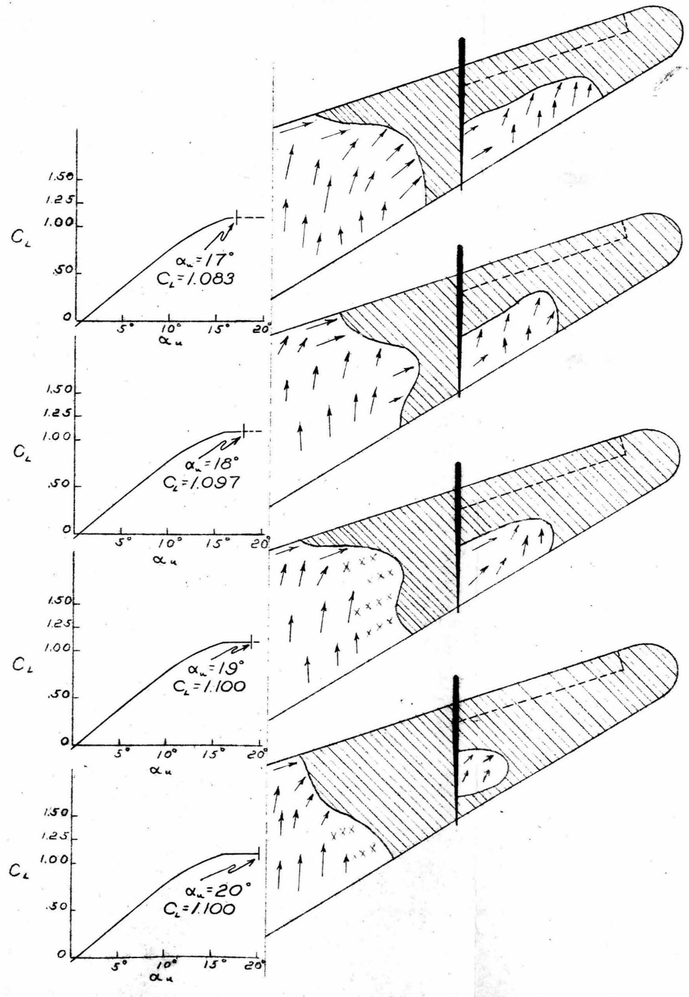
α_w = 17°
C_L = 1.083
α_w = 18°
C_L = 1.097
α_w = 19°
C_L = 1.100
α_w = 20°
C_L = 1.100
C_L
α_u

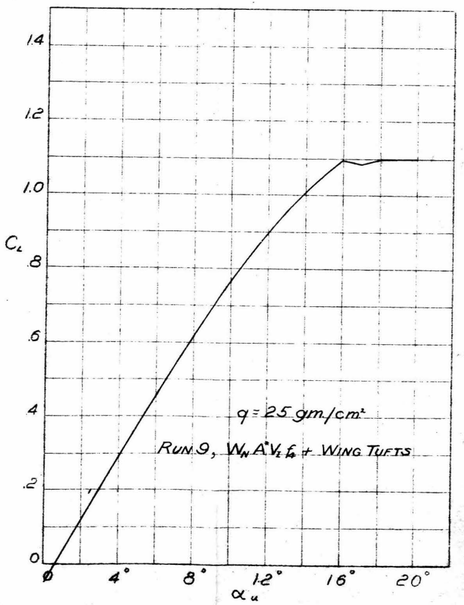
q = 2.5 gm./cm²
RUN 9, $W_N A^* V_I f_4$ + WING TUFTS
C_L
α_u

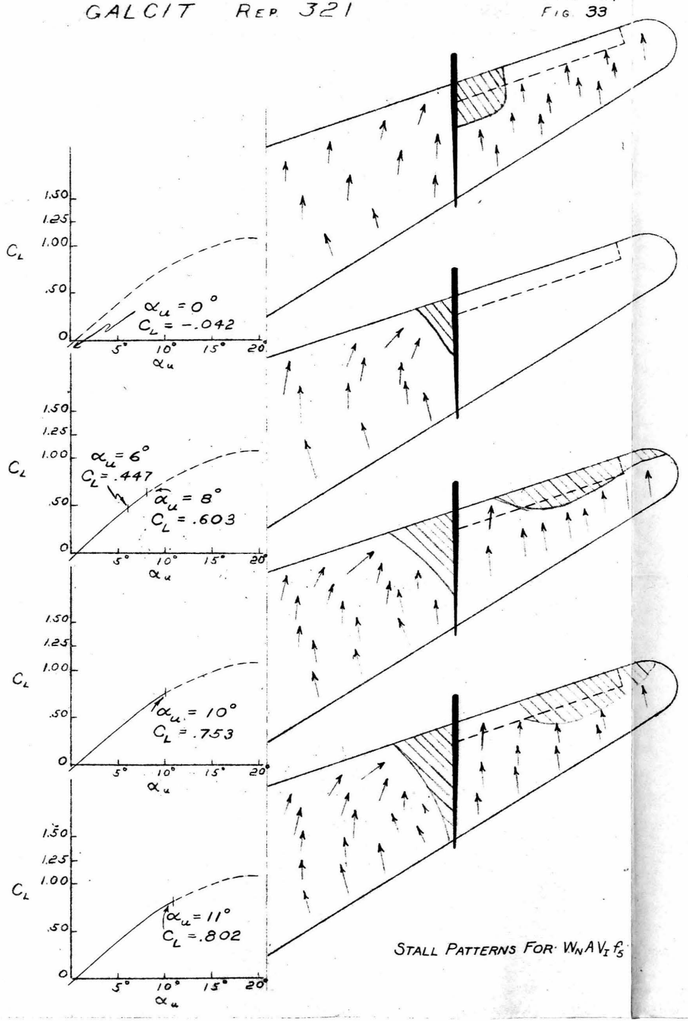

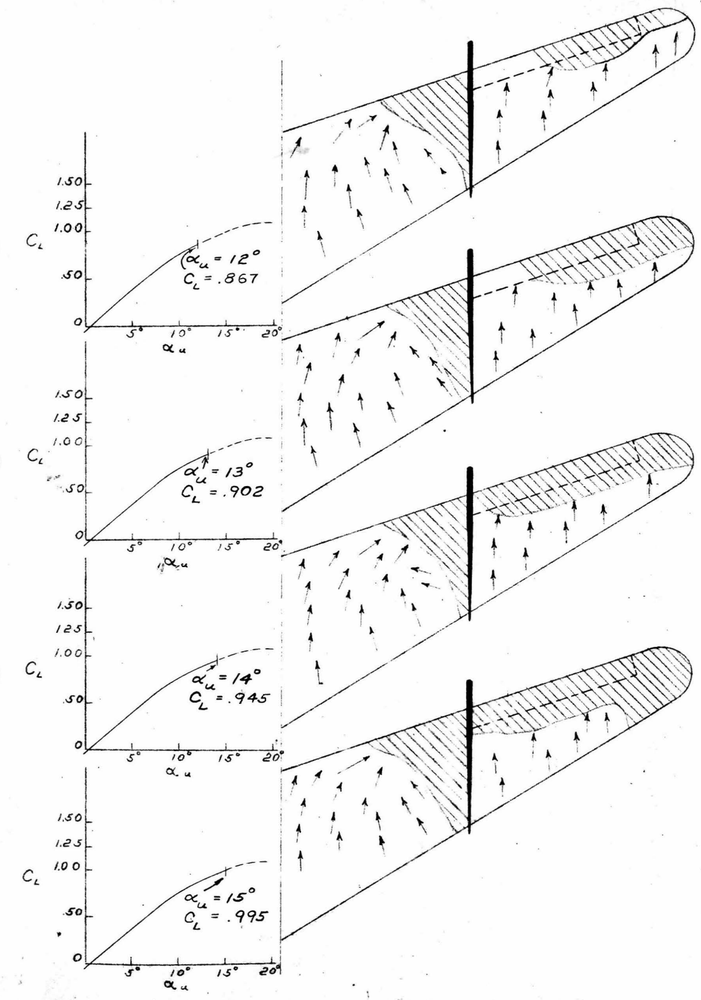

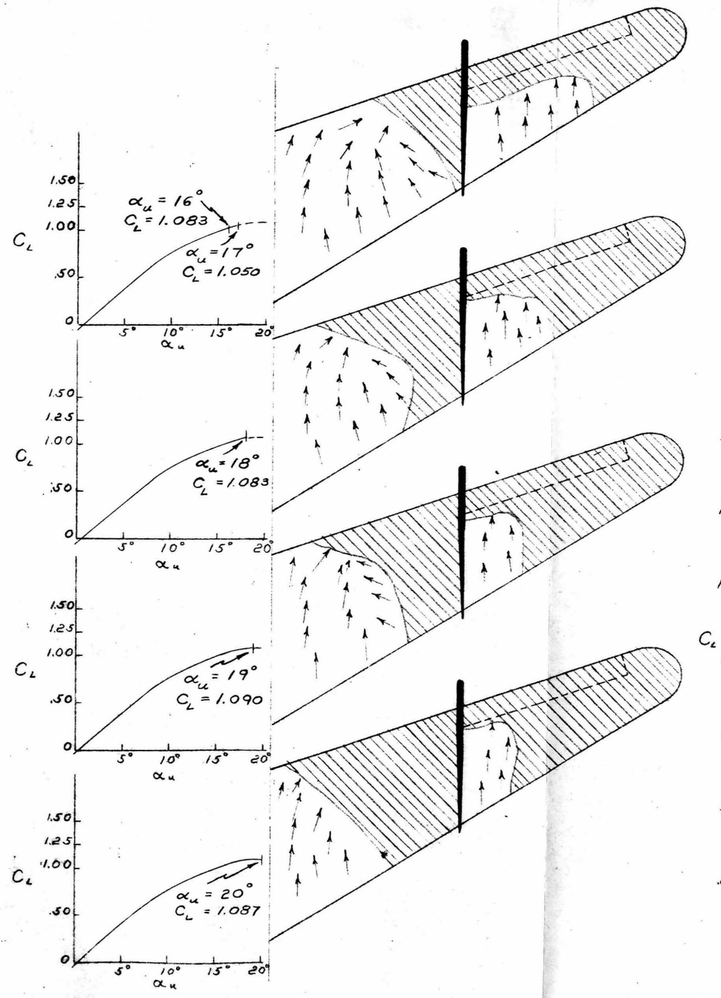

STALL PATTERNS FOR $W_N A V_1 f_5$

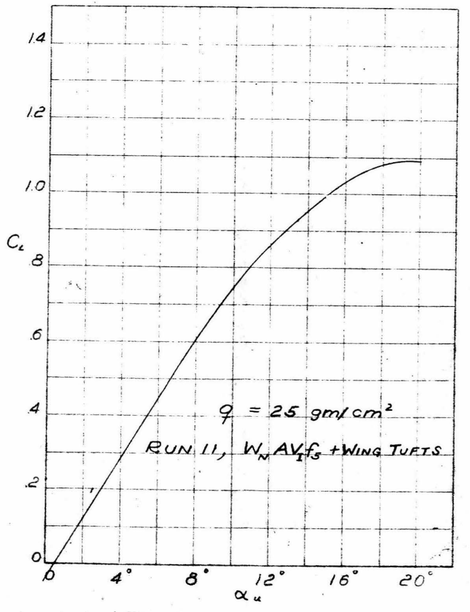

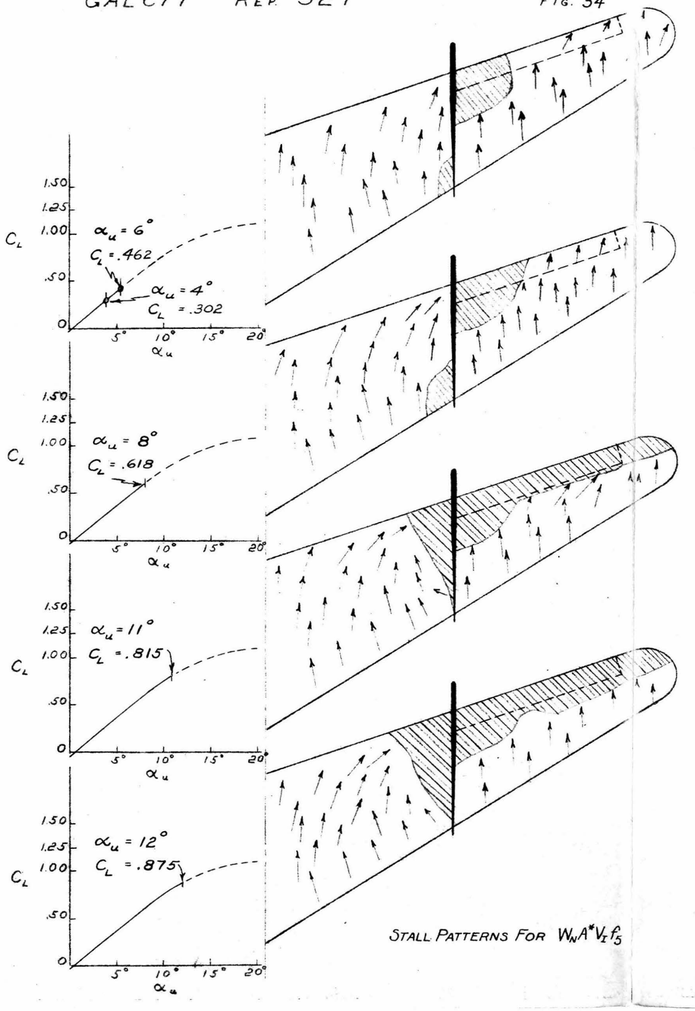

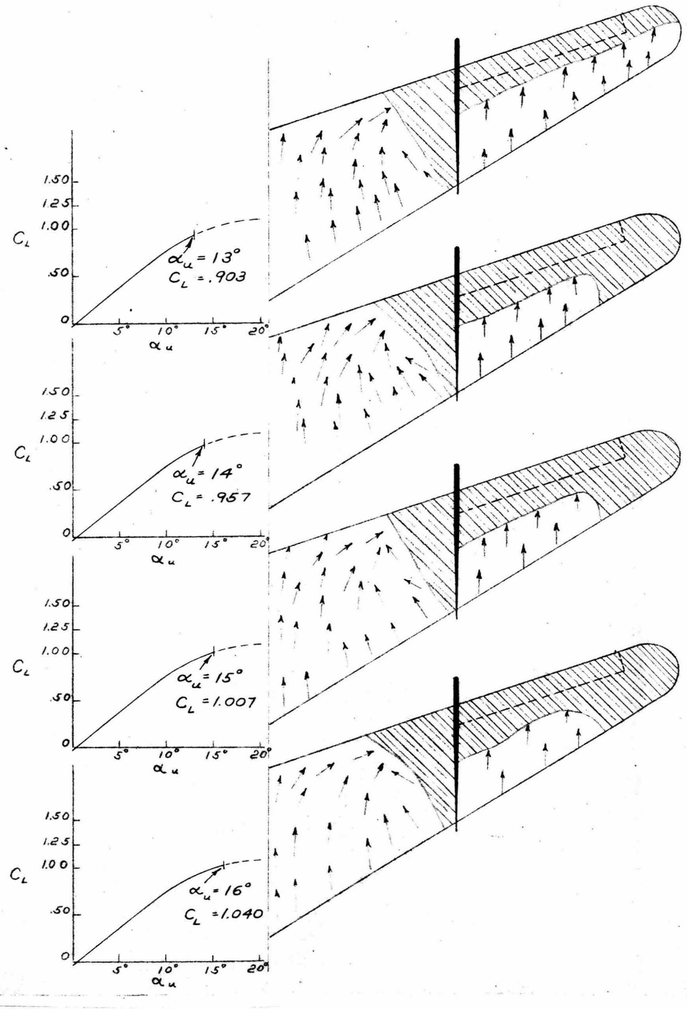

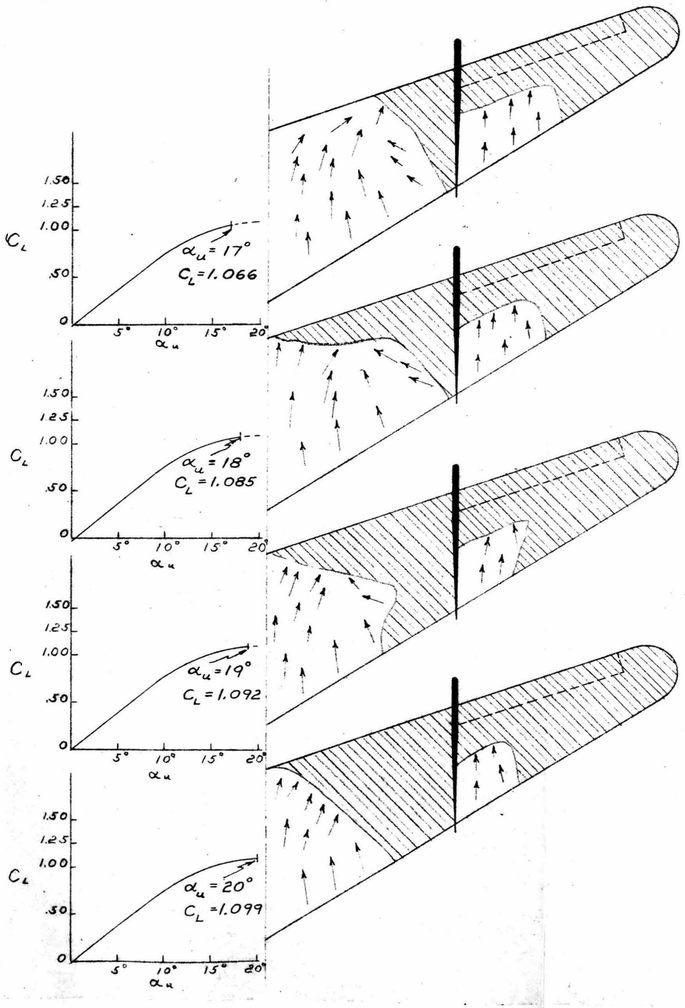

STALL PATTERNS FOR $W_N A^* V_I f_S$

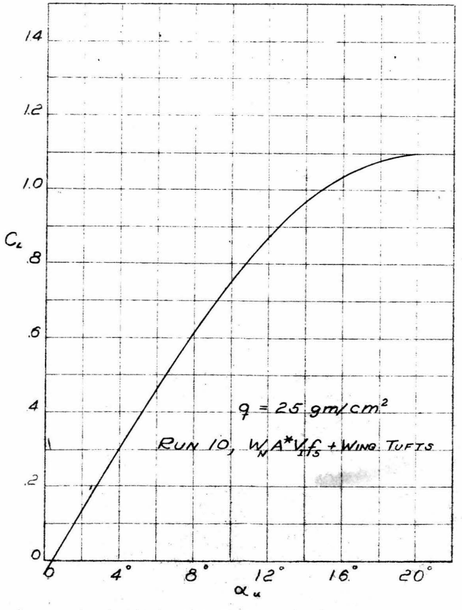

$q = 25\ gm/cm^2$, $\alpha_t = \alpha_l = r = 0°$, $i = 2.25°$

- ⊙ $W_N A^* V_2 B_N D$ + WING TUFTS, RUN 14
- △ $W_N A^* V_2 X_N B_N D$ " , " 15
- □ $W_N A^* V_2 X_N B_N D f_4$ " , " 16
- ▽ $W_N A V_2 X_N B_N D f_4$ " , " 17

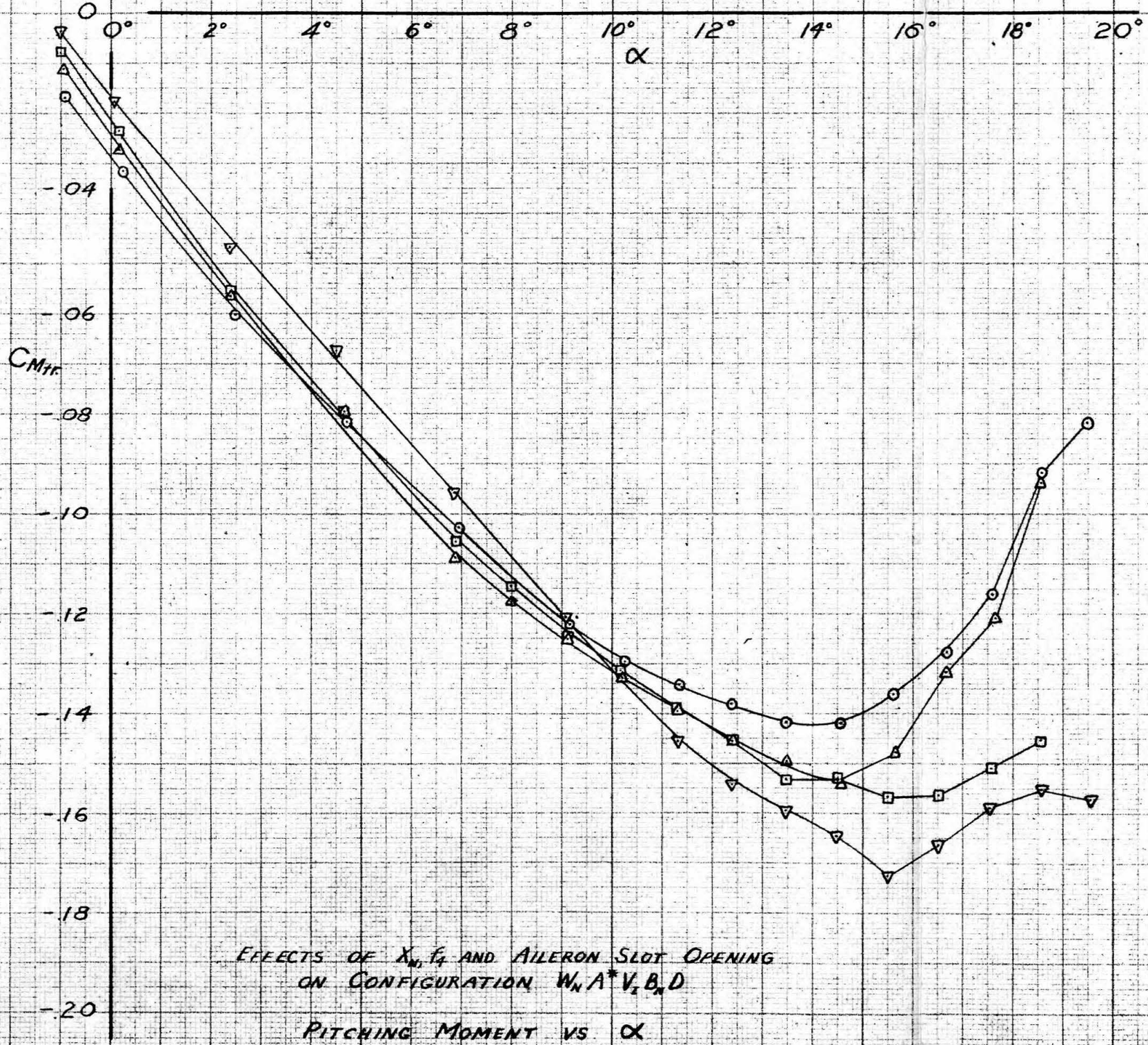

EFFECTS OF X_N, f_4 AND AILERON SLOT OPENING ON CONFIGURATION $W_N A^* V_2 B_N D$

PITCHING MOMENT VS α

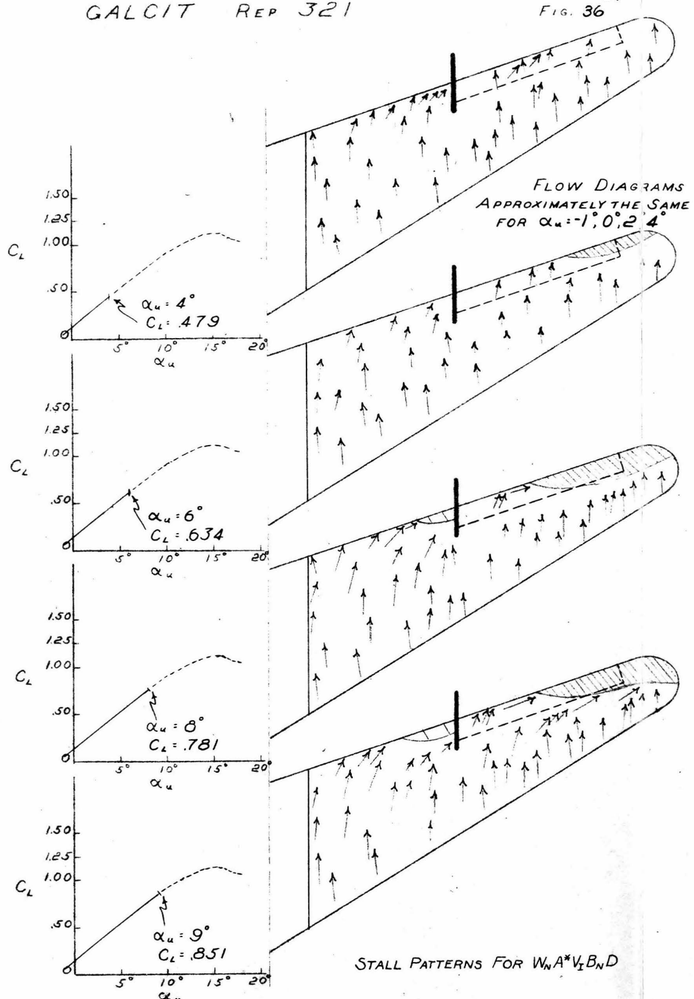

STALL PATTERNS FOR $W_N A^* V_2 B_N D$

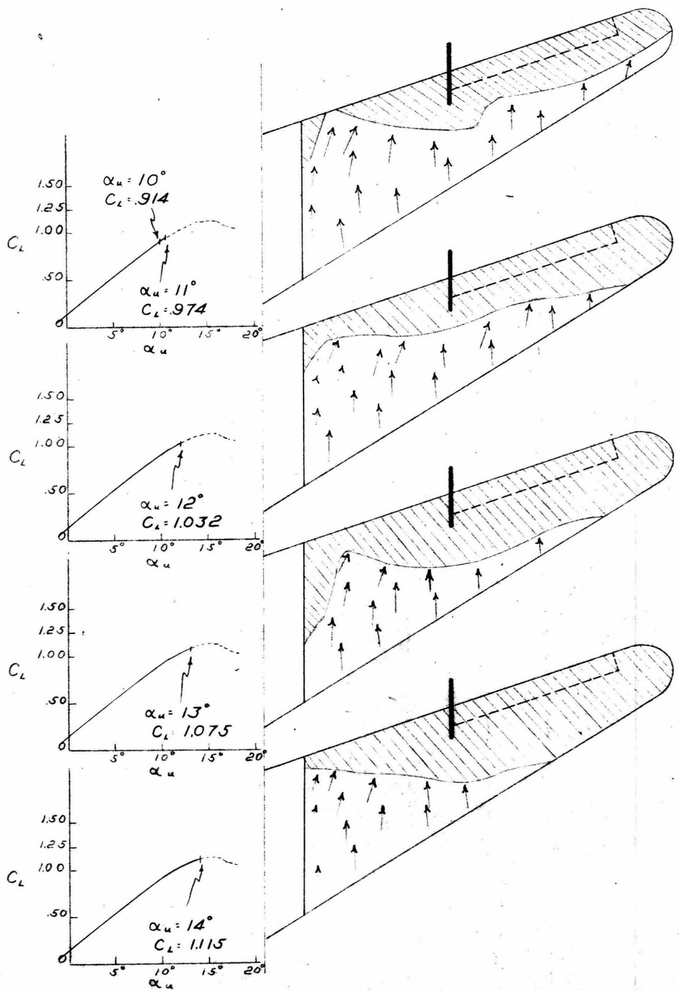

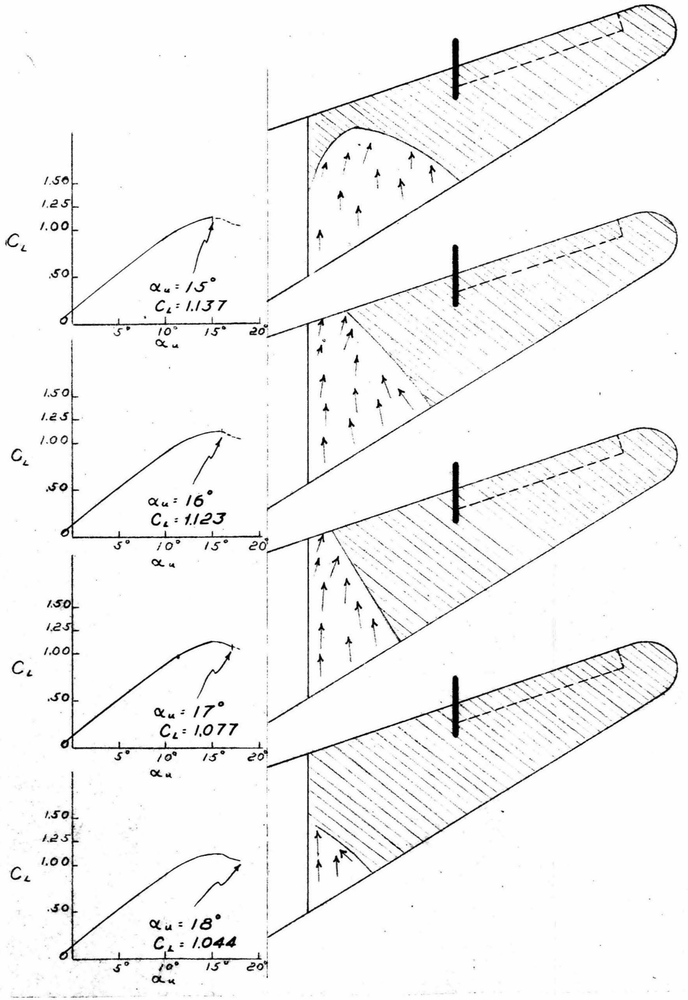

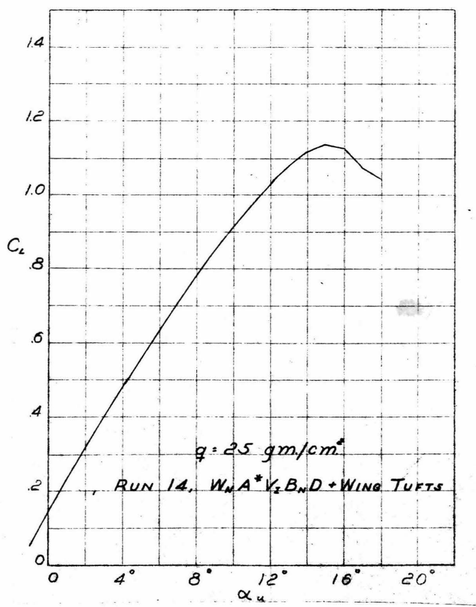

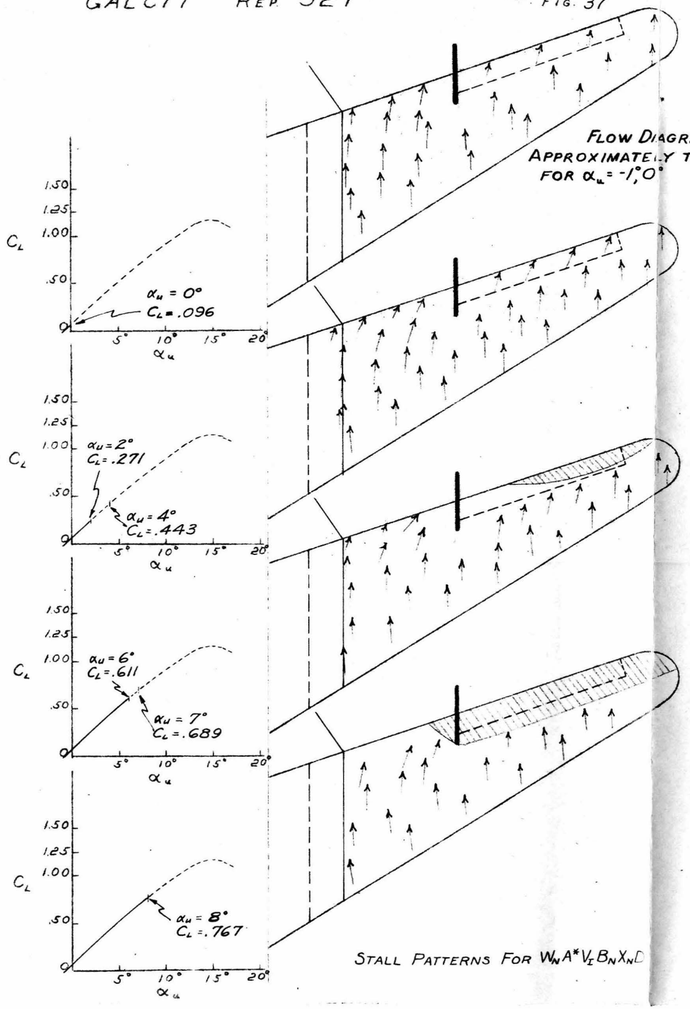
FLOW DIAGRAMS
APPROXIMATELY THE SAME
FOR $\alpha_u = -1°, 0°$
$\alpha_u = 0°$
$C_L = .096$
$\alpha_u = 2°$
$C_L = .271$
$\alpha_u = 4°$
$C_L = .443$
$\alpha_u = 6°$
$C_L = .611$
$\alpha_u = 7°$
$C_L = .689$
$\alpha_u = 8°$
$C_L = .767$
STALL PATTERNS FOR $W_N A^* V_E B_N X_N D$

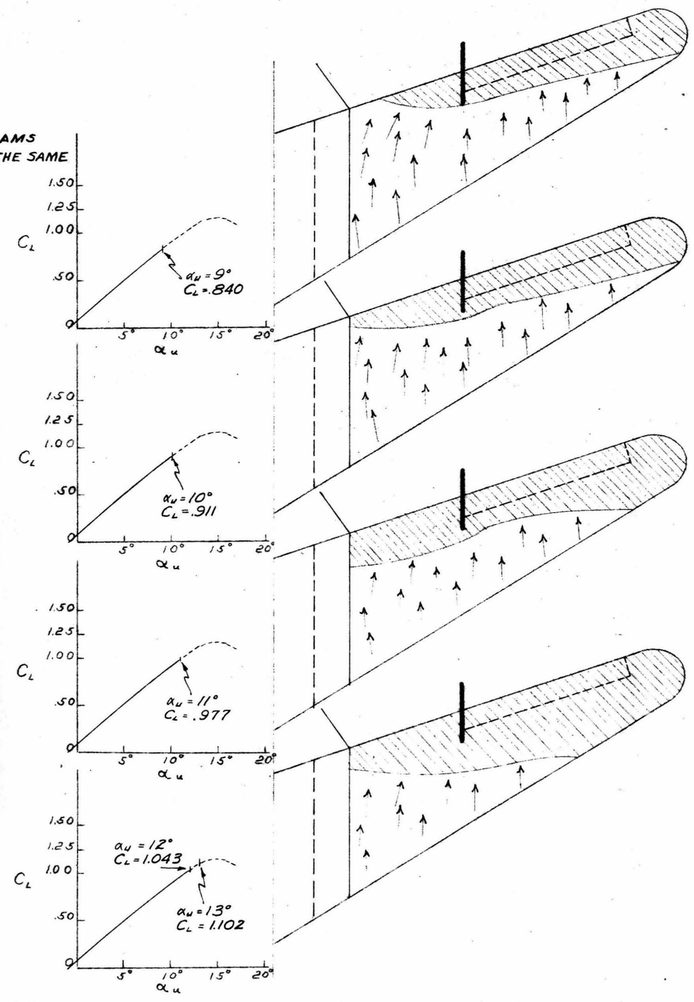
$\alpha_u = 9°$
$C_L = .840$
$\alpha_u = 10°$
$C_L = .911$
$\alpha_u = 11°$
$C_L = .977$
$\alpha_u = 12°$
$C_L = 1.043$
$\alpha_u = 13°$
$C_L = 1.102$

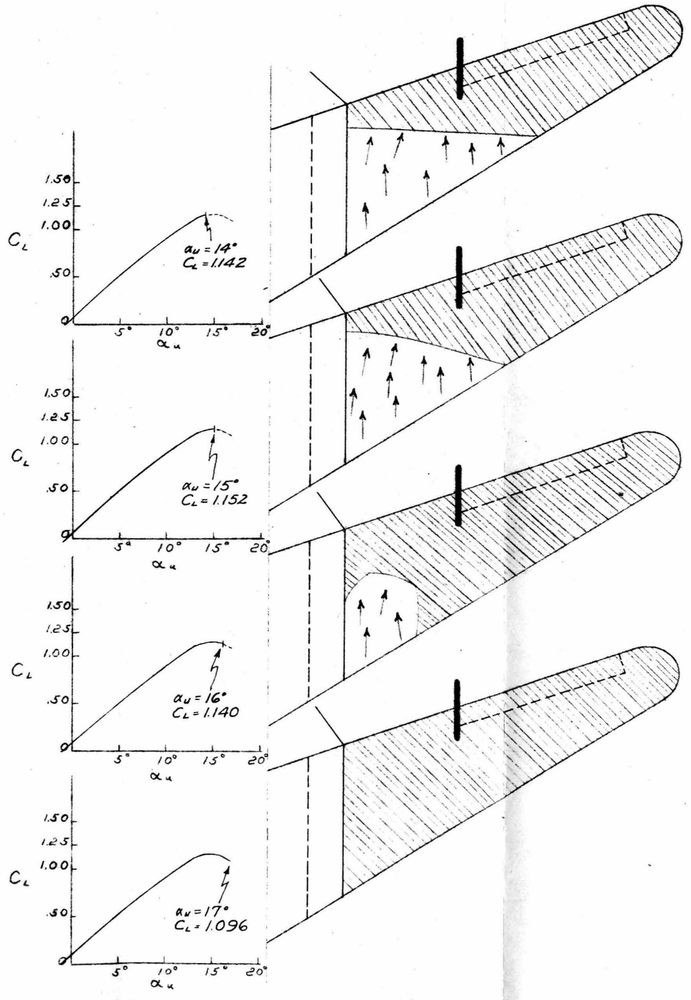
$\alpha_u = 14°$
$C_L = 1.142$
$\alpha_u = 15°$
$C_L = 1.152$
$\alpha_u = 16°$
$C_L = 1.140$
$\alpha_u = 17°$
$C_L = 1.096$

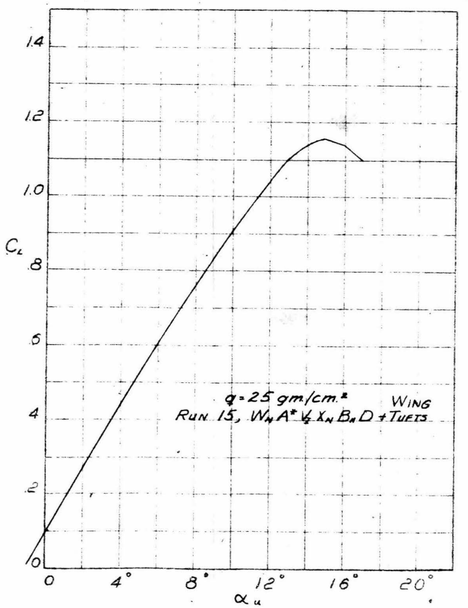
$q = 25$ gm/cm.²
WING
RUN 15, $W_N A^* V_E X_N B_N D$ + TUFTS

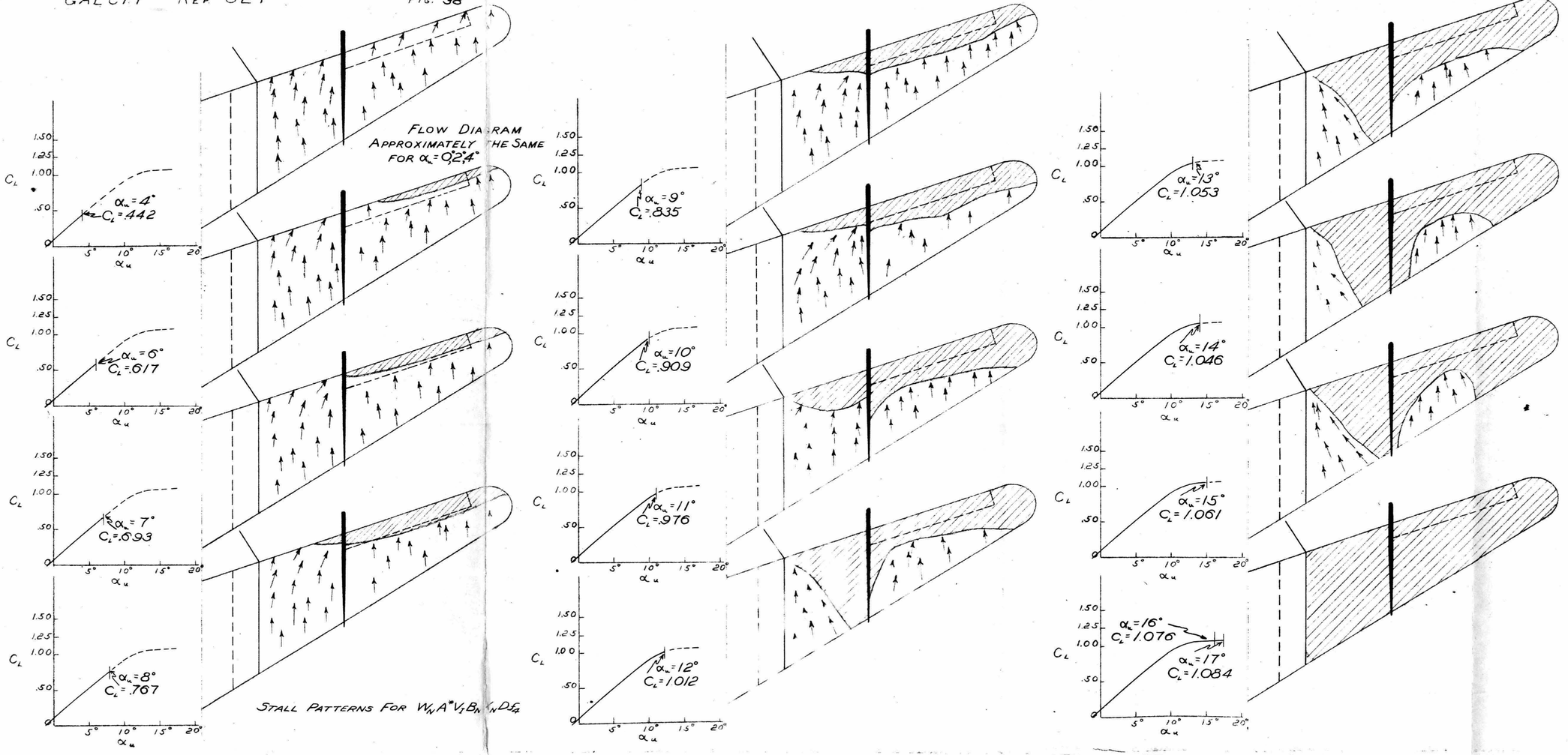
FLOW DIAGRAM
APPROXIMATELY THE SAME
FOR $\alpha_L = 0, 2, 4°$
$\alpha_u = 4°$
$C_L = .442$
$\alpha_u = 6°$
$C_L = .617$
$\alpha_u = 7°$
$C_L = .693$
$\alpha_u = 8°$
$C_L = .767$
$\alpha_u = 9°$
$C_L = .835$
$\alpha_u = 10°$
$C_L = .909$
$\alpha_u = 11°$
$C_L = .976$
$\alpha_u = 12°$
$C_L = 1.012$
$\alpha_u = 13°$
$C_L = 1.053$
$\alpha_u = 14°$
$C_L = 1.046$
$\alpha_u = 15°$
$C_L = 1.061$
$\alpha_u = 16°$
$C_L = 1.076$
$\alpha_u = 17°$
$C_L = 1.084$
C_L
α_u
STALL PATTERNS FOR $W_N A^* V_t B_N X_N D \ell_t$

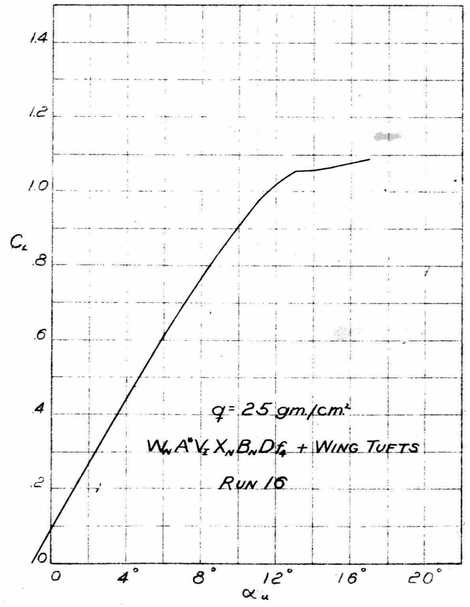
C_L
α_u
$q = .25$ gm./cm.²
$W_N A^* V_t X_N B_N D \ell_t$ + WING TUFTS
RUN 16

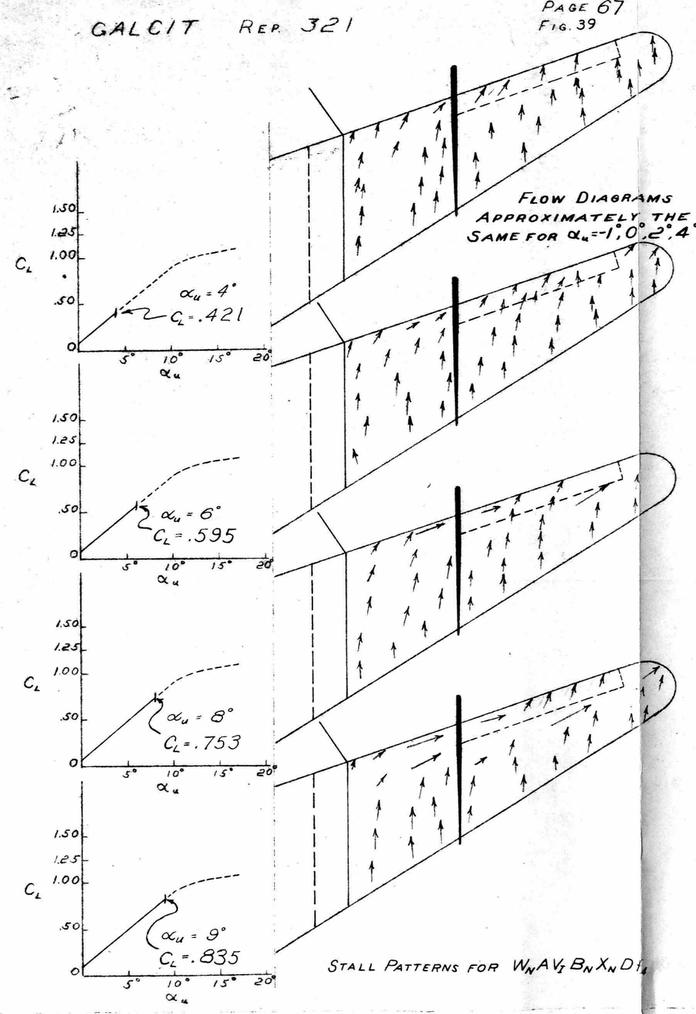
FLOW DIAGRAMS APPROXIMATELY THE SAME FOR α_u = -1°, 0°, 2°, 4°
α_u = 4°
C_L = .421
α_u = 6°
C_L = .595
α_u = 8°
C_L = .753
α_u = 9°
C_L = .835
C_L
α_u
STALL PATTERNS FOR $W_N A V_1 B_N X_N D f_4$

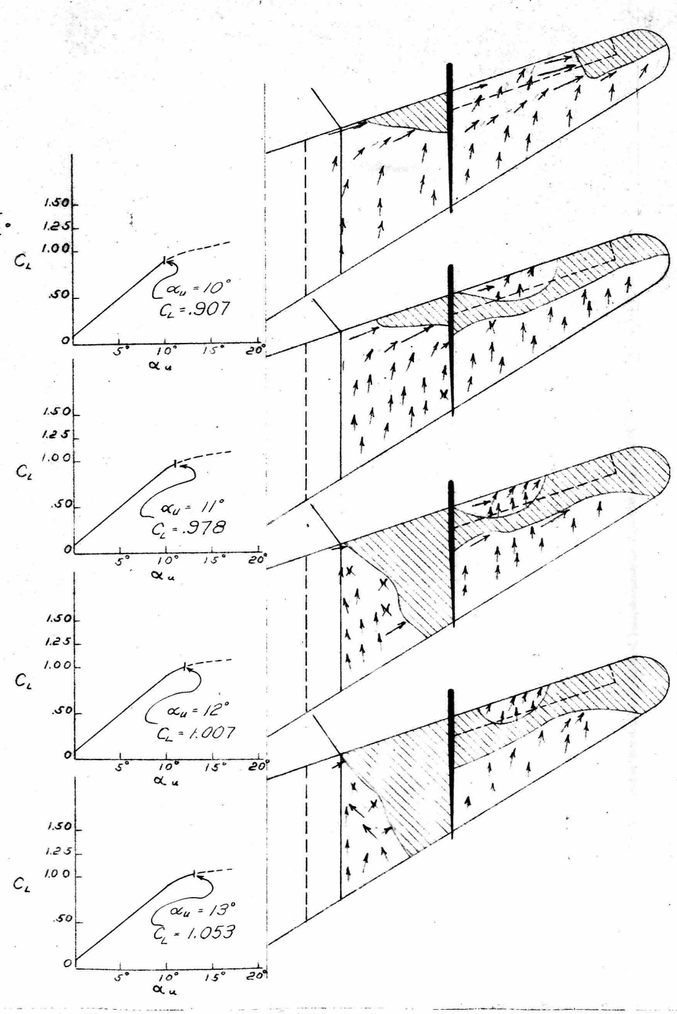
α_u = 10°
C_L = .907
α_u = 11°
C_L = .978
α_u = 12°
C_L = 1.007
α_u = 13°
C_L = 1.053
C_L
α_u

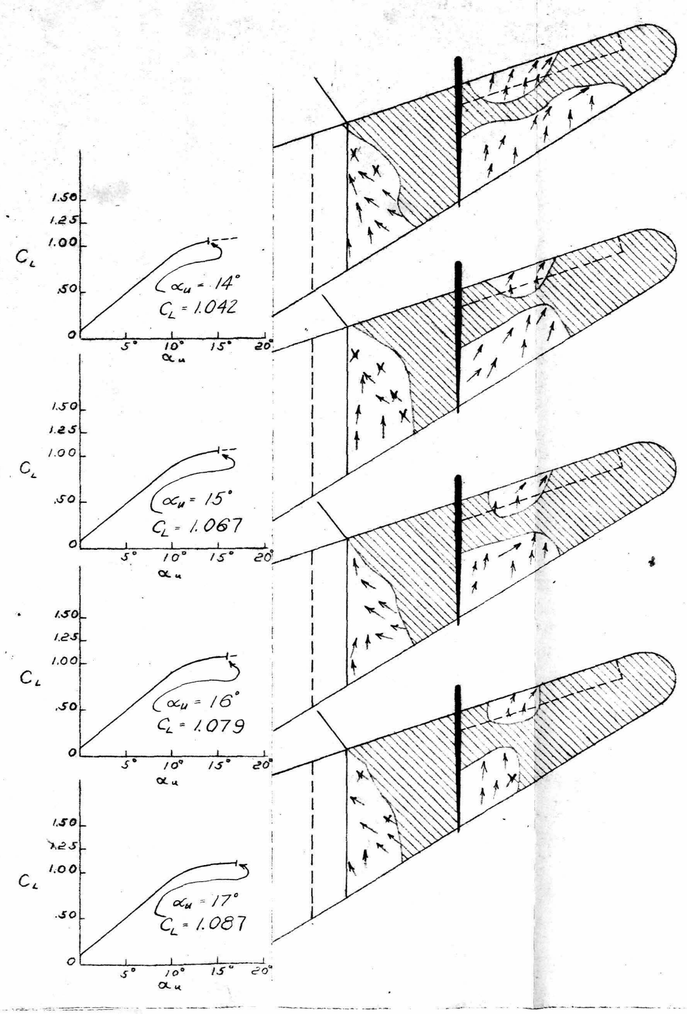
α_u = 14°
C_L = 1.042
α_u = 15°
C_L = 1.067
α_u = 16°
C_L = 1.079
α_u = 17°
C_L = 1.087
C_L
α_u

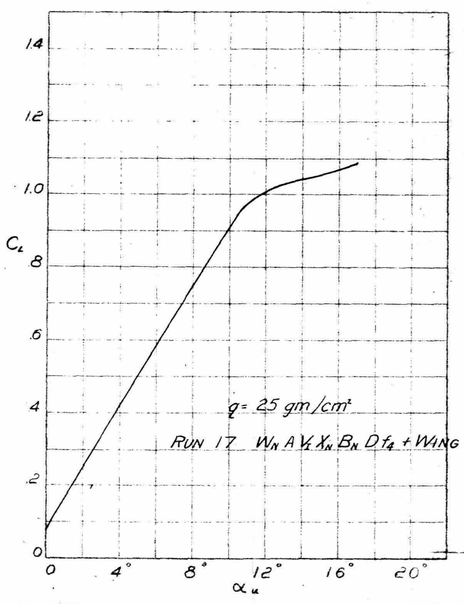
q = 25 gm/cm²
RUN 17 $W_N A V_1 X_N B_N D f_4$ + WING TUFTS
C_L
α_u

$q = 25\ gm/cm^2$, $a_r = a_\ell = r_r = r_\ell = 0°$, $i = 2.25°$

○ $W_N A V_1 X_N B_N D f_4$ +WING TUFTS, RUN 17 (SEE FIG. 39)
△ " + S_i + " " , " 18
□ " + S_m + " " , " 19
▽ " + S_i^6 + " " , " 20

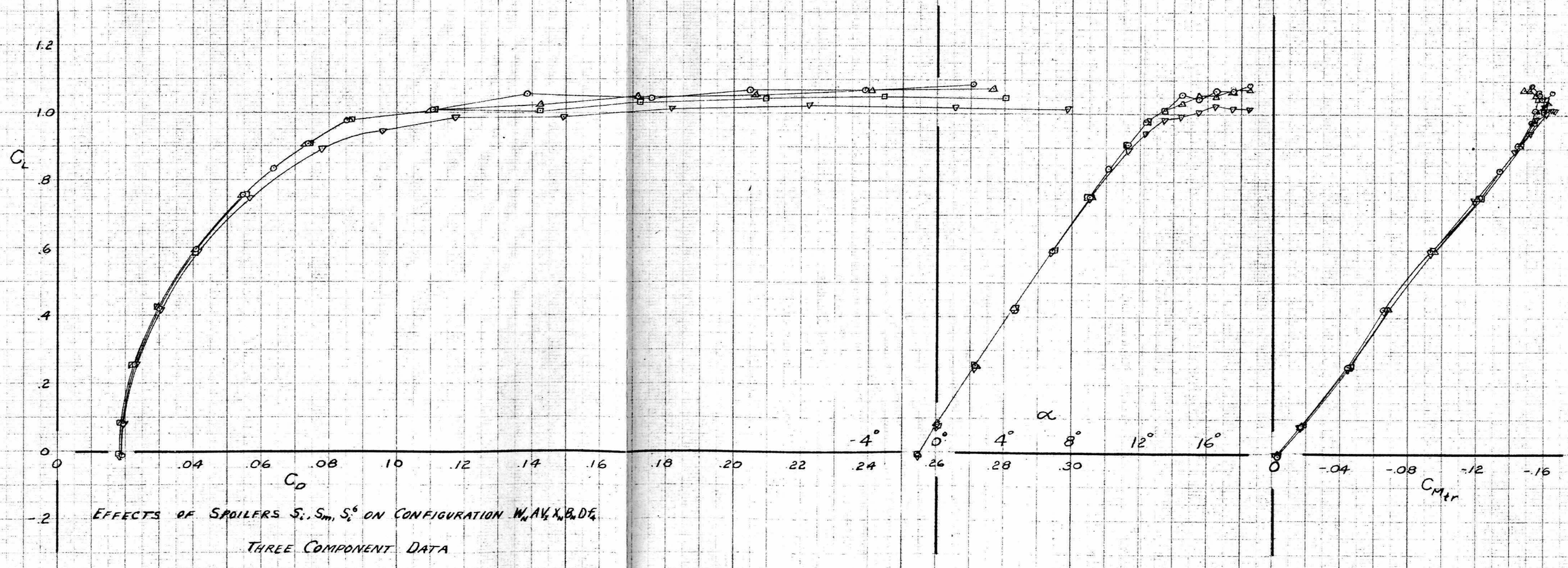

EFFECTS OF SPOILERS S_i, S_m, S_i^6 ON CONFIGURATION $W_N A V_1 X_N B_N D f_4$

THREE COMPONENT DATA

FIG. 41

$q = 25\ gm/cm^2$, $a_r = a_l = r_r = r_l = 0°$, $i = 2.25°$

○ $W_N A V_1 X_N B_N D f_4$ + WING TUFTS, RUN 17 (SEE FIG. 39)

△ " + S_i + " " , " 18

□ " + S_m + " " , " 19

▽ " + S_i^6 + " " , " 20

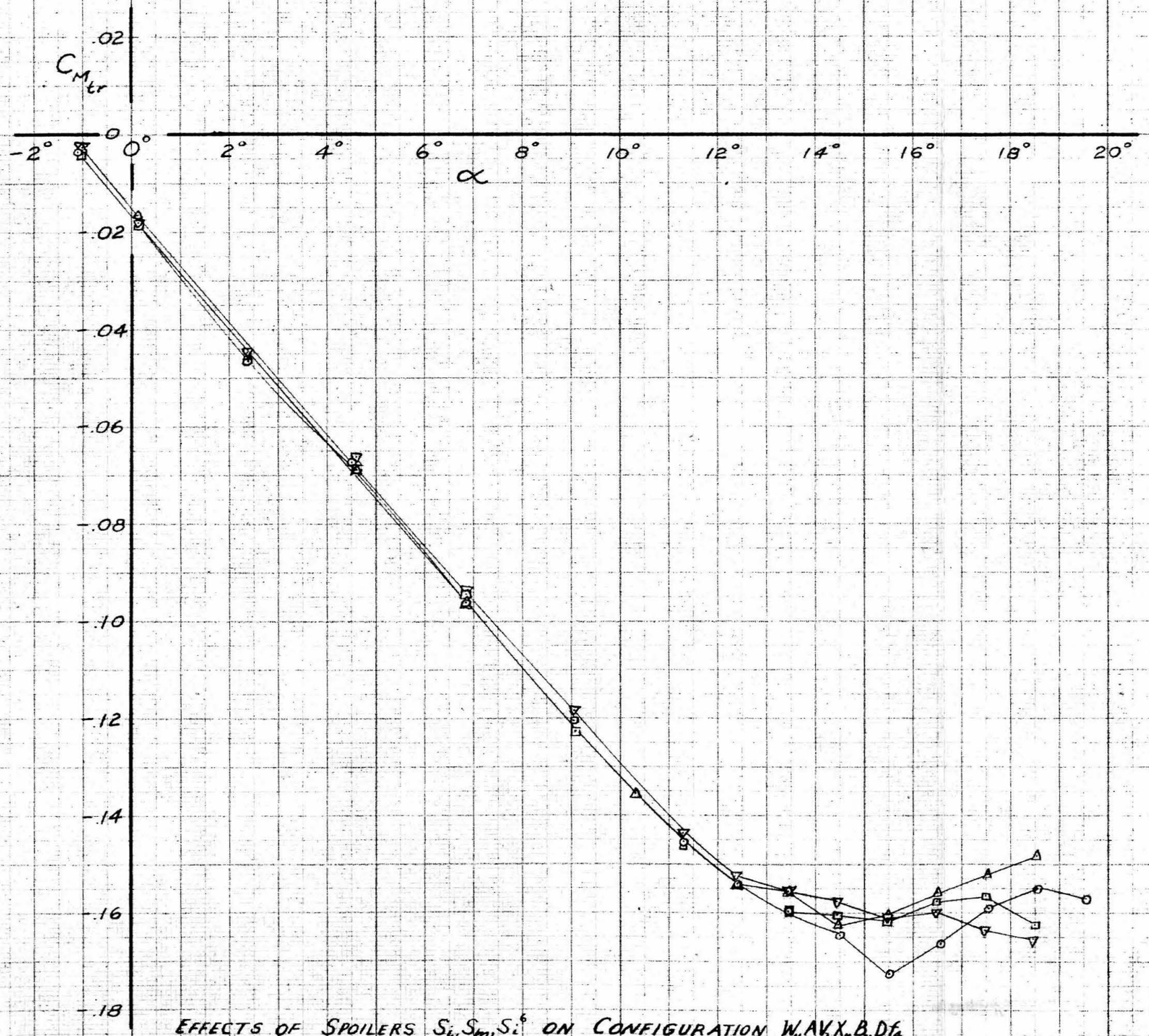

EFFECTS OF SPOILERS S_i, S_m, S_i^6 ON CONFIGURATION $W_N A V_1 X_N B_N D f_4$

PITCHING MOMENT VS α

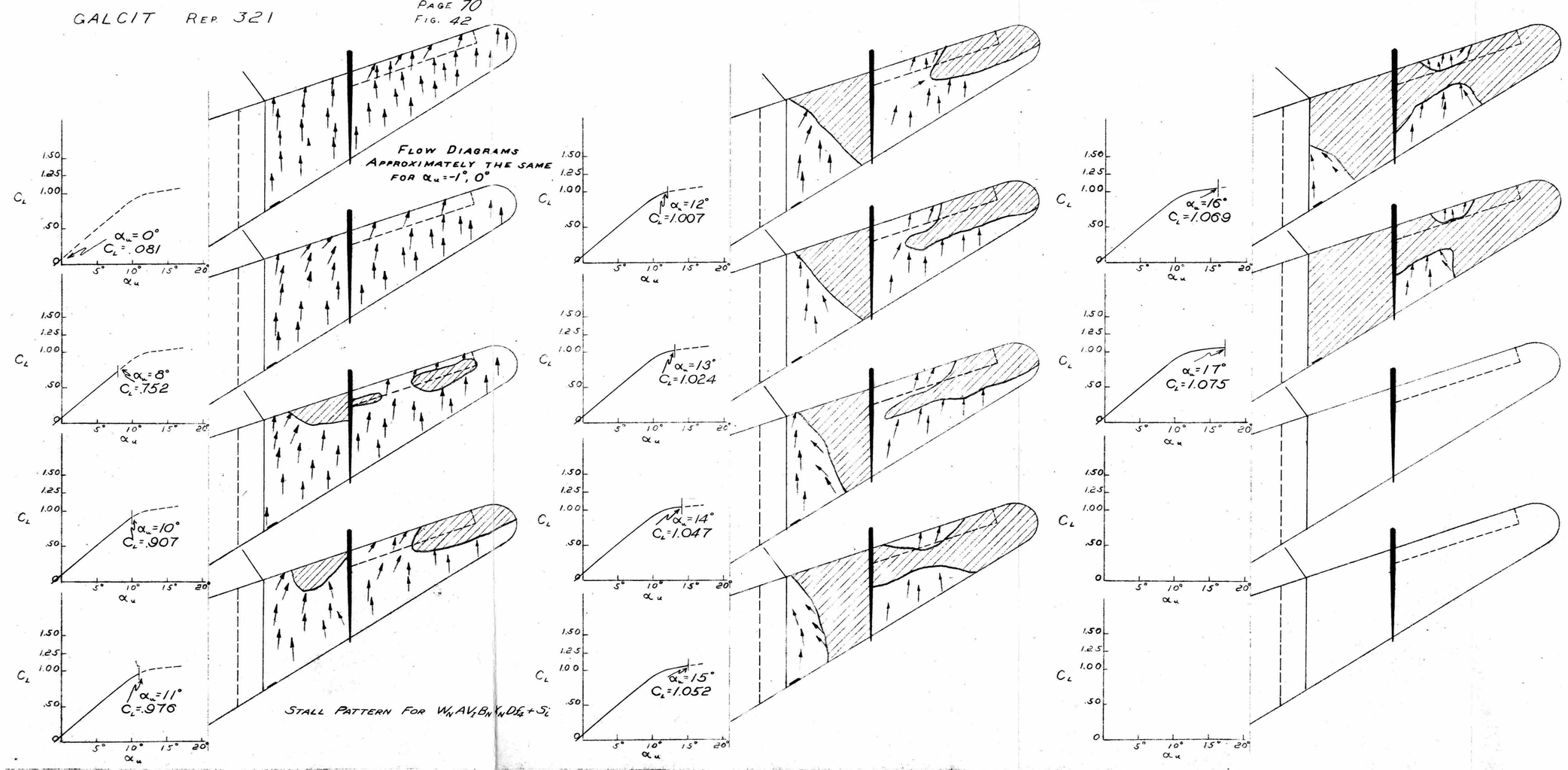
FLOW DIAGRAMS APPROXIMATELY THE SAME FOR $\alpha_u = -1°, 0°$
$\alpha_u = 0°$ $C_L = .081$
$\alpha_u = 8°$ $C_L = .752$
$\alpha_u = 10°$ $C_L = .907$
$\alpha_u = 11°$ $C_L = .976$
$\alpha_u = 12°$ $C_L = 1.007$
$\alpha_u = 13°$ $C_L = 1.024$
$\alpha_u = 14°$ $C_L = 1.047$
$\alpha_u = 15°$ $C_L = 1.052$
$\alpha_u = 16°$ $C_L = 1.069$
$\alpha_u = 17°$ $C_L = 1.075$
STALL PATTERN FOR $W_N A V_2 B_N V_N D f_4 + S_1$
C_L
α_u

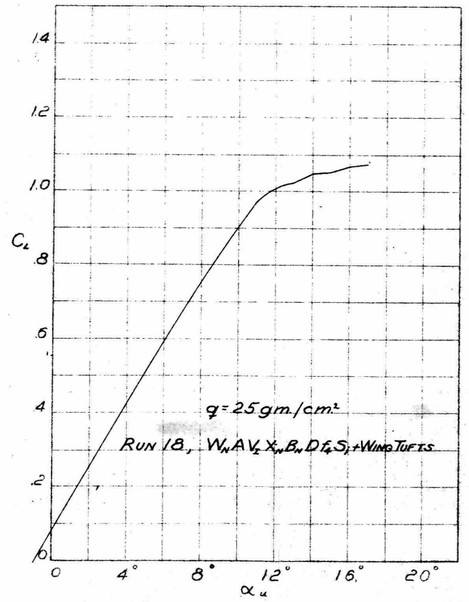
C_L
α_u
$q = 25 gm/cm^2$
RUN 18, $W_N A V_2 X_N B_N D f_4 S_1$ + WING TUFTS

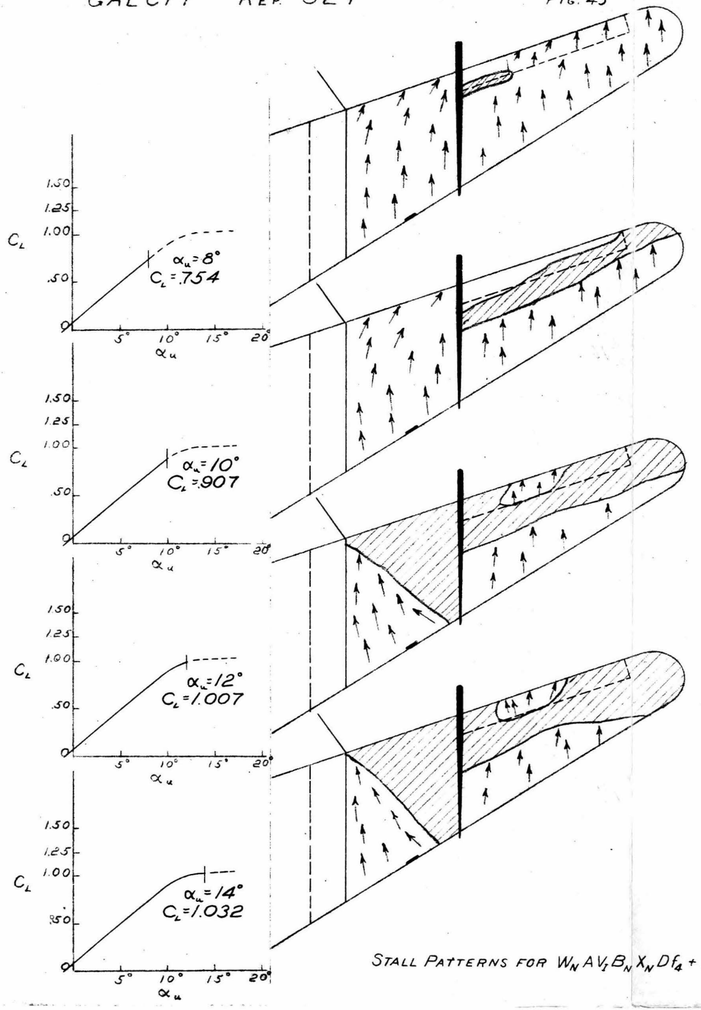

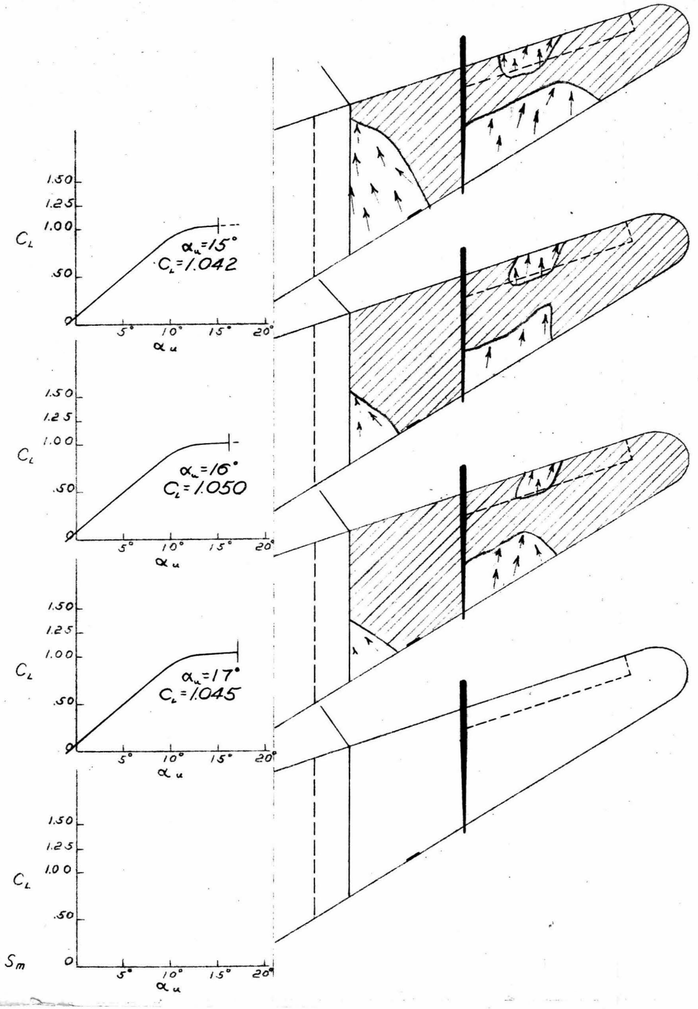

STALL PATTERNS FOR $W_N A V_1 B_N X_N D f_4 + S_m$

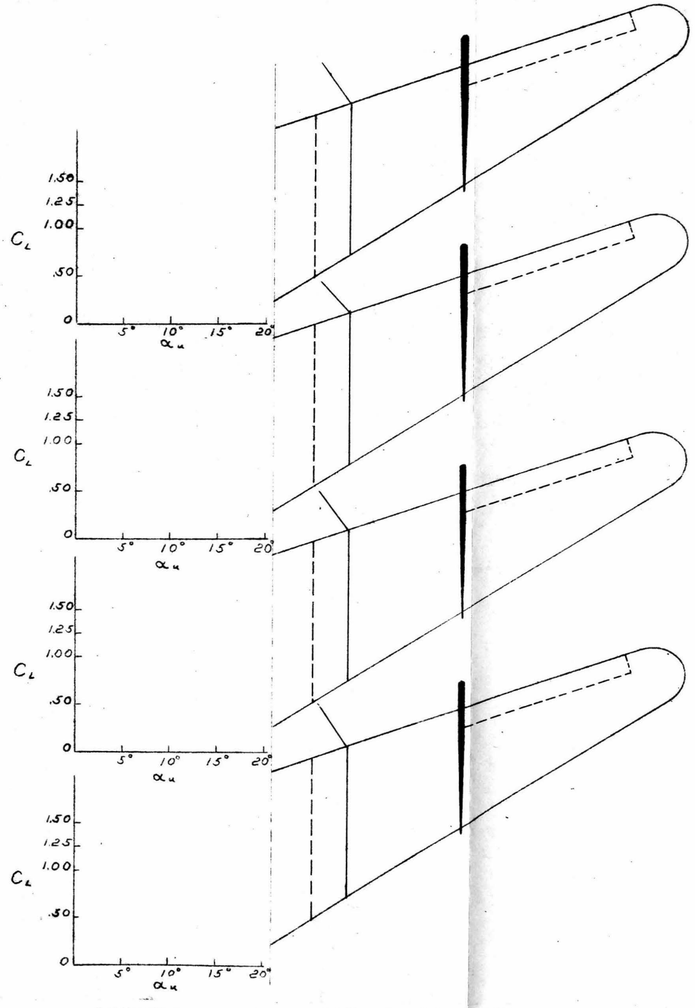

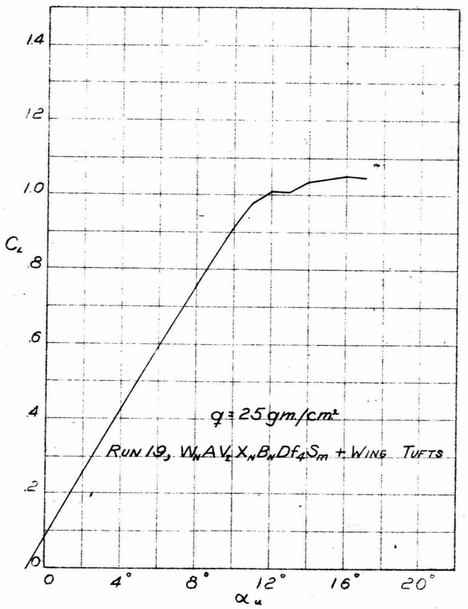

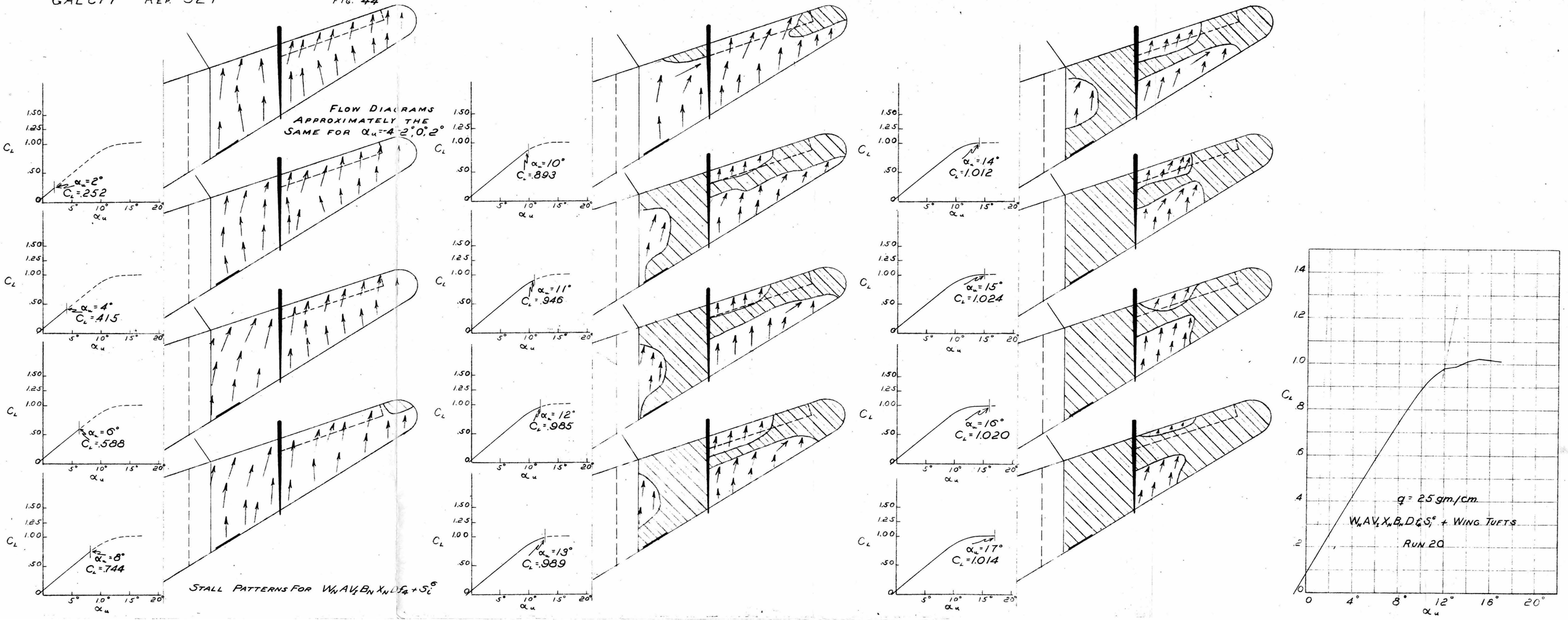
FLOW DIAGRAMS APPROXIMATELY THE SAME FOR α_u = -4°, -2°, 0°, 2°
α_u = 2°
C_L = .252
α_u = 4°
C_L = .415
α_u = 6°
C_L = .588
α_u = 8°
C_L = .744
α_u = 10°
C_L = .893
α_u = 11°
C_L = .946
α_u = 12°
C_L = .985
α_u = 13°
C_L = .989
α_u = 14°
C_L = 1.012
α_u = 15°
C_L = 1.024
α_u = 16°
C_L = 1.020
α_u = 17°
C_L = 1.014
C_L
α_u
STALL PATTERNS FOR $W_N A V_1 B_N X_N D \phi + S_i^\circ$
q = 25 gm./cm.
$W_N A V_1 X_N B_N D \phi S_i^\circ$ + WING TUFTS
RUN 20

$q = 25\ gm/cm^2$, $a_r = a_l = 0°$, $r = 0°$, $i = 2.25°$

x	$W_N A^* V_1 B_N X_N f_4 P^{30}_{RRW}$	+	WING TUFTS		,	RUN 31
⊙	"	+	"	+ S^2_Δ	,	" 44
△	"	+	"	+ S^3_Δ	,	" 45
⊡	"	+	"	+ S'_Δ	,	" 46

FOR P^{30}_{RRW}, $J = 1.59$

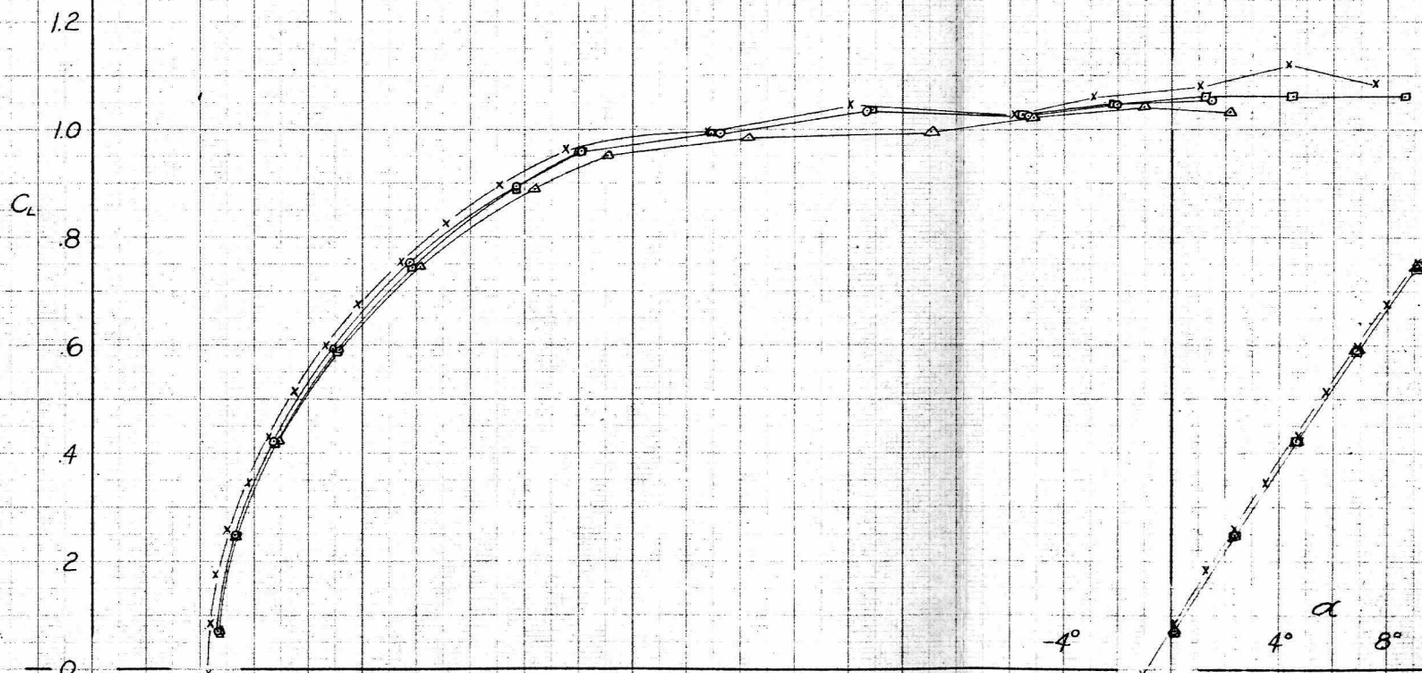

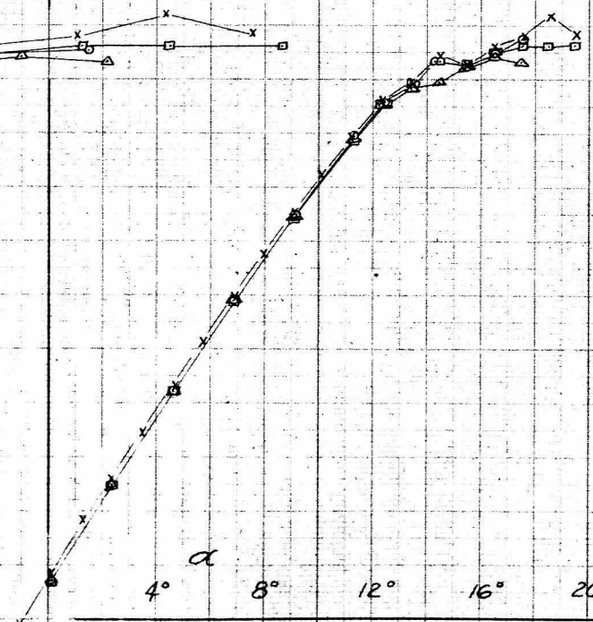

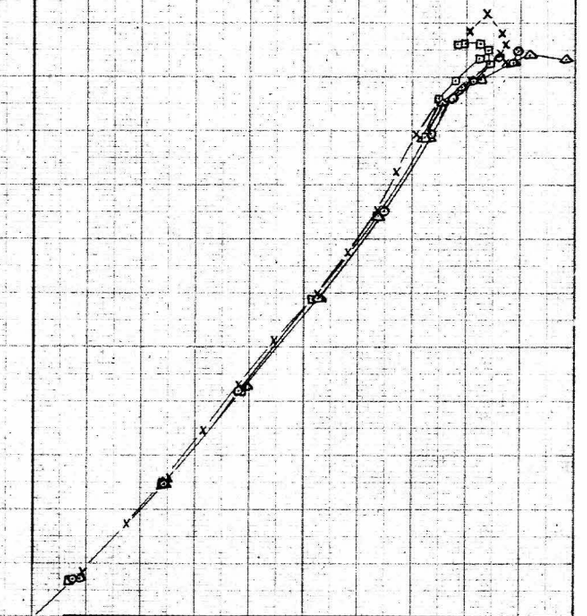

EFFECTS OF SPOILERS S'_Δ, S^2_Δ AND S^3_Δ ON CONFIGURATION
$W_N A^* V_1 B_N X_N f_4 P^{30}_{RRW}$

THREE COMPONENT DATA

$q = 25\ gm/cm^2$; $a_r = a_2 = r = 0°$; $i = 2.25°$

× $W_N A^* V_I B_N X_N f_4 P^{30}_{RRW}$ + WING TUFTS, RUN 31
⊙ " + " $+S^2_\Delta$, " 44
△ " + " $+S^3_\Delta$, " 45
□ " + " $+S^1_\Delta$, " 46

FOR P^{30}_{RRW}, $J = 1.59$

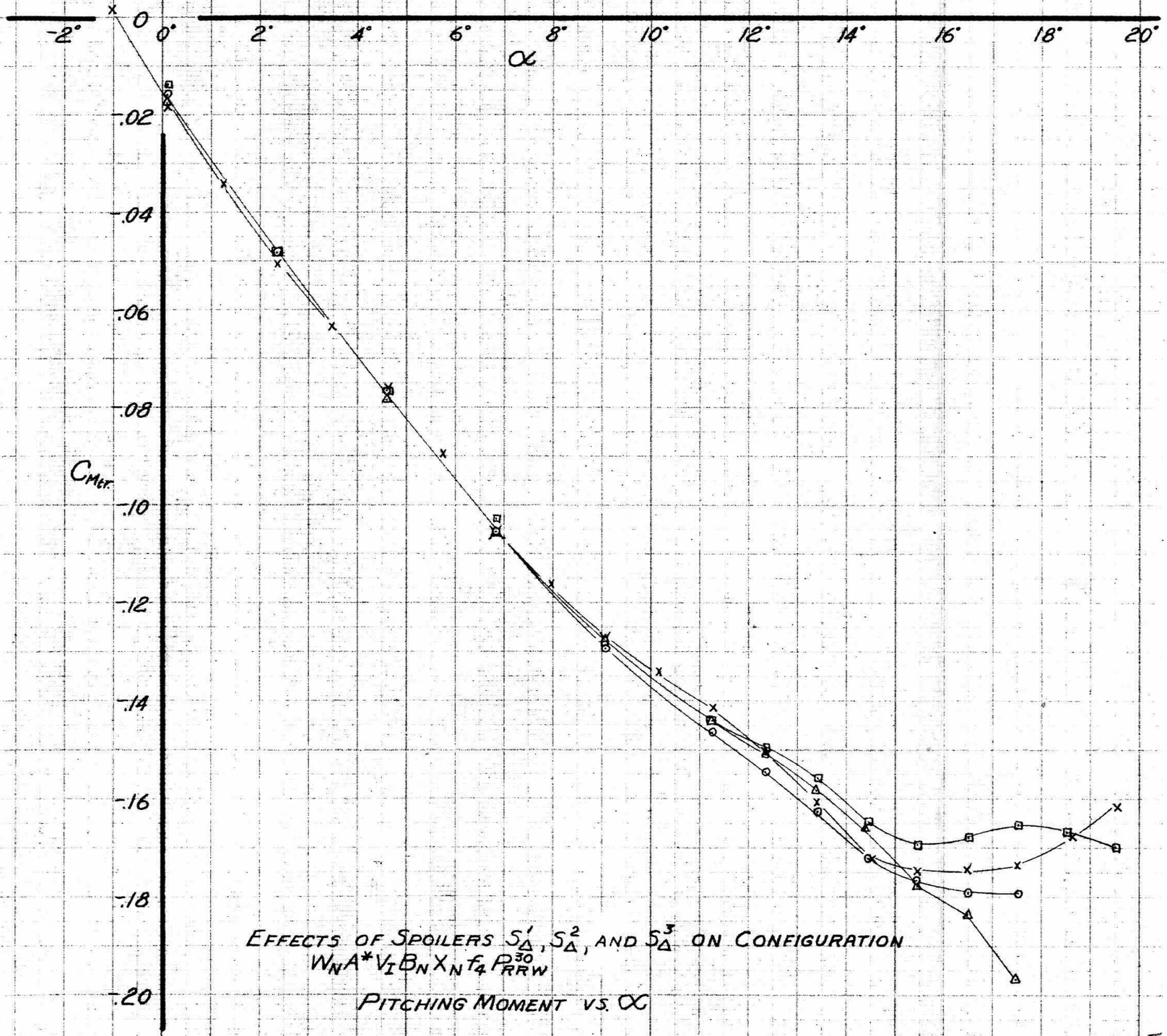

EFFECTS OF SPOILERS S^1_Δ, S^2_Δ, AND S^3_Δ ON CONFIGURATION $W_N A^* V_I B_N X_N f_4 P^{30}_{RRW}$

PITCHING MOMENT VS. α

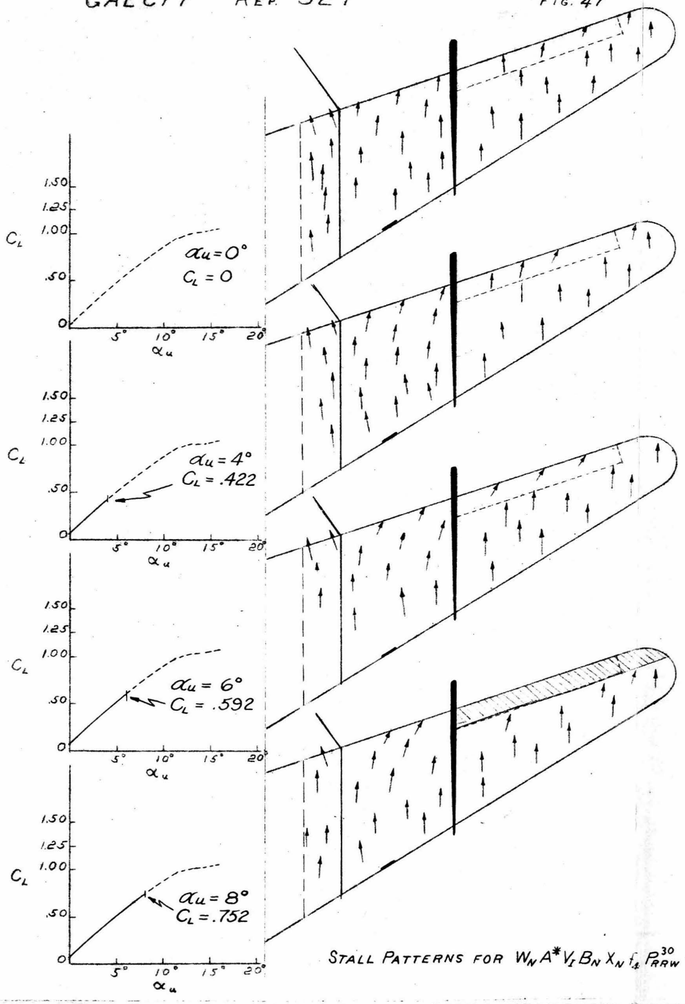

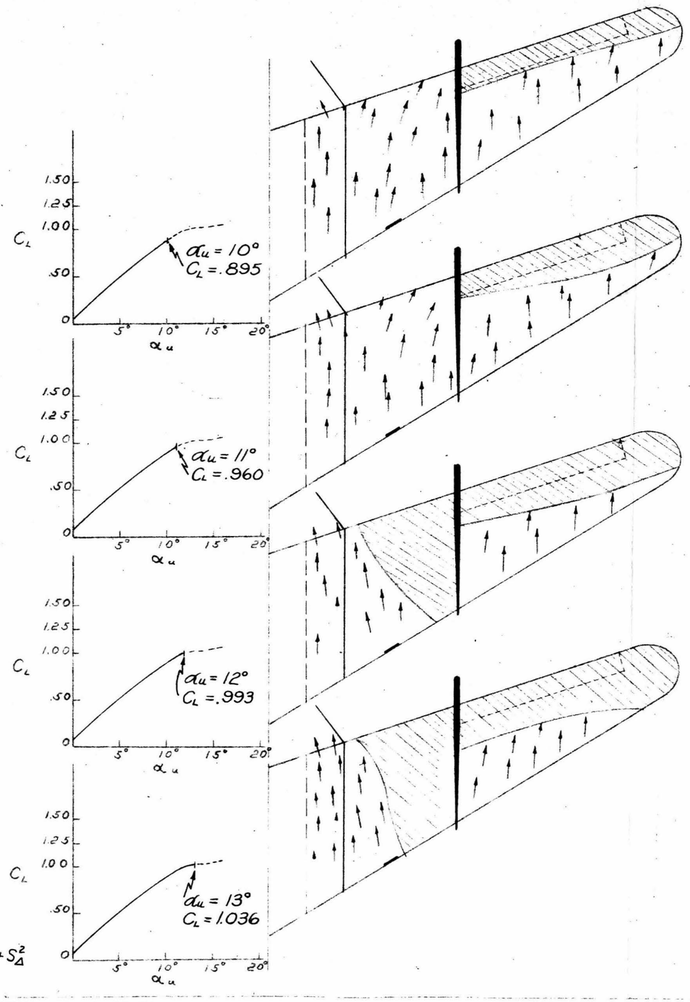

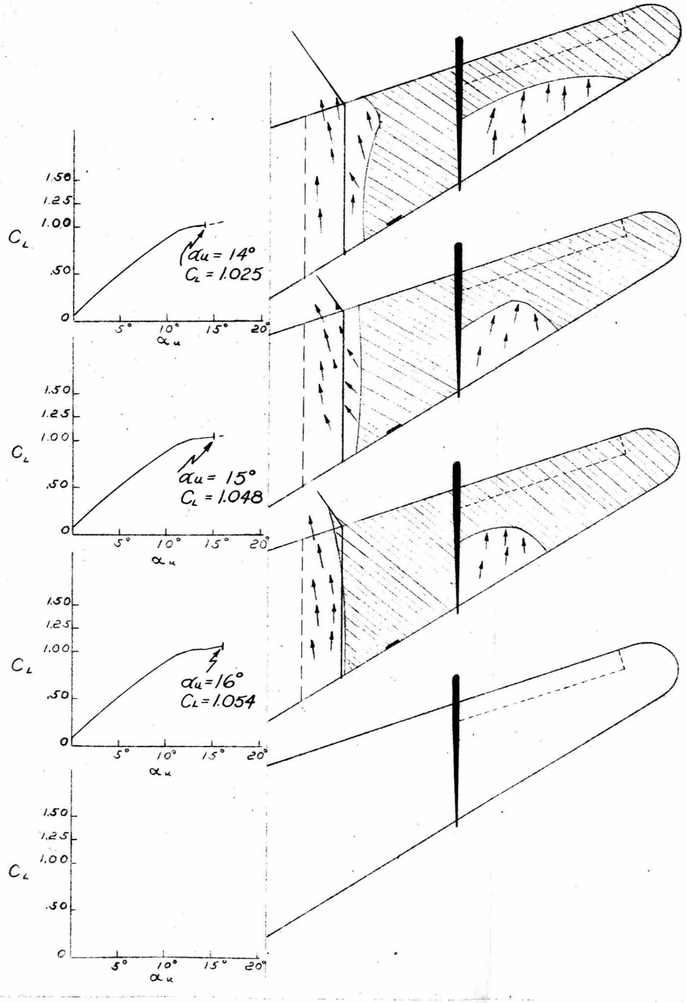

STALL PATTERNS FOR $W_N A^* V_t B_N X_N f_s P_{RRW}^{30} + S_\Delta^2$

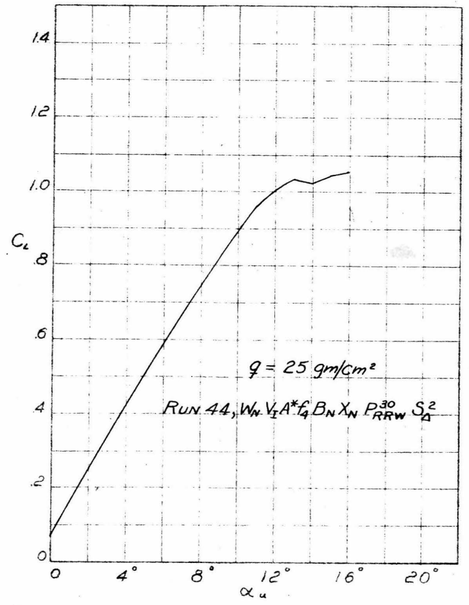

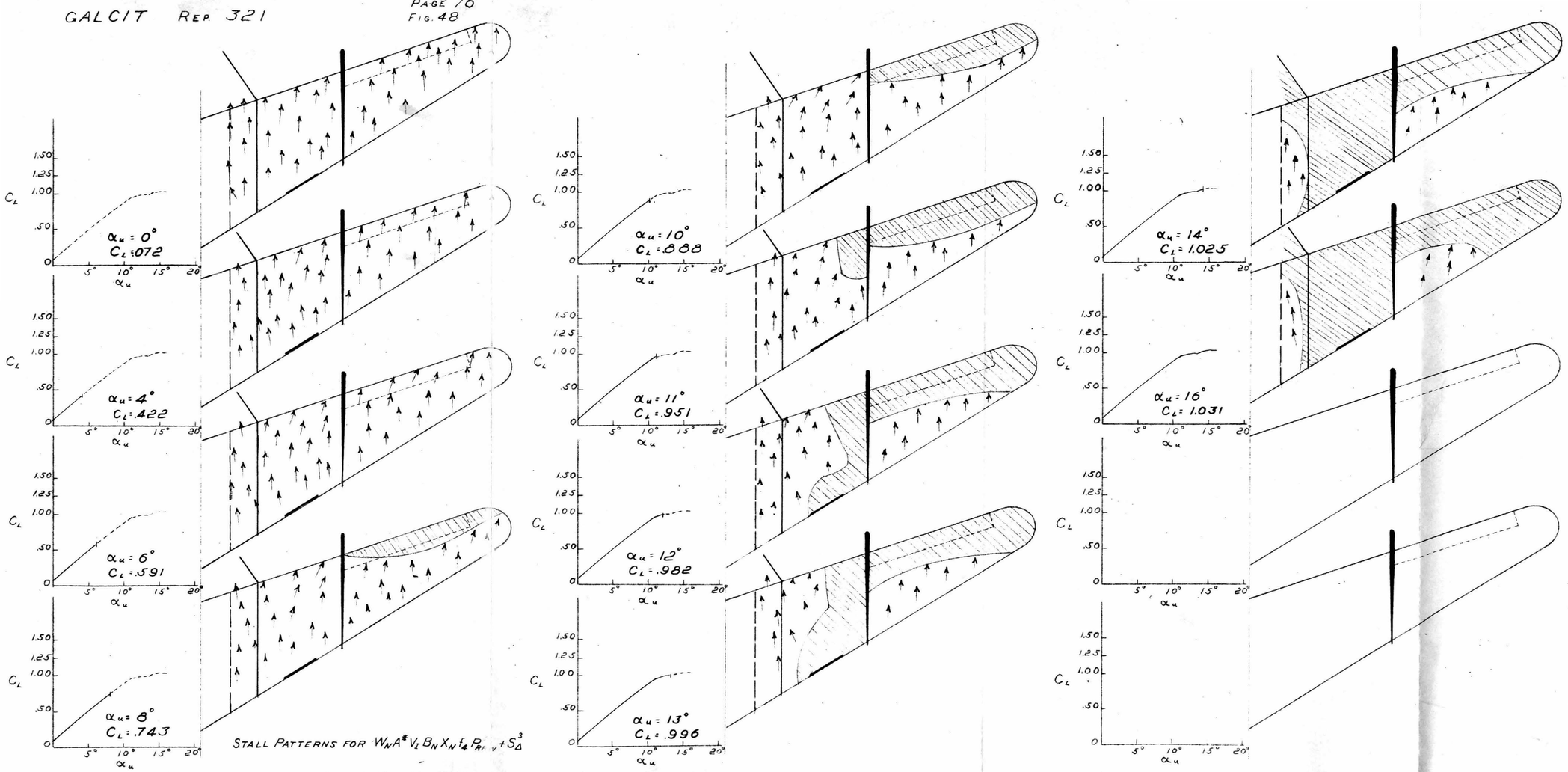

STALL PATTERNS FOR $W_N A^{*} V_1 B_N X_N f_4 P_{RN} + S_\Delta^3$

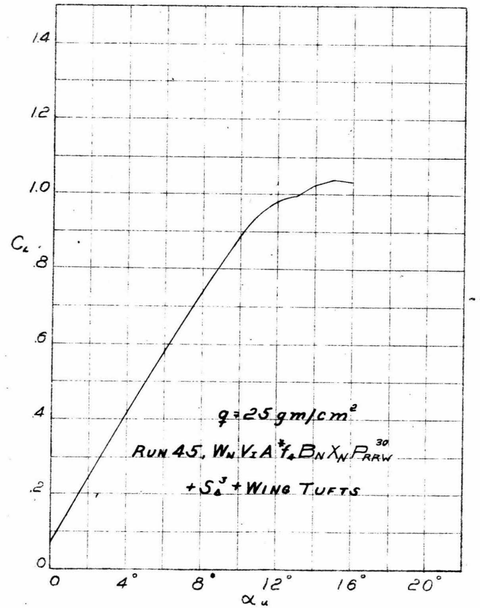

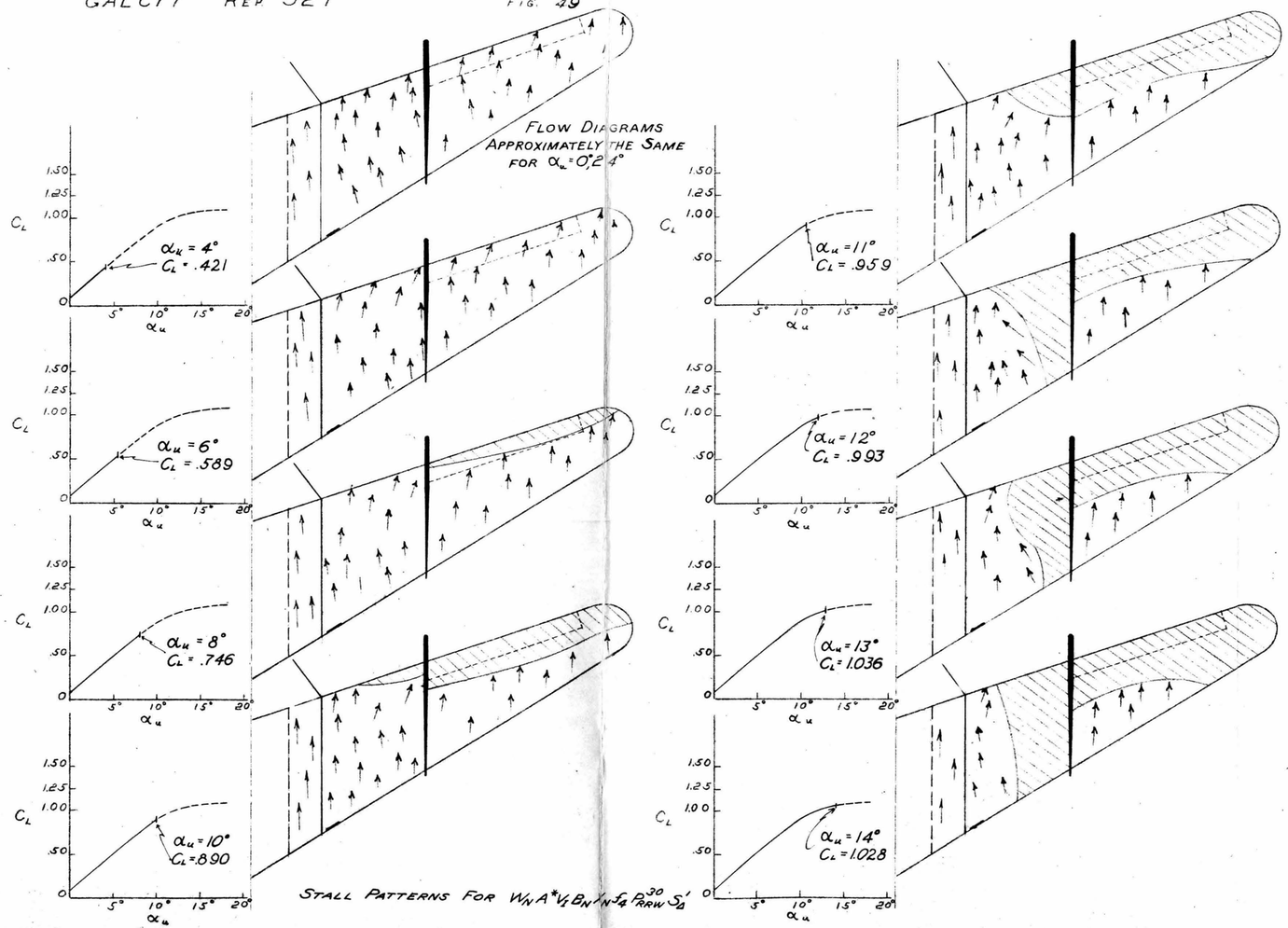

STALL PATTERNS FOR $W_N A^* \frac{1}{2} B_N Y_N \frac{1}{4} P^{30}_{RRW} S_A'$

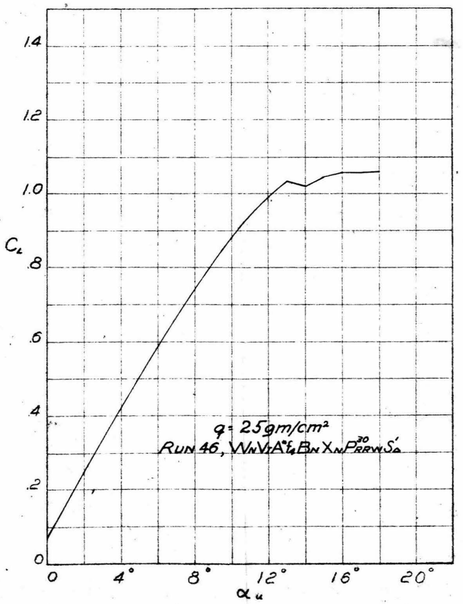

$q = 25$ gm./cm.^{2}, $i = 225°$, $a_r = a_l = -10°$, $r = 0°$

○ $W_N A^* V_I B_N X_N L L_N P^{30}_{RRW} F^{+5} f_4$ + WING TUFTS , RUN 27

△ " " + S_Δ , " 28

FOR P^{30}_{RRW}, $J = 1.59$

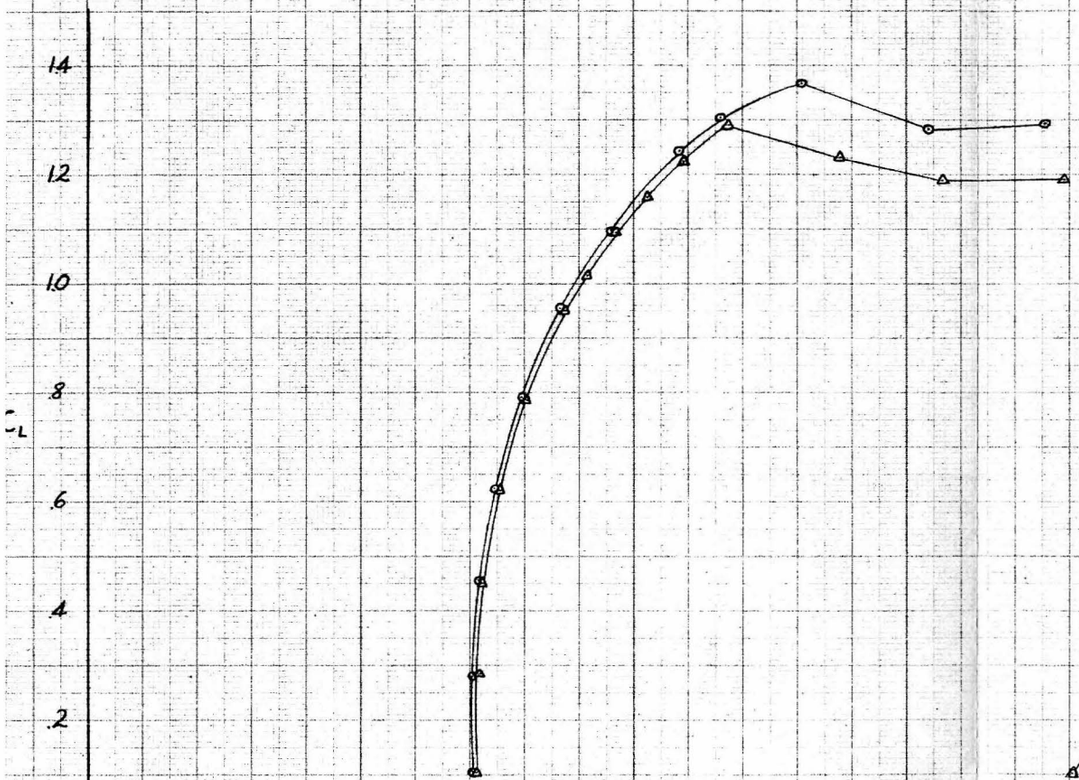

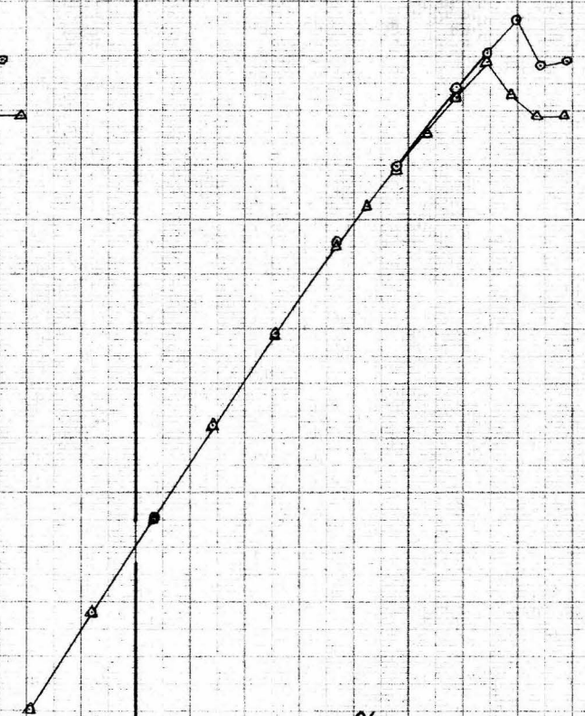

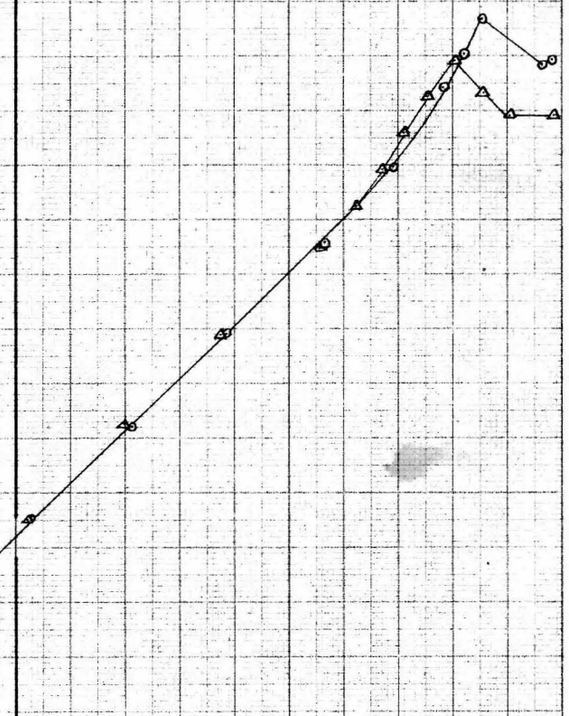

EFFECT OF SPOILER S_Δ ON CONFIGURATION $W_N A^* V_I B_N X_N L L_N P^{30}_{RRW} F^{+5} f_4$
WITH AILERONS UP 10°

THREE COMPONENT DATA

$q = 25\ gm/cm^2$, $\epsilon = 2.25°$, $\nu = 0°$

- $W_N A V_F S_4 X_N B_N R^{30}_{RRW} F^{45}$ + WING TUFTS, $a_n = a_\ell = -10°$, RUN 25A
- $W_N A^* V_F S_4 X_N B_N R^{30}_{RRW} F^{45}$ + " " $a_n = a_\ell = -10°$ " 26
- " + ΔL_N + " " $a_n = a_\ell = -10°$ " 27
- " + $\Delta L_N S_\Delta$ + " " $a_n = a_\ell = -10°$ " 28
- " + ΔL_N ± " " $a_n = a_\ell = 0°$ " 29
- $W_N A^* V_F X_N B_N L L_N R^{30}_{RRW} F^{45}$ + " " $a_n = a_\ell = 0°$ " 30

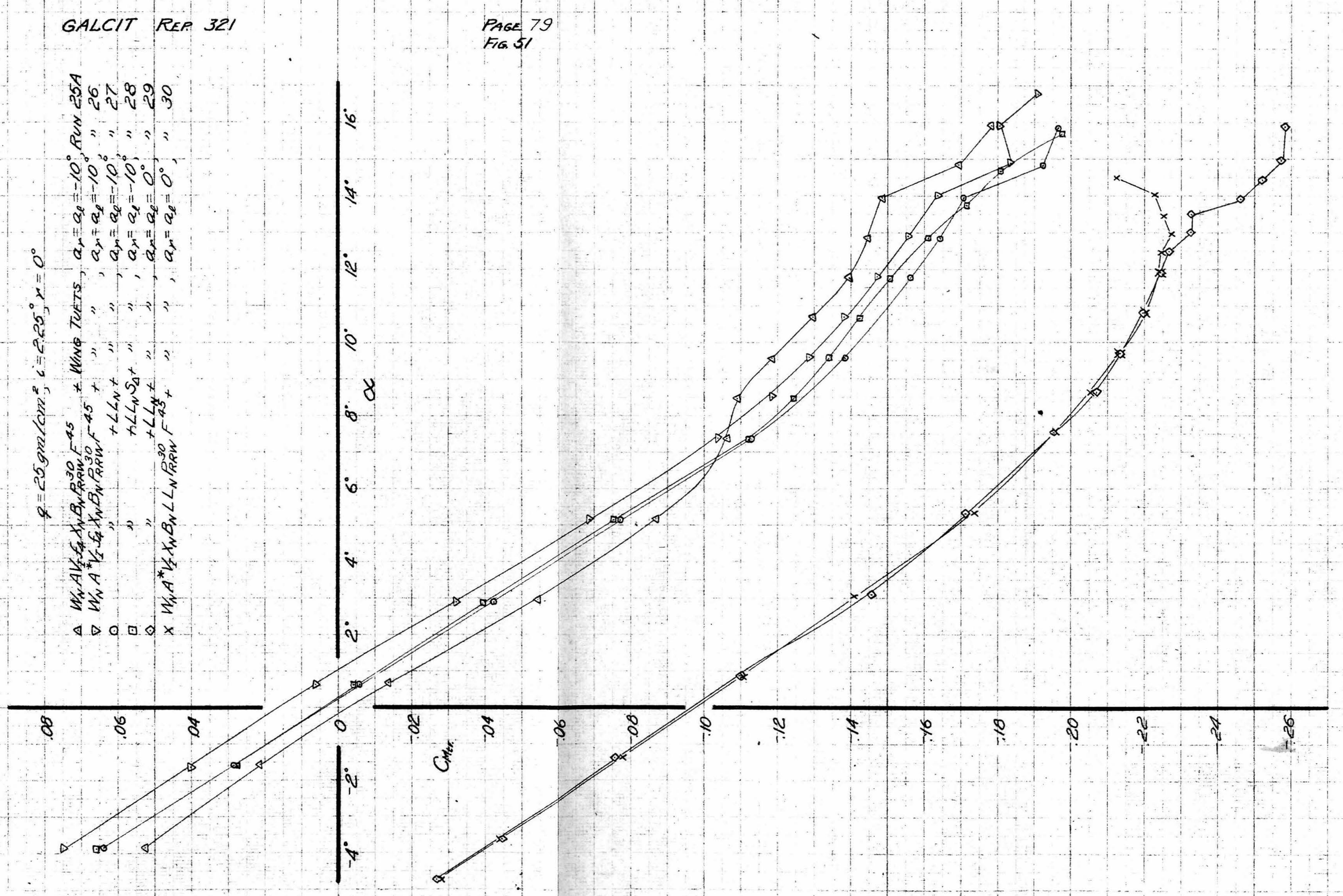

EFFECT OF f_4, AILERON DEFLECTION, AILERON GAP, AND SPOILER S_Δ WITH DEFLECTED FLAPS

PITCHING MOMENT VS α

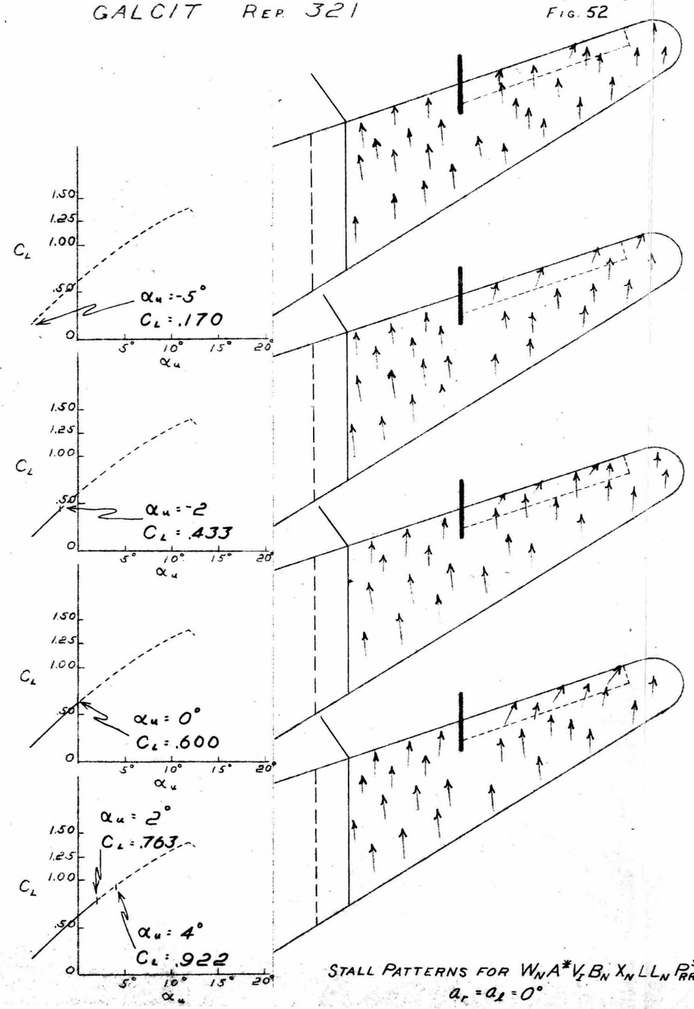

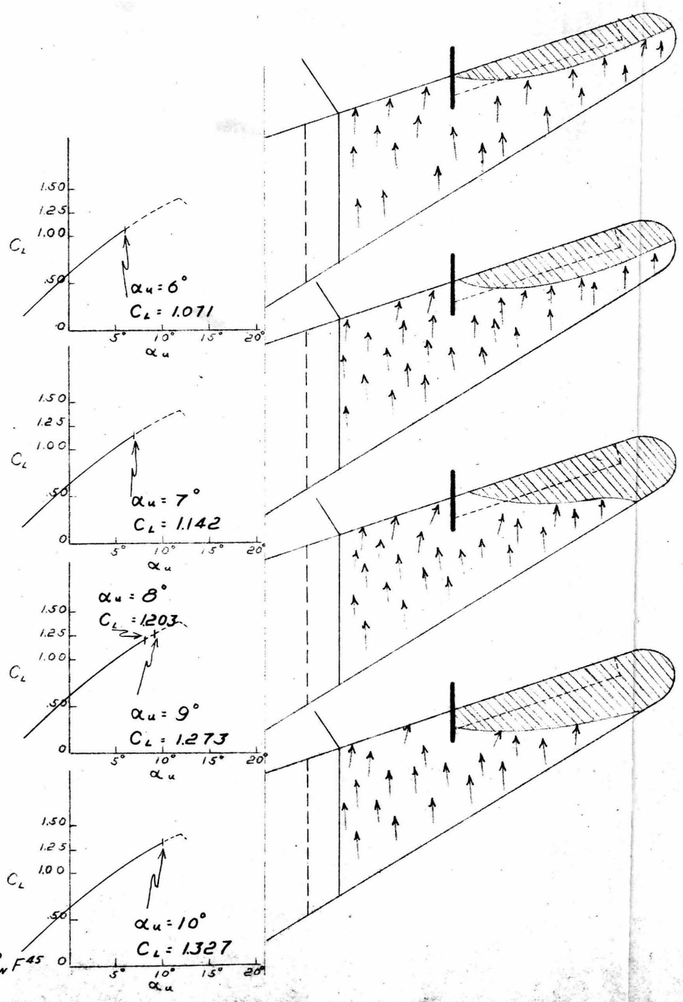

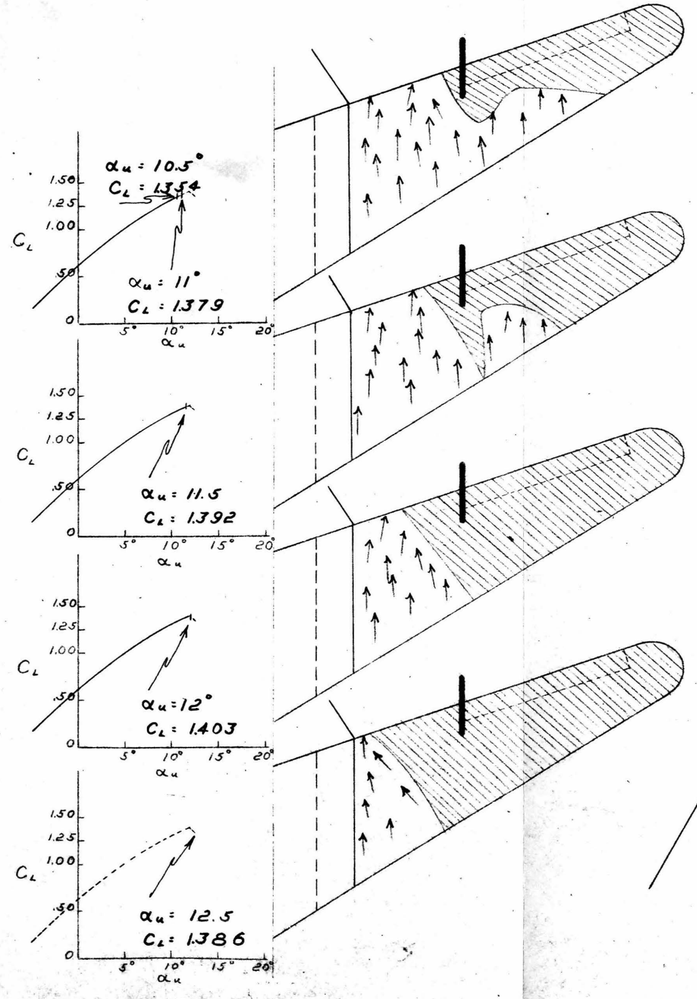

STALL PATTERNS FOR $W_N A^* V_t B_N X_N LL_N P^{30}_{RRW} F^{45}$
$a_r = a_t = 0°$

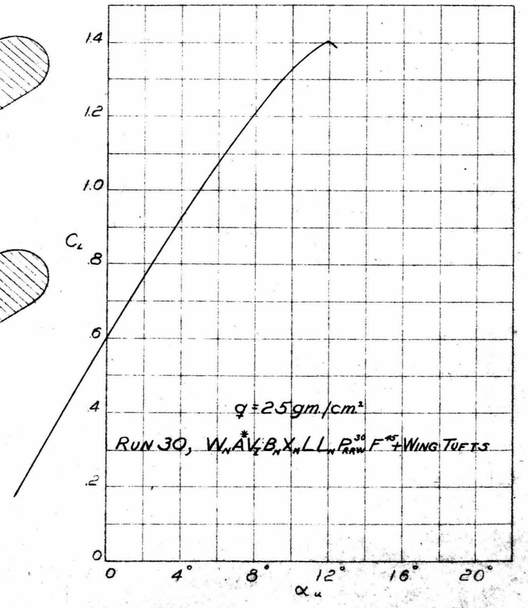

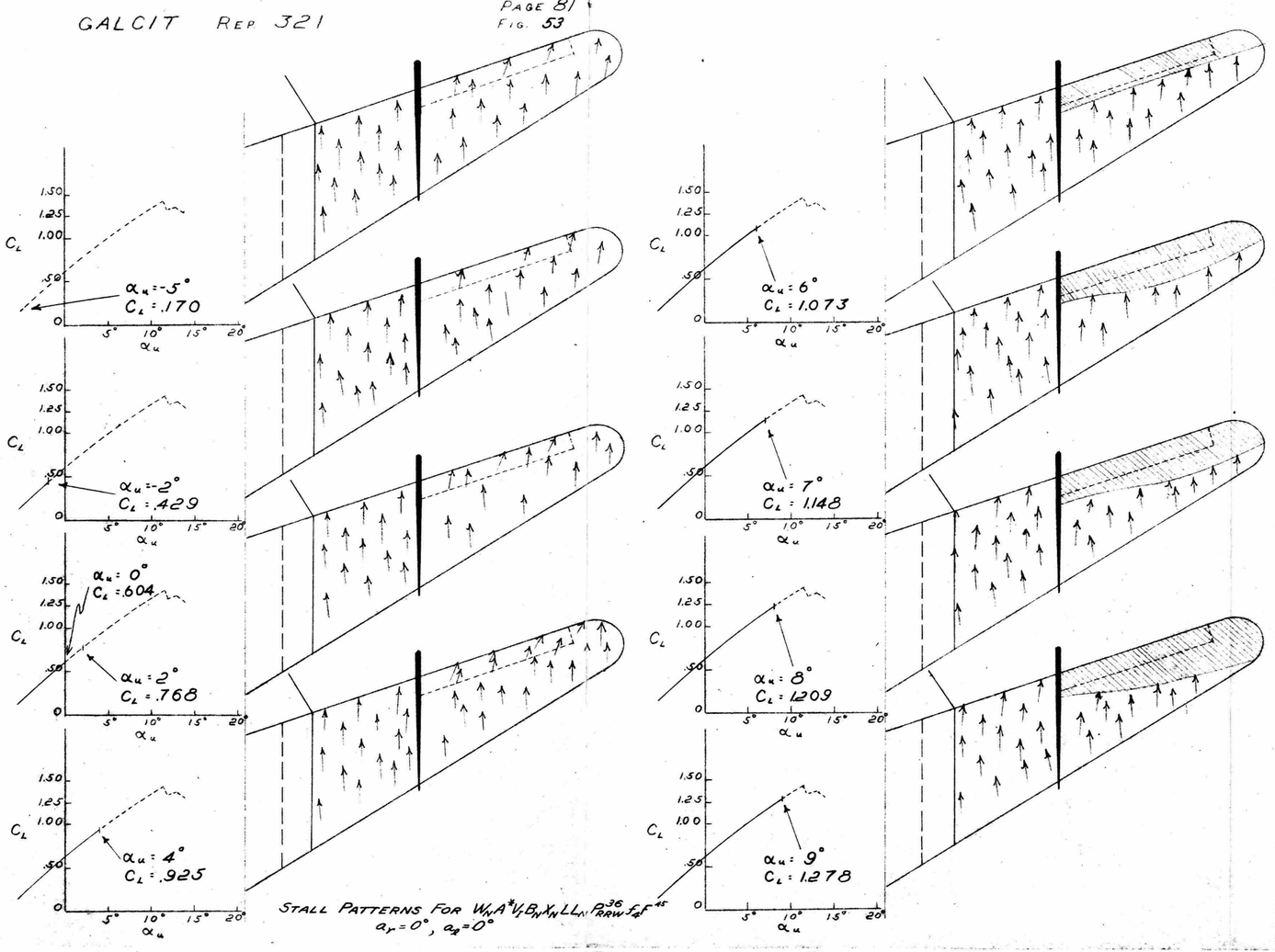

STALL PATTERNS FOR $W_N A^* V_2 B_N X_N LL_N P_{RRW}^{36} f_4 F^{45}$
$a_r = 0°$, $a_d = 0°$

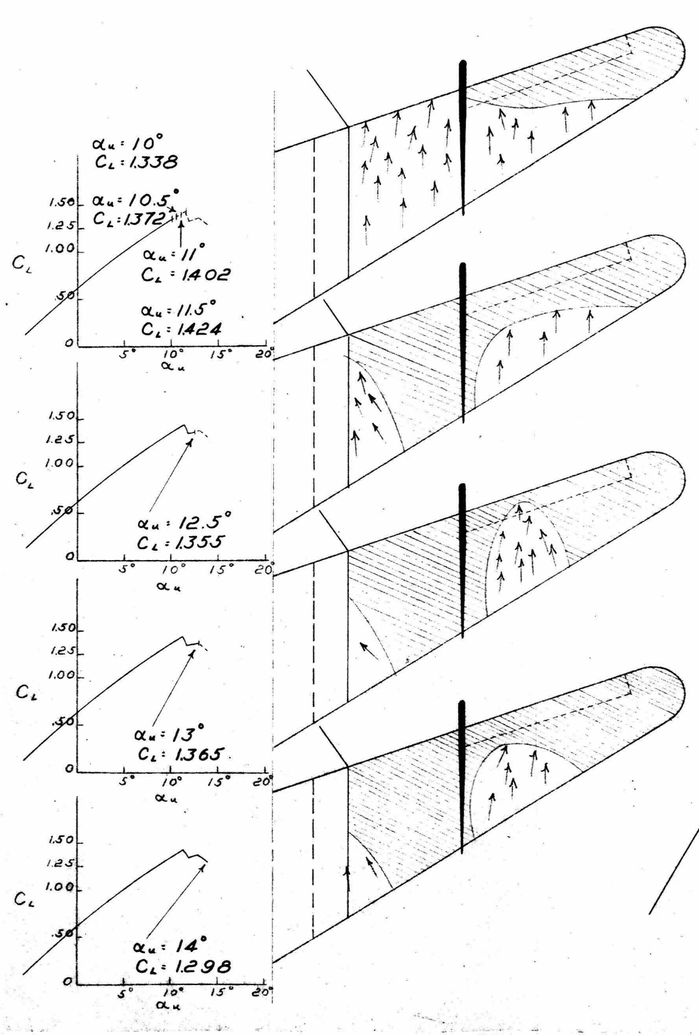

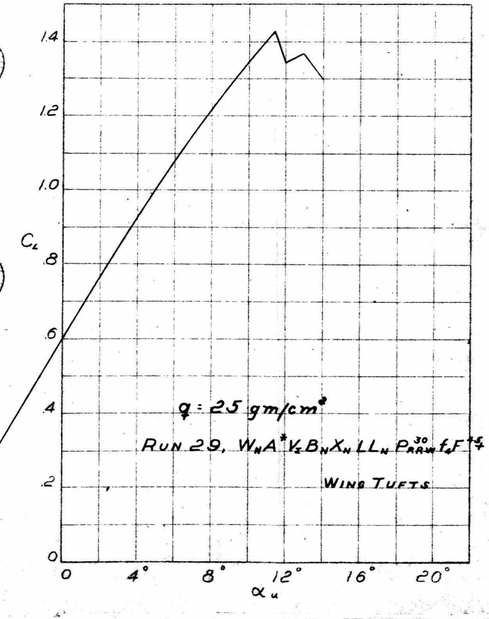

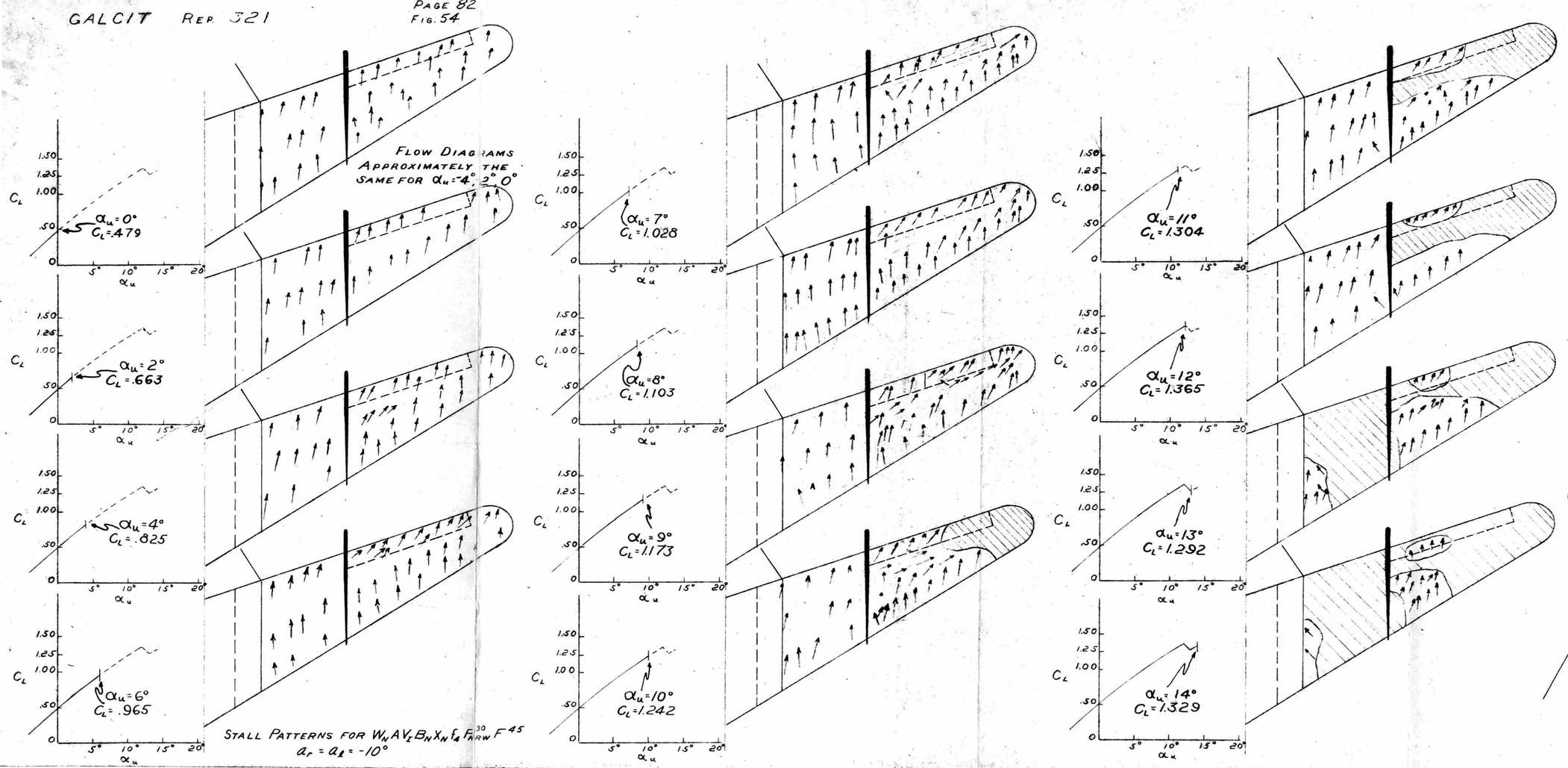
FLOW DIAGRAMS APPROXIMATELY THE SAME FOR $\alpha_u = -4°, 2°, 0°$
$\alpha_u = 0°$ $C_L = .479$
$\alpha_u = 2°$ $C_L = .663$
$\alpha_u = 4°$ $C_L = .825$
$\alpha_u = 6°$ $C_L = .965$
$\alpha_u = 7°$ $C_L = 1.028$
$\alpha_u = 8°$ $C_L = 1.103$
$\alpha_u = 9°$ $C_L = 1.173$
$\alpha_u = 10°$ $C_L = 1.242$
$\alpha_u = 11°$ $C_L = 1.304$
$\alpha_u = 12°$ $C_L = 1.365$
$\alpha_u = 13°$ $C_L = 1.292$
$\alpha_u = 14°$ $C_L = 1.329$
C_L
α_u
STALL PATTERNS FOR $W_N A V_L B_N X_N f_4 F^{30}_{FRRW} F^{45}$
$a_r = a_\ell = -10°$

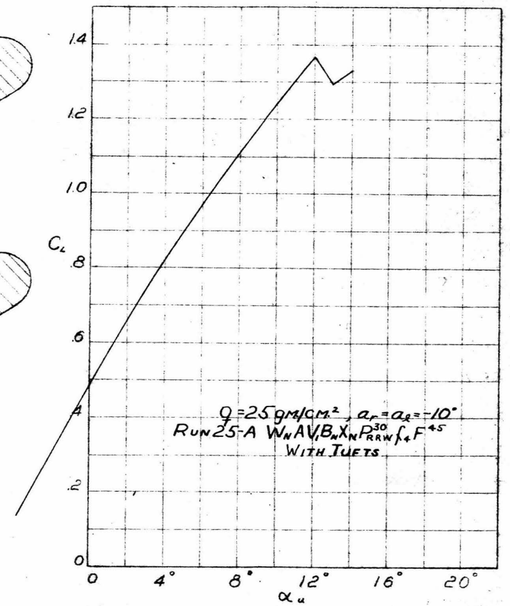
C_L
α_u
$Q = 25$ gm/cm²
$a_r = a_\ell = -10°$
RUN 25-A $W_N A V_L B_N X_N F^{30}_{FRRW} f_4 F^{45}$
WITH TUFTS

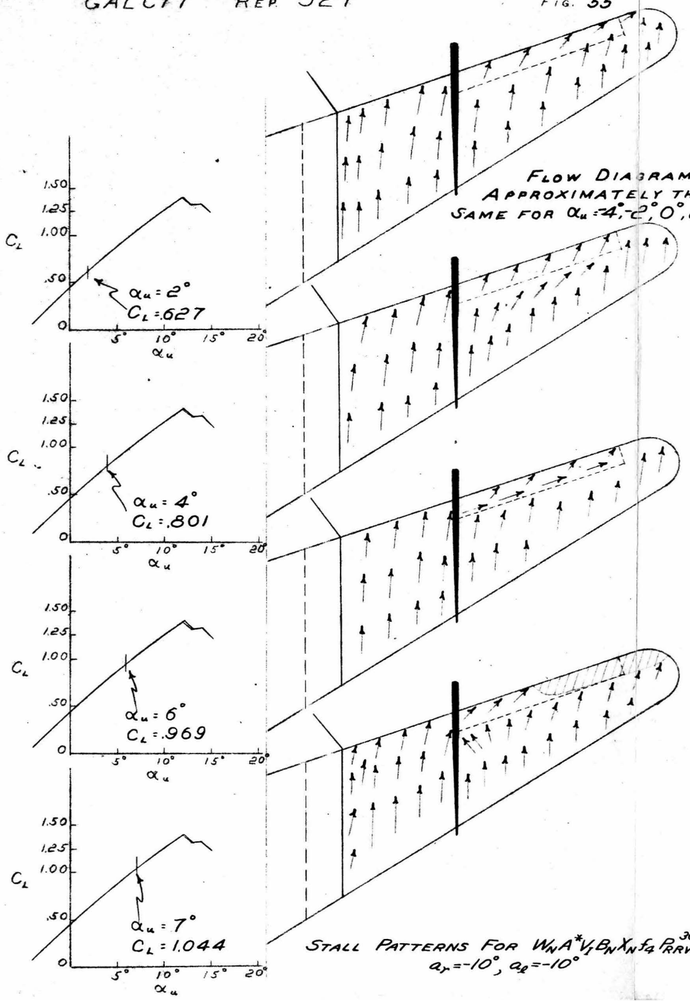

FLOW DIAGRAMS APPROXIMATELY THE SAME FOR $\alpha_u = 4°, 2°, 0°, 2°$

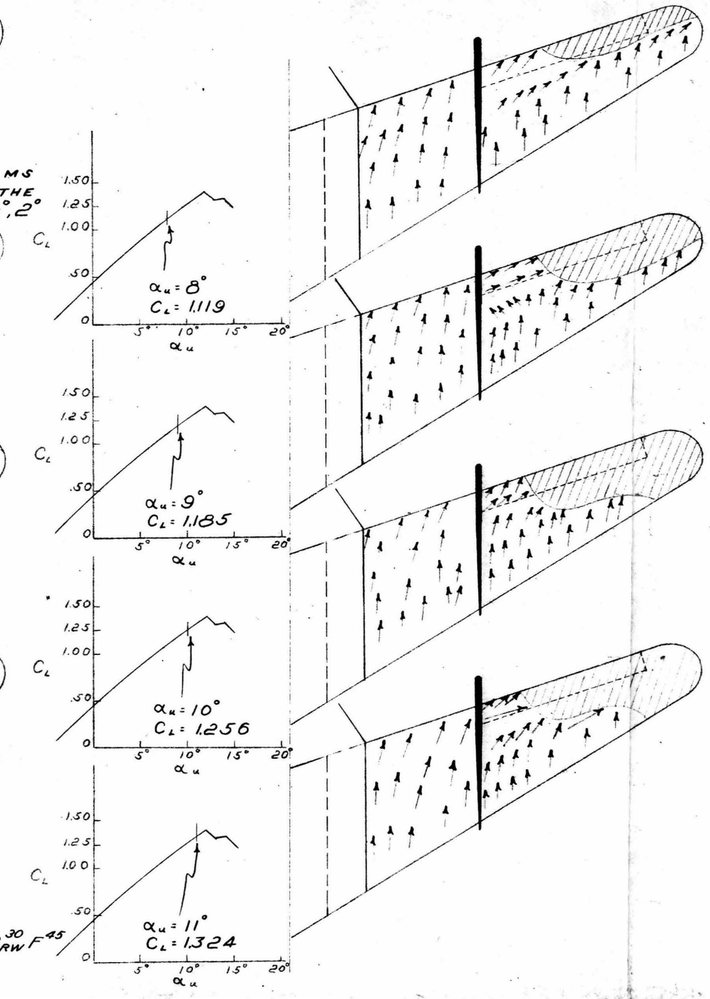

STALL PATTERNS FOR $W_N A^* V_1 B_N X_N f_4 P_{RRW}^{30} F^{45}$
$a_r = -10°$, $a_e = -10°$

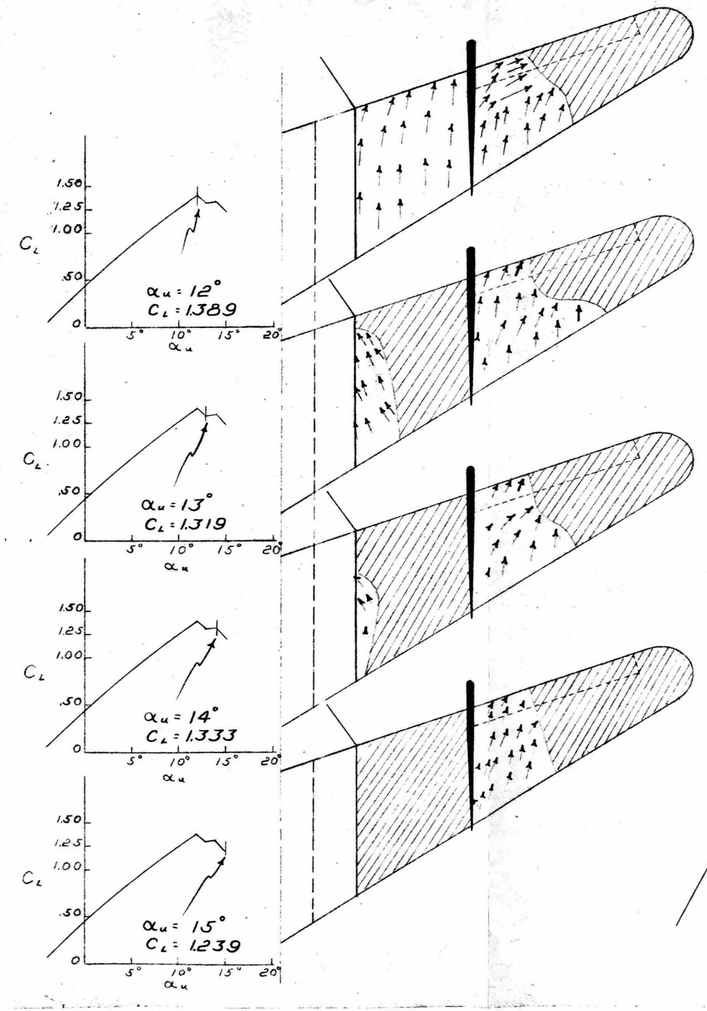

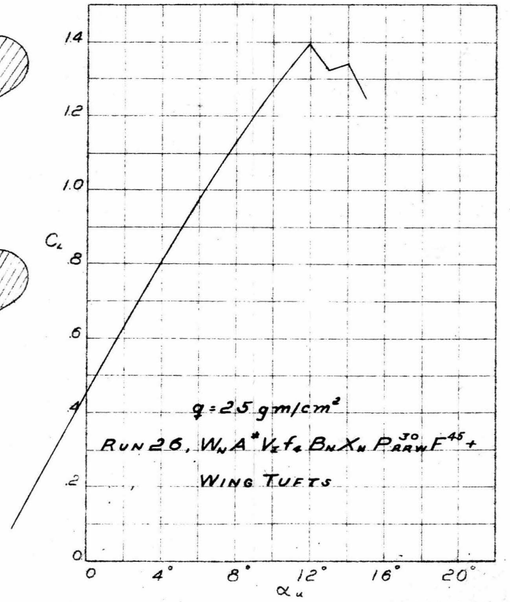

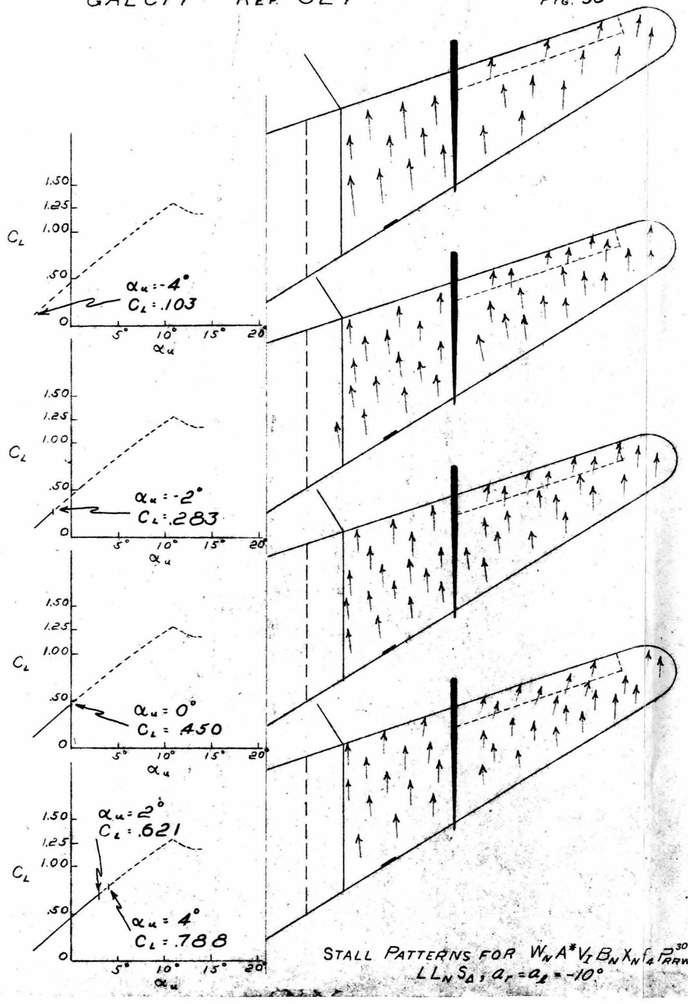

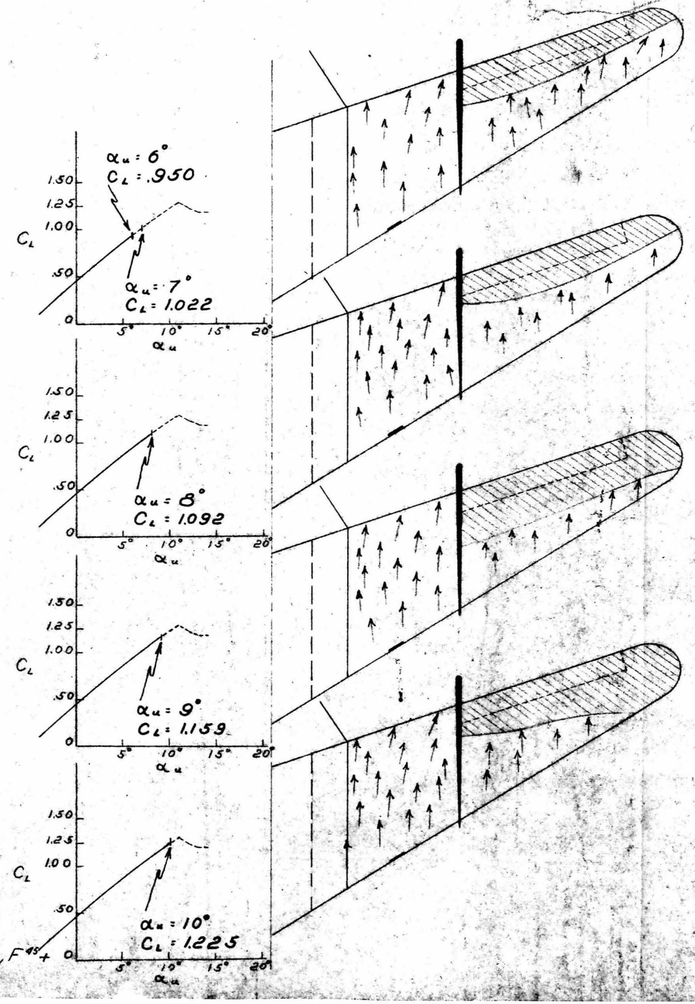

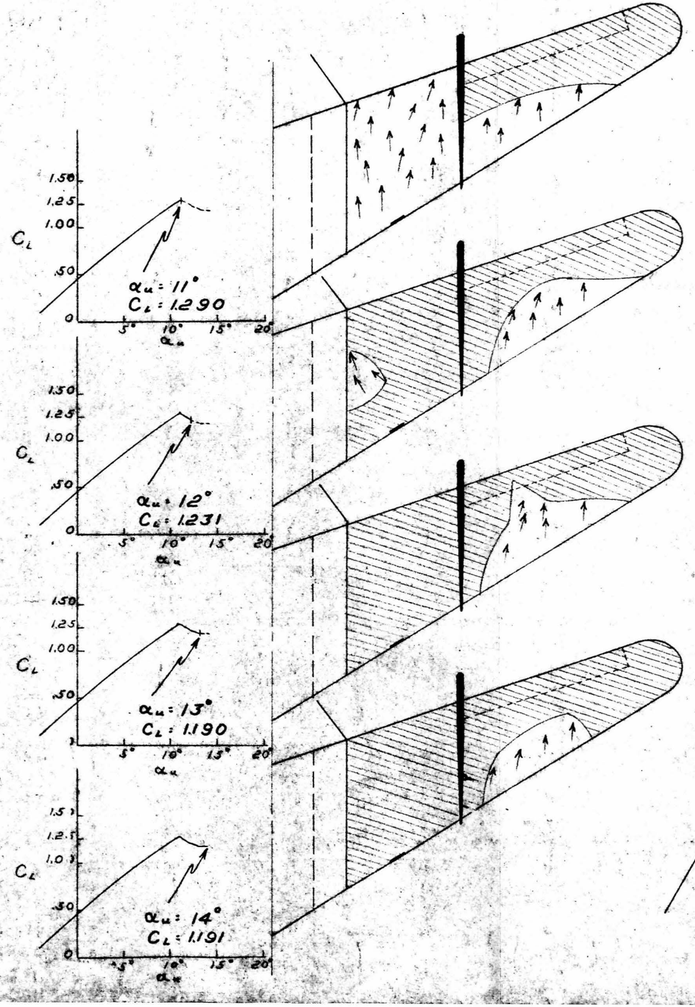

STALL PATTERNS FOR $W_N A^* V_t B_N X_N L L_N P_{PROP}^{30} F^{40} +$
$L L_N S_\Delta ; a_r = a_t = -10°$

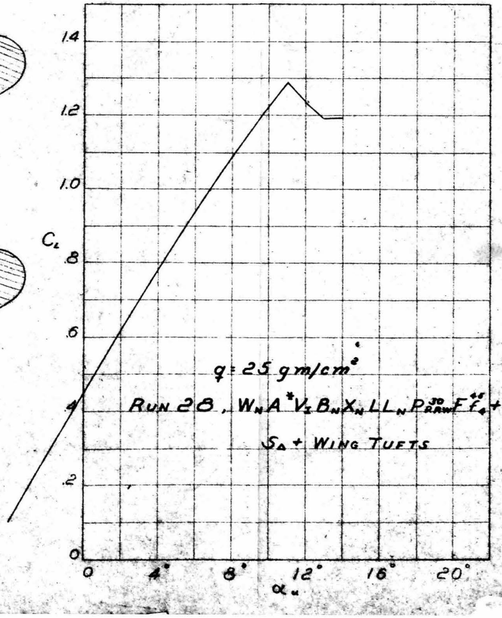

PHOTO 1.
$W_N AV_I f_1$, lower side view showing f_1

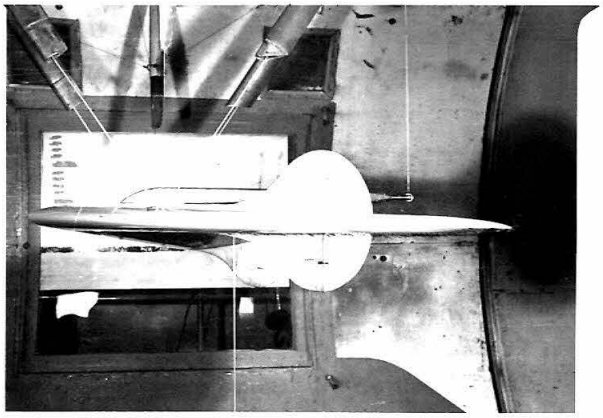

PHOTO 2.
$W_N AV_I f_2$, side view showing f_2

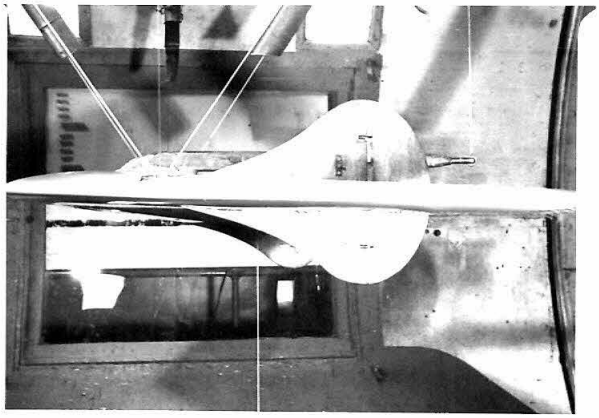

PHOTO 3.
$W_N AV_I f_3$, side view showing f_3

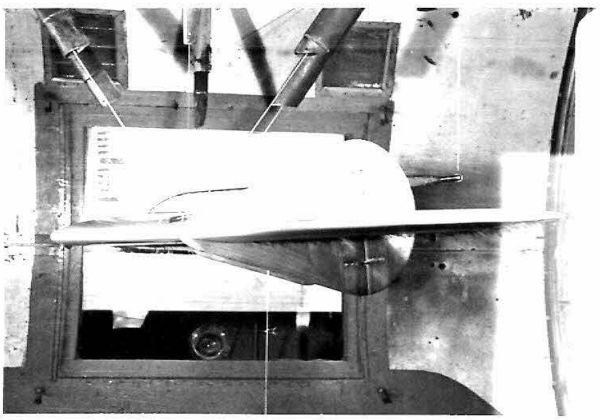

PHOTO 4.
$W_N AV_I f_4$, side view showing f_4

PHOTO 5.
$W_N A^* V_I f_5$, side view showing f_5

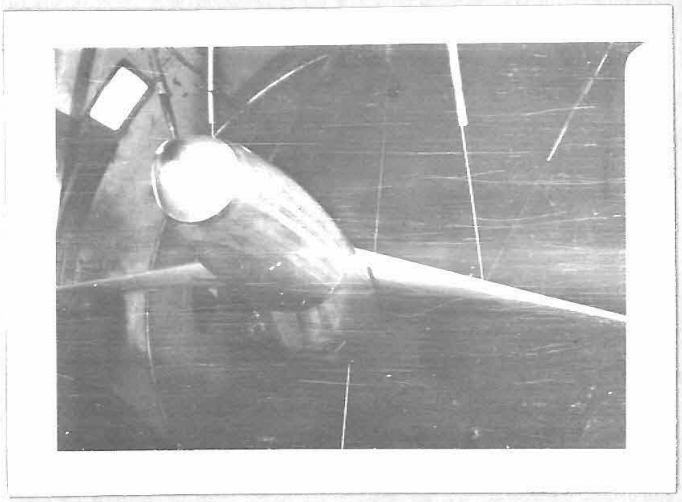

PHOTO 6.
$W_N A^* V_I B_N D$, 3/4 front view

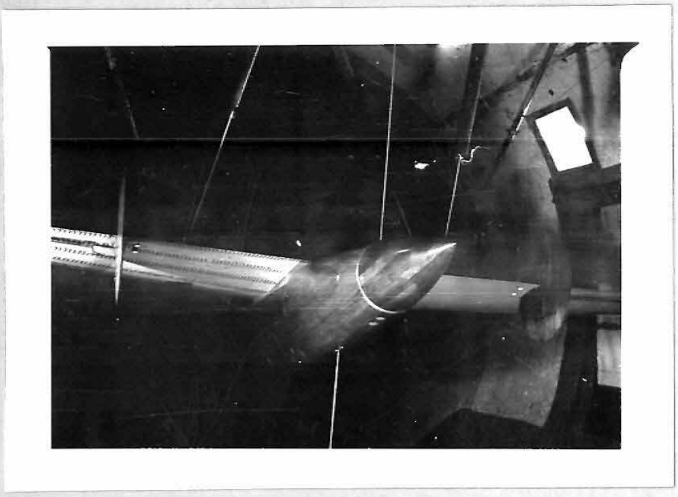

PHOTO 7.
$W_N A^* V_I B_N D$+Wing Tufts, 3/4 rear view

PHOTO 8.
$W_N A^* V_I B_N D$, side view

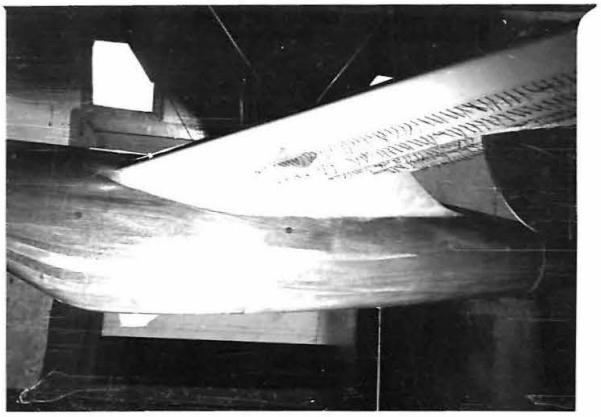

PHOTO 9.
$W_N A^* V_I B_N X_N D$ + Wing Tufts, side view showing fillet X_N

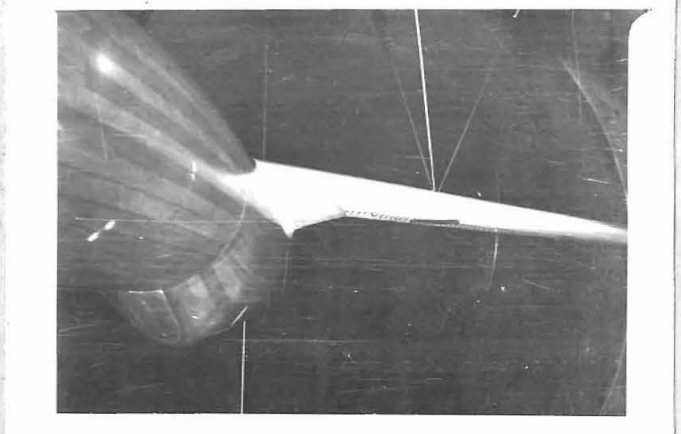

PHOTO 10
$W_N A^* V_I B_N X_N D$ + Wing Tufts, front view showing fillet X_N

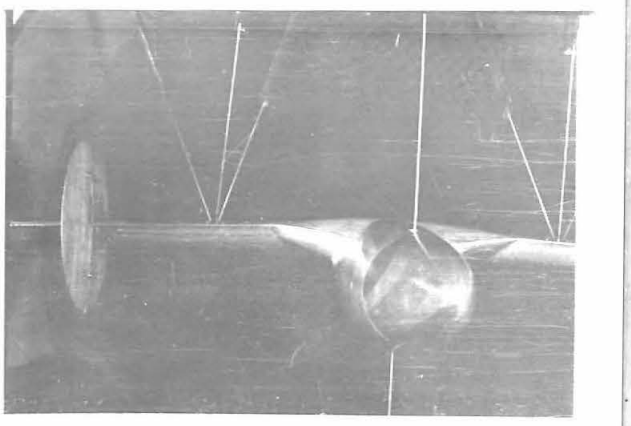

PHOTO 11
$W_N A^* V_I B_N X_N D$ + Wing Tufts, rear view showing fillet X_N

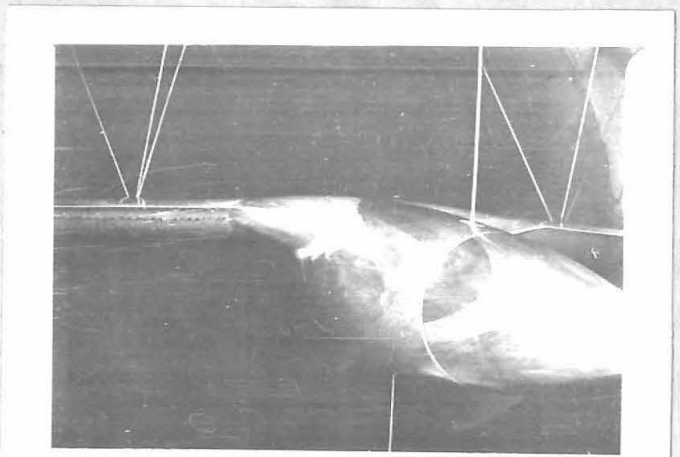

PHOTO 12
$W_N A^* V_I B_N X_N D$ + Wing Tufts, 3/4 rear view showing fillet X_N

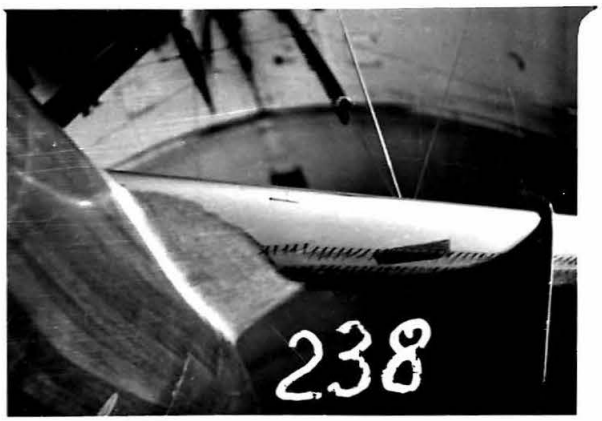

PHOTO 13
$W_N AV_I X_N B_N Df_4 S_i$ + Wing Tufts, upper front view showing spoiler S_i

PHOTO 14
$W_N AV_I X_N B_N Df_4 S_m$ + Wing Tufts, upper front view showing spoiler S_m

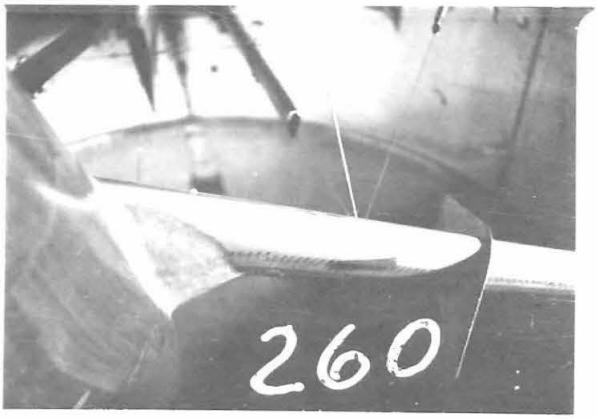

PHOTO 15
$W_N AV_I X_N B_N Df_4 S_i^6$ + Wing Tufts, upper front view showing spoiler S_i^6

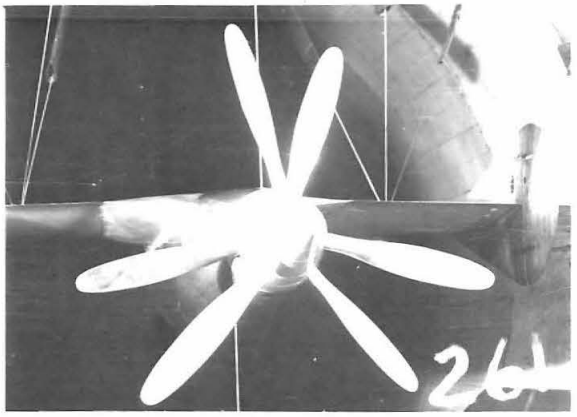

PHOTO 16
$W_N A*V_I X_N B_N f_4 P_{FLW}^{30} P_{RRW}^{30}$, rear view

PHOTO 17
$W_N A^* V_I X_N B_N f_4 P^{30}_{FLW} P^{30}_{RRW}$, side view

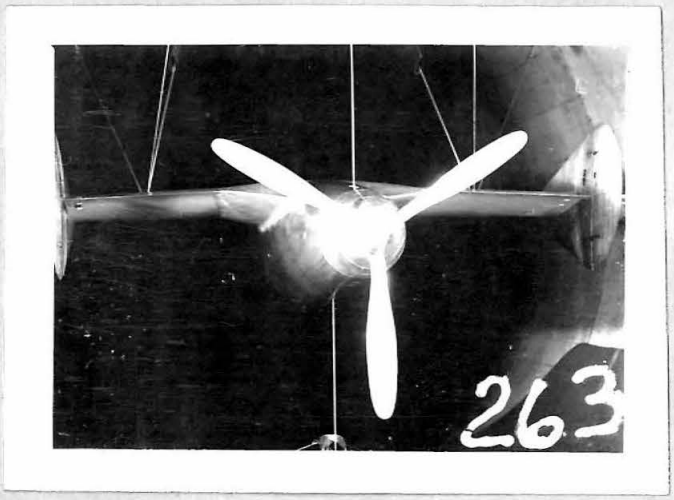

PHOTO 18
$W_N A^* V_I f_4 B_N X_N P^{30}_{RRW}$, rear view

PHOTO 19
$W_N A^* V_I f_4 B_N X_N P^{30}_{RRW}$, side view

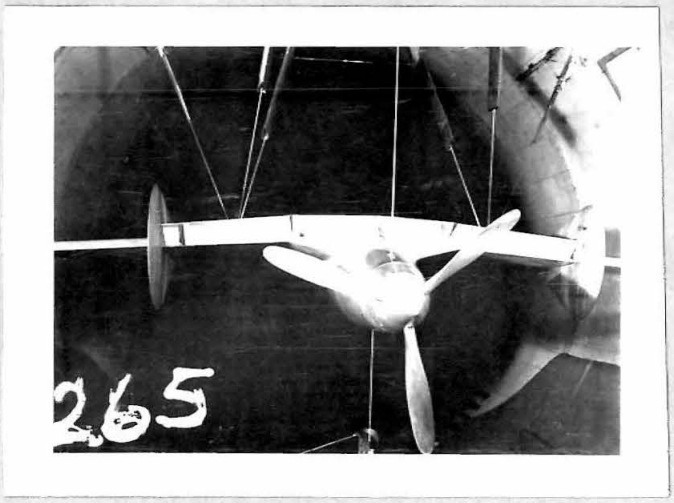

PHOTO 20
$W_N A^* V_I f_4 B_N X_N P^{30}_{RRW} F^{45}$, rear view showing flaps F^{45}

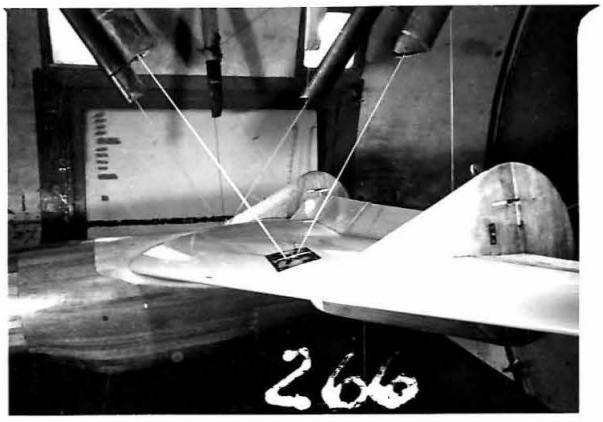

PHOTO 21
$W_N A^* V_I f_4 B_N X_N P^{30}_{RRW} F^{45}$, 3/4 side view showing flaps F^{45}

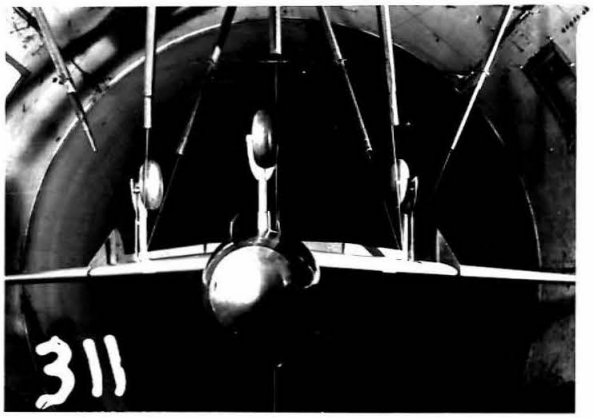

PHOTO 22
$W_N A^* V_I f_4 B_N X_N LL_N P^{30}_{RRW} F^{45} S_\Delta$ + Wing Tufts, front view showing landing gear LL_N and spoiler S_Δ

PHOTO 23
$W_N A^* V_I f_4 B_N X_N LL_N P^{30}_{RRW} F^{45} S_\Delta$ + Wing Tufts, side view showing landing gear LL_N and spoiler S_Δ

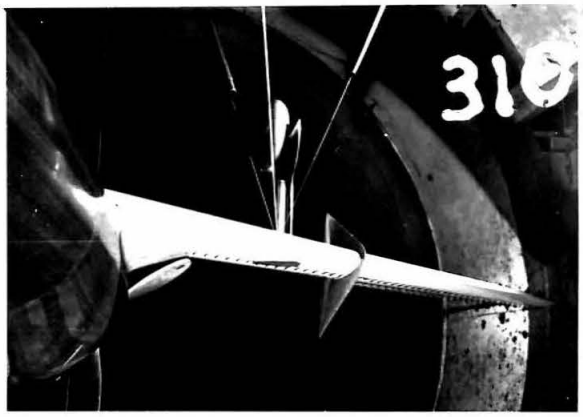

PHOTO 24
$W_N A^* V_I f_4 B_N X_N LL_N P^{30}_{RRW} F^{45} S_\Delta$ + Wing Tufts, front view of right wing showing landing gear LL_N and spoiler S_Δ

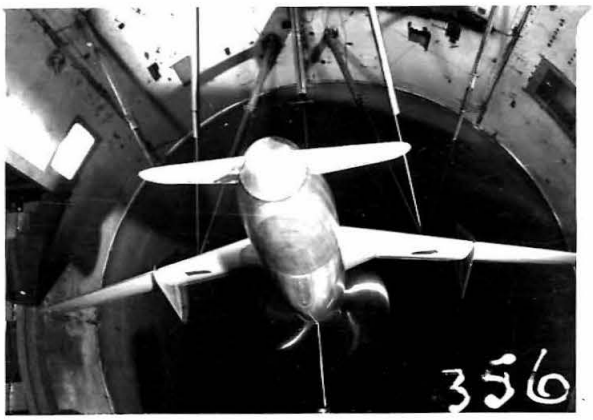

PHOTO 25
$W_N A^* V_I f_4 B_N X_N H_1 P^{30}_{RRW}$, front view showing tail H_1

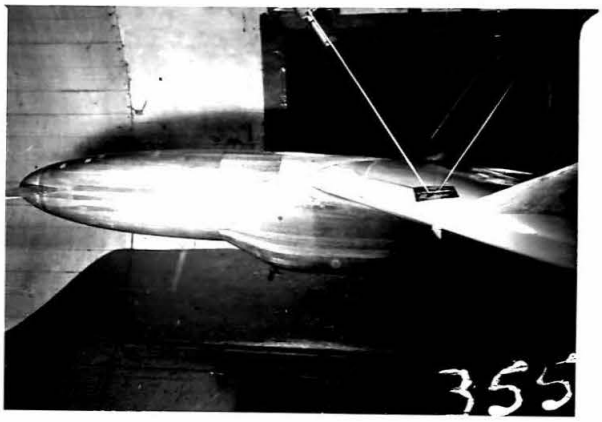

PHOTO 26
$W_N A^* V_I f_4 B_N X_N H_1 P^{30}_{RRW}$, side view showing tail H_1